Faculty of Engineering

Salinity Reduction of Borneo Tropical Brackish Peat Water with Electrocoagulation Treatment

Calvin Anak Jose Jol

Master of Engineering
2023

Salinity Reduction of Borneo Tropical Brackish Peat Water with Electrocoagulation Treatment

Calvin Anak Jose Jol

A thesis submitted

In fulfillment of the requirements for the degree of Master of Engineering

(Chemical Engineering)

Faculty of Engineering
UNIVERSITI MALAYSIA SARAWAK
2023

DECLARATION

I declare that the work in this thesis was carried out in accordance with the regulations of Universiti Malaysia Sarawak. Except where due acknowledgement has been made, the work is that of the author alone. The thesis has not been accepted for any degree and is not concurrently submitted in candidature of any other degree.

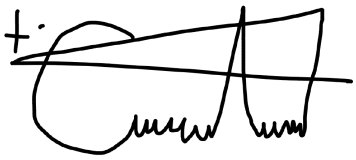

.....

Signature

Name: Calvin Anak Jose Jol

Matric No.: 20020368

Faculty of Engineering

Universiti Malaysia Sarawak

Date: 22nd June 2023

Puji Tuhan!

Dituju ka bapa ku, Jose Jol Anak Endru, ngan aku sayangi, kami sakamarukant,

guru guru ku, sekaraunganku ngan selalu

mare kata perangsang kita

ka aku sampe aku bajaya kania.

Puji Tuhan!

Ditujuka ngagai Indai aku, Reeta Anak Seli, ka dikesayauka, bala kami sebilik,

bala pengajar enggau bala pangan ti dikerinduka aku ti selalu

meri aku jaku peransang enggau

ading ti ngasuh aku tulihka pemujur.

ACKNOWLEDGEMENT

The author would like to thank all individuals, parties, and organizations that have contributed and cooperated throughout the study completion. This endeavour would not have been possible without my supervisor, Dr Nazeri Abdul Rahman for his willingness to share knowledge, experiences, support, and ultimate guidance. The assistance provided by Miss Allene Albania Linus is greatly appreciated especially in terms of knowledge sharing and moral support. The author would like to express his thankfulness to his beloved parents, family members, teachers, and friends who were either directly or indirectly involved in providing their support and motivation to complete the study. May the Almighty God bless you all always.

ABSTRACT

Sarawak located on Borneo Island has vast availability of brackish peat water sources especially in some coastal rural areas. However, brackish peat water is currently underutilized as the source for water treatment plants in the state due to excessive salinity levels. As such, this study aims to investigate the salinity reduction in brackish peat water sources for domestic consumption in Sarawak coastal rural areas by utilizing continuous electrocoagulation treatment with aluminium electrodes. Correspondingly, this study analyzes the effects of seawater percentage, electric current, and flow rate on salinity reduction with electrocoagulation treatment. This study has found that the treated salinity levels in brackish peat water with 30% of seawater percentage meet the Malaysia Class I standard in National Water Quality Standard. The study has also identified both monolayer and multilayer adsorption that occur in electrocoagulation treatment as the precursor to salinity reduction. In addition, the presence of in-situ aluminium hydroxides coagulants could adsorb some sodium chloride from brackish peat water with 70% of seawater percentage at 2,503 mg/g of maximum adsorption capacity and 2.65 min^{-1} of adsorption rate. From the statistical analysis conducted, this study found that electrocoagulation treatment could achieve 91.78% of maximum salinity reduction efficiency with an optimum electric current of 5 A and flow rate of 1.2 L/min in brackish peat water with a 30% of seawater percentage. This treatment system costs only RM 0.29 per meter cubic of treated brackish peat water at optimum conditions. Overall, this study demonstrates that continuous electrocoagulation treatment could reduce the salinity levels in brackish peat water with 30% of seawater percentage which is considered safe for domestic consumption in Sarawak coastal rural areas at reasonable cost.

Keywords: Brackish peat water, electrocoagulation, salinity reduction, adsorption

Pengurangan Kadar Garam dalam Air Gambut Masin Tropikal Borneo dengan Sistem Rawatan Elecktrokogulasi

ABSTRAK

Sarawak yang terletak di kepulauan Borneo mempunyai sumber air yang dikenali sebagai Air Gambut Masin Tropikal. Namun, sumber air tersebut tidak dapat digunakan dalam loji rawatan air di negeri tersebut kerana mengandungi garam yang berlebihan. Oleh itu, kajian ini melakukan rawatan elektrokogulasi dengan menggunakan elektrok aluminium untuk mengurangkan kadar garam dalam air gambut masin bagi kegunaan domestik di pedalaman persisiran negeri Sarawak. Kajian ini juga mengkaji kesan kadar kegaraman, arus elektik, dan aliran air semasa penyahgaraman dalam rawatan elektrokoagulasi. Sehubungan itu, kajian ini telah mendapati rawatan air gambut masin yang mempunyai 30% kadar kegaraman telah mencapai taraf Kumpulan Satu dalam Standard Kualiti Air Kebangsaan di Malaysia. Selain itu, kajian ini juga mengenalpasti pengurangan kegaraman dalam air gambut masin adalah disebabkan oleh penjerapan mono yang berbilang lapisan. Penghasilan koagulan aluminum hidroksida juga menjerap beberapa natrium klorida daripada air gambut masin yang mempunyai 70% kegaraman pada kadar 2,503 mg/g keupayaan penjerapan tertinggi dan 2.65 min^{-1} penjerapan dalam bentuk floks. Melalui analisa statistikal, rawatan elektrokoagulasi mencapai 91.78% pengurangan garam dengan kadar 5 A arus elektrik and 1.2 L/min aliran air serta 30% nilai kegaraman yang optimum. Kos rawatan tersebut hanya memerlukan RM 0.29 bagi setiap isipadu air gambut masin yang terawat. Kesimpulannya, sistem rawatan elektrokoagulasi telah menyahgaram air gambut masin yang mempunyai 30% nilai kegaraman untuk kegunaan domestik di pedalaman persisiran negeri Sarawak pada kadar kos yang berpatutan.

Kata Kunci: *Air gambut masin, elektrokoagulasi, pengurangan garam, penjerapan*

TABLE OF CONTENTS

		Page
DECLARATION		i
DEDICATION		ii
ACKNOWLEDGEMENT		iii
ABSTRACT		iv
ABSTRAK		v
TABLE OF CONTENTS		vi
LIST OF TABLES		xii
LIST OF FIGURES		xiv
LIST OF ABBREVIATIONS		xvi
LIST OF NOMENCLATURES		xviii
CHAPTER 1: INTRODUCTION		1
1.1	Background of the Study	1
1.2	Research Problems	3
1.3	Research Hypothesis	5
1.4	Aim and Objectives	6
1.5	Research Scopes	6
1.6	Significances of the Study	7

CHAPTER 2: LITERATURE REVIEW 8

2.1 Introduction 8

2.2 Brackish Peat Water in Sarawak 8

2.2.1 Coastal Peatlands 8

2.2.2 Coastal Rural Areas 10

2.2.3 Water Supply Issues 10

2.2.4 Characteristics of Peat Water 11

2.2.5 Brackish Peat Water 12

2.3 Brackish Peat Water Treatment 13

2.3.1 Chemical Coagulation 13

2.3.2 Membrane-Related Process 15

2.4 Electrocoagulation Treatment 16

2.4.1 Fundamentals of Electrocoagulation 16

2.4.2 Mechanism of Electrocoagulation 17

2.5 Operating Parameters 19

2.5.1 Electric Current 19

2.5.2 Seawater Percentage 20

2.5.3 Flow Rate 21

2.6 Past Studies on Electrocoagulation 22

2.6.1 Peat Water 23

2.6.2 Seawater 24

2.6.3 Brackish Water 25

2.7 Water Quality Analysis 25

2.8 Energy Operating Cost Analysis 28

2.9 Adsorption Mechanisms in Electrocoagulation 29

2.9.1 Adsorption Isotherm Model 29

2.9.2 Langmuir Adsorption Isotherm 30

2.9.3 Freundlich Isotherm Adsorption 32

2.9.4 Application of Langmuir and Freundlich Isotherm Models in Electrocoagulation 34

2.10 Kinetic Modeling 34

2.10.1 Pseudo-First Order Kinetic Model 35

2.10.2 Linear Pseudo-First Order Kinetic Model 35

2.10.3 Non-Linear Pseudo First Order Kinetic Model 36

2.10.4 Evaluation of Model Validity 37

2.10.5 Application of Pseudo-First Order Kinetic Model in Electrocoagulation 38

2.11 Electrocoagulation Flocs Analysis 39

2.11.1 Electrocoagulation Flocs 39

2.11.2 Electrocoagulation Flocs Analysis with Energy Dispersive X-Ray 40

2.12 Statistical Model 41

2.12.1 Response Surface Methodology 42

2.12.2 Screening and Selection of Independent Factors and Responses 42

2.12.3 Experimental Design Strategy 43

2.12.4 Running the Experiments and Obtaining Results 44

2.12.5 Experimental Data Fitting to the Mathematical Model 45

2.12.6 Model Validation 46

2.12.7 Model Optimization 47

2.13 Summary 48

CHAPTER 3: RESEARCH METHODOLOGY 49

3.1 Introduction 49

3.2 Stage 1: Experimental Study of Salinity Reduction in Brackish Peat Water. 50

3.2.1 Characterization of Brackish Peat Water 51

3.2.2 Continuous Electrocoagulation Treatment System 53

3.2.3 Effects of Seawater Percentage and Electric Current on Salinity Reduction in Brackish Peat Water 54

3.2.4 Effects of Seawater Percentage and Flow Rate on Salinity Reduction in Brackish Peat Water 55

3.2.5 Water Quality Analysis 56

3.2.6 Energy Operating Cost Analysis for the Treatment of Brackish Peat Water with Electrocoagulation 57

3.3 Stage 2: Formulation of Adsorption and Kinetic Models and Conduct Electrocoagulation Flocs Analysis 59

3.3.1 Formulation of Adsorption Isotherm Models 60

3.3.2 Formulation of Pseudo-First Order Kinetics Models 62

3.3.3 Electrocoagulation Flocs Analysis 64

3.4 Stage 3: Development of Statistical Model with Response Surface Methodology 65

3.4.1 Design of Experiment 65

3.4.2 Mathematical Model Fitting 66

3.4.3 Analysis of Variance 68

3.4.4 Statistical Model Analysis 68

CHAPTER 4: RESULTS AND DISCUSSIONS 70

4.1 Introduction 70

4.2 Stage 1: Salinity Reduction of Brackish Peat Water with Electrocoagulation Treatment 70

4.2.1 Salinity Reduction of Brackish Peat Water with Varied Seawater Percentage and Electric Current 70

4.2.2 Salinity Reduction of Brackish Peat Water with Varied Seawater Percentage and Flow Rate 77

4.2.3 Comparison of Untreated and Treated Brackish Peat Water to the National Water Quality Standards in Malaysia 82

4.2.4 Analysis of Energy Operating Cost for Brackish Peat Water Treatment with Continuous Electrocoagulation System 84

4.3 Stage 2: Adsorption Kinetic Models and Analysis of Electrocoagulation Flocs 90

4.3.1 Langmuir and Freundlich Adsorption Isotherm Models 91

4.3.2 Linear and Non-Linear Pseudo-First Order Kinetic Models 95

4.3.3 Energy Dispersive X-Ray Analysis of Electrocoagulation Flocs 98

4.4 Stage 3: Statistical Analysis of Salinity Reduction with Electrocoagulation Treatment 101

4.4.1 Experimental Statistical Design 101

4.4.2 Mathematical Quadratic Equations 103

4.4.3 Model Validation with Analysis of Variance 105

4.4.4 Three-Dimensional (3D) Response Surface Plots 106

CHAPTER 5: CONCLUSIONS 110

REFERENCES 112

APPENDICES 146

LISTS OF TABLES

		Page
Table 2.1	National Water Quality Standards (NWQS) in Malaysia (Department of Environment, 2020)	26
Table 2.2	Water Classifications (Department of Environment, 2020)	27
Table 2.3	Application of Langmuir and Freundlich Adsorption Isotherm Models in Electrocoagulation Treatment	34
Table 2.4	Key Terms in Statistical Analysis	41
Table 2.5	Mathematical Model Validation Source (Acharya et al., 2018; Hendaoui et al., 2018; Shamaei et al., 2018)	46
Table 3.1	Formation of Brackish Peat Water from Intrusion of Seawater into Peat Water Sources	53
Table 3.2	List of Variables for Experimental Study for The Effects of Seawater Percentage and Electric Current on Salinity Reduction in Brackish Peat Water	55
Table 3.3	List of Variables for Experimental Study for The Effects of Seawater Percentage and Flow Rate on Salinity Reduction in Brackish Peat Water	56
Table 3.4	National Water Quality Standards (NWQS) in Malaysia (Department of Environment, 2020)	57
Table 3.5	Experimental Design of Actual and Coded Values of Independent Variables	67
Table 3.6	Statistical Goals, Limits, Weights, and Importance for The Treatment of Brackish Peat Water with Continuous Electrocoagulation Treatment	68
Table 4.1	Energy Operating Cost for The Treatment of Brackish Peat Water with Continuous Electrocoagulation Treatment at 5 A of Electric Current	87
Table 4.2	Comparison of Energy Operating Cost between Electrocoagulation and Other Water Treatment Processes	89
Table 4.3	Comparison of Adsorption Capacity (qe) for Salinity Reduction in Brackish Peat Water with Langmuir and Freundlich Adsorption Isotherm Models	92
Table 4.4	Parameters for Adsorption Process for Salinity Reduction in Brackish Peat Water with Adsorption Isotherm Models	92

Table 4.5	Pseudo-First Orders Kinetic Model Parameters for Salinity Reduction in Brackish Peat Water with Continuous Electrocoagulation Treatment	95
Table 4.6	Kinetic Parameters for Salinity Reduction in Brackish Peat Water with Non-Linear Pseudo-First-Order Model	97
Table 4.7	Elemental Mass Percentage on Electrocoagulation Flocs from Brackish Peat Water with Seawater Percentage That Ranged from 0% to 90%	100
Table 4.8	Central Composite Design (CCD) Experimental Statistical Design	102
Table 4.9	ANOVA and Statistical Parameters of Salinity Reduction Efficiency and Energy Operating Cost	105
Table 4.10	Electrocoagulation Treatment of Brackish Peat Water at Optimum 5 A of Electric Current, 1.2 L/min of Flow Rate, and 30% of Seawater Percentage	109

LIST OF FIGURES

		Page
Figure 2.1	Distribution of Coastal Peatlands in Sarawak (Department of Irrigation & Drainage Sarawak, 2020)	9
Figure 2.2	Estuaries Environment in Coastal Peatlands (Takahashi et al., 2021)	13
Figure 2.3	Formation of Electrocoagulation Flocs (Liu et al., 2018)	39
Figure 2.4	Energy Dispersive X-Ray Spectroscopy (Colpan et al., 2018)	40
Figure 3.1	Stages in Research Methodology	49
Figure 3.2	Kampung Metang Terap in Lundu district (Google Map, 2022).	51
Figure 3.3	Brackish peat water from Kampung Metang Terap in Lundu at Varied Seawater Percentage (A) 0%, (B) 10%, (C) 30%, (D) 50%, (E) 70%, (F) 80%, and (G) 90%.	52
Figure 3.4	Continuous Electrocoagulation Treatment System	53
Figure 4.1	Effect of Electric Current on Salinity Levels Changes with Varied Seawater Percentage and Time	71
Figure 4.2	Effect of Electric Current on Salinity Reduction Efficiency with Varied Seawater Percentage and Time	72
Figure 4.3	Effects of Seawater Percentage and Electric Current on Salinity Reduction Efficiency in Brackish Peat Water	73
Figure 4.4	Effect of Flow Rate on Salinity Levels Changes with Varied Seawater Percentage and Time	78
Figure 4.5	Effect of Flow Rate on Salinity Reduction Efficiency with Varied Seawater Percentage and Time	79
Figure 4.6	Effect of Seawater Percentage and Flow Rate on Salinity Reduction Efficiency in Brackish Peat Water	80
Figure 4.7	Comparison of Untreated and Treated Salinity Levels in Brackish Peat Water to the National Water Quality Standards in Malaysia at 5 A of Electric Current, 1.2 L/min of Flow Rate, and 30% of Seawater Percentage	83
Figure 4.8	Effects of Electric Current and Flow Rate on Energy Operating Cost with Electrocoagulation Treatment of Brackish Peat Water with 30% of Seawater Percentage	85

Figure 4.9	Effect of Flow Rate on Specific Electrical Energy Consumption (SEEC) with Electrocoagulation Treatment at 5 A of Electric Current in Brackish Peat Water with 30% of Seawater Percentage	88
Figure 4.10	Illustration of Salinity Reduction with Adsorption Process in Continuous Electrocoagulation Treatment	91
Figure 4.11	Experimental Data Fitting to Langmuir and Freundlich Adsorption Isotherm Models	94
Figure 4.12	Linear Pseudo-first Order Kinetic for Salinity Reduction in Brackish Peat Water with Electrocoagulation Treatment	96
Figure 4.13	Non-Linear Pseudo-First Order Kinetic Models for Salinity Reduction in Brackish Peat Water with Electrocoagulation Treatment	97
Figure 4.14	Analysis of Electrocoagulation Flocs from Brackish Peat Water with Energy Dispersive X-Ray	99
Figure 4.15	Relationship Between Salinity Reduction Efficiency, Sodium Chloride, and Aluminium Hydroxides in Electrocoagulation Treatment	101
Figure 4.16	Regression Coefficient of Mathematical Equation for Salinity Reduction Efficiency	104
Figure 4.17	Regression Coefficient of Mathematical Model for Energy Operating Cost	104
Figure 4.18	Relationship between Seawater Percentage and Electric Current on Salinity Reduction Efficiency at 1.2 L/min of Flow Rate	107
Figure 4.19	Relationship between Seawater Percentage and Flow Rate on Salinity Reduction Efficiency at 5 A of Electric Current	107
Figure 4.20	Relationship between Flow Rate and Electric Current on Salinity Reduction Efficiency at 30% of Seawater Percentage	107
Figure 4.21	Relationship between Electric Current and Seawater Percentage on Energy Operating Cost at 1.2 L/min of Flow Rate	108
Figure 4.22	Relationship between Flow Rate and Seawater Percentage on Energy Operating Cost at 5 A of Electric Current	108
Figure 4.23	Relationship between Electric Current and Flow Rate on Energy Operating Cost at 30% of Seawater Percentage	108

LIST OF ABBREVIATIONS

AC	Alternating Current
AN	Ammoniacal Nitrogen
ANOVA	Analysis of Variance
APHA	American Public Health Association
ASTM	American Society Testing Materials
BOD	Biochemical Oxygen Demand
CCD	Central Composite Design
COD	Chemical Oxygen Demand
DC	Direct Current
DOC	Dissolved Organic Carbon
DOE	Department of Environment
DoE	Design of Experiment
EPU	Economic Planning Unit
EQA	Environmental Quality Act
FC	Feacal Coliform
JBALB	Jabatan Bekalan Air Luar Bandar
KWB	Kuching Water Board
NTU	Nephelometric Turbidity unit
NWQS	National Water Quality Standard
PACl	Polyaluminium Chloride
pH	Potential of Hydrogen
RO	Reverse Osmosis

RSM	Response Surface Methodology
SAWAS	Sarawak Alternative Water Supply
SS	Suspended Solids
SWB	Sibu Water Board
TCU	True Colour Unit
TDS	Total Dissolved Solids
TOC	Total Organic Content
TSS	Total Suspended Solids

LIST OF NOMENCLATURES

α	Axial Point
C_e	Equilibrium Salinity Levels
C_o	Initial Salinity Levels
C_t	Final Salinity Levels
I	Electric Current
k_1	Reaction Rate Constant
K_f	Freundlich Constant
K_L	Langmuir Constant
M	Molecular Weight
n_f	Empirical Constant
Q	Volume
q_e	Equilibrium Adsorption Capacity
q_{max}	Maximum Adsorption Capacity
R^2	Regression Coefficient
R_L	Langmuir Separation Factor
T	Residence Time
V	Voltage
Z	Faraday Constant

CHAPTER 1

INTRODUCTION

1.1 Background of the Study

A significant decline in the quality and quantity of available freshwater has an adverse impact on human health and the ecosystem (Dessu et al., 2018). Realizing this issue, the United Nations has placed 'Clean Water and Sanitation' as number six target for achieving Sustainable Development Goals by 2030 in order to mitigate water scarcity issue (Sullivan et al., 2018). Despite the immense supply of natural water sources on Borneo Island, water shortage issues especially in Sarawak coastal rural areas have not been sufficiently addressed (Khalid, 2018).

The coastal rural areas in Sarawak are endowed with a vast availability of unutilized brackish peat water sources. Brackish peat water is mainly derived from peat swamp forestry in the form of water residues and could not be consumed as potable water without a proper water treatment process (Grzegorzek & Majewska-Nowak, 2017). According to Gosch et al. (2018), most coastal peatlands are constituted by brackish peat water sources owing to the occurrence of seawater intrusion into this region during water tide. Due to this circumstance, the salinity levels in brackish peat water will vary considerably depending on the amount of freshwater (<500 mg/L) and seawater (between 15,000 mg/L and 48,000 mg/L) (Dijk et al., 2017).

The concerns of prolonged water supply issue especially in remote coastal rural areas have embarked the need to implement standalone water treatment system. This undertaken should has least impact on the environment, reliable, and user-friendly (Pooi & Ng, 2018; Gunten, 2018). Even though brackish peat water could be treated with chemical coagulation and membrane-related processes, these processes have

disadvantages in terms of sludge generation as well as membrane fouling and degradation issues (Gohil & Surest, 2017; Barrera-Diaz et al., 2018).

Electrocoagulation is a simple water treatment process that generates in-situ aluminium hydroxide coagulants to separate pollutants from water sources in the form of flocs. In comparison to conventional chemical coagulation, electrocoagulation has zero secondary pollution and requires less maintenance (Moussa et al., 2017). The process to treat water sources with electrocoagulation generally consists of three successive steps. Initially, the sacrificial aluminium electrodes are dissociated to form aluminium ions as shown by **Equation 1.1**. This treatment process also involves water splitting reaction, as shown by **Equation 1.2**, through cathode reduction to generate hydroxides ions. Both aluminium and hydroxides ions bind to each other as shown in **Equation 1.3** and subsequently form gelatinous white aluminium hydroxide coagulants (Garcia-Segura et al., 2017).

Anode Oxidation:

$$Al \rightarrow Al^{3+}_{(aq)} + 3e^- \quad \textbf{(1.1)}$$

Cathode Reduction:

$$3H_2O + 3e^- \rightarrow \frac{3}{2}H_{2(g)} + OH^- \quad \textbf{(1.2)}$$

Formation of Aluminium Hydroxide:

$$Al^{3+}_{aq} + 3H_2O \rightarrow Al(OH)_3 + 3H^+ \quad \textbf{(1.3)}$$

The electro dissolution of anode electrode causes metal concentration in water sources to rise and finally precipitates electrocoagulation flocs where the organic pollutants act as a ligand (Garcia-Segura et al., 2017). Aluminium hydroxide coagulants also operate as a charge shield in the charge neutralization mechanism that aims in compressing the double layer of pollutants and favouring the formation of aggregates and eventually, precipitation (Rusdianasari et al., 2019). The adsorption of organic pollutants with aluminium hydroxide coagulants that occurs on the active sites of

adsorbent surfaces will precipitate and eventually form electrocoagulation flocs. Ghernaout (2019) informed that electrocoagulation treatment could remove many pollutants from water sources due to the nature of electrocoagulation flocs that have high adsorption capacity.

Several published studies in the literature had reported that electrocoagulation treatment could be utilized to treat peat water (Rusdianasari et al., 2019; Rahman et al., 2020a; Rahman et al., 2020b; Rahman et al., 2020c), brackish water (Sari & Chellam et al., 2017; Zhang et al., 2019), and seawater (Abdulkarem et al., 2017). A study conducted by Al-Raad et al. (2019) on saline water treatment reported that electrocoagulation treatment is found to be effective at low energy operating costs. As added by Al-Raad and Hanafiah (2021), electrocoagulation destabilizes finely dispersed particles and complex pollutants such as greases, hydrocarbons, heavy metals, and suspended solids from water sources to form flocs. Although electrocoagulation is effective to treat various water sources, its application for brackish peat water treatment has not been reported in the literature. As such, the purpose of this study is to conduct an experimental investigation to reduce the salinity levels in brackish peat water with electrocoagulation treatment system.

1.2 Research Problems

Brackish peat water found in coastal peatlands contains high salinity levels which is harmful for domestic consumption (Wildayana et al., 2017). The treatment of brackish peat water with conventional treatment systems particularly chemical coagulation and reverse osmosis have some drawbacks in terms of harmful sludge generation, membrane fouling and degradation (Zhang et al., 2020; Verbeke et al., 2020). Realizing these issues, the application of electrocoagulation treatment system

for salinity reduction in brackish peat water could unlock its potential as an alternative water technology in Sarawak coastal rural areas. Despite the effectiveness of electrocoagulation system in removing various types of contaminants, the effects of key operating parameters particularly seawater percentage, electric current, and flow rate on salinity reduction have not been investigated.

According to El-Ashtouky et al. (2020), the formation of aluminium hydroxide coagulants through redox reactions in electrocoagulation treatment is associated to the number of salts ions that available in water sources. To date, no study has reported the applicability of electrocoagulation treatment to reduce the salinity levels in brackish peat water with varied seawater percentage. Additionally, electric current is the main precursor that led to contaminants reduction with electrocoagulation treatment due to the formation of in-situ aluminium hydroxide coagulants (Shahedi et al., 2020). In electrocoagulation, the flow rate agitates the water to ensure an effective adsorption process between aluminium hydroxides and contaminants through in-situ mixing process (Nugroho et al., 2021; Ashraf et al., 2021).

The adsorption kinetics and electrocoagulation flocs analysis for salinity reduction in brackish peat water have not been reported in the published literature. A study conducted by Budhiary and Sumantri (2021) informed that the adsorption kinetic models and electrocoagulation flocs analysis could explain the mechanisms that lead to contaminants reduction in electrocoagulation. Although there are several adsorption theorems that are available in the literature, these models possess some limitations to describe the adsorption mechanism precisely (Liu et al., 2019; Laskar & Hashisho, 2020; Azizian & Eris, 2021).

The energy operating cost analysis needs to be conducted when electrocoagulation treatment is employed for water treatment (Khorram & Fallah,

2020). According to Tones et al. (2020), response surface methodology (RSM) is a statistical tool used for process optimization. In developing a statistical model, the implementation of RSM requires careful consideration of experimental design, selection of responses variables, and its accuracy (Bajpai et al., 2020). As such, RSM could be employed to optimize the energy consumption in electrocoagulation treatment system through statistical model analysis (Bajpai et al., 2020).

1.3 Research Hypothesis

Continuous electrocoagulation treatment is utilized to reduce the salinity levels of brackish peat water at varied seawater percentage, electric current, and flow rate. The adsorption process that occurs in electrocoagulation treatment reduces salinity levels in brackish peat water with the aid of in-situ aluminium hydroxide coagulants. In addition, the effectiveness of electrocoagulation treatment to reduce salinity levels could be assessed in terms of water quality analysis and energy operating cost. The adsorption kinetic models are formulated to analyze the salinity reduction efficiency based on adsorption capacity and rate. Moreover, the occurrence of salinity adsorption with aluminium hydroxide coagulants is identified with electrocoagulation flocs analysis. The optimal salinity reduction efficiency and energy operating cost of electrocoagulation treatment could be determined by regulating the seawater percentage, electric current, and flow rate. In accordance with the problem statement which has been mentioned previously, this study hypothesizes that continuous electrocoagulation treatment is utilized to reduce salinity levels in brackish peat water for domestic consumption in Sarawak coastal rural areas at reasonable electric current and flow rate.

1.4 Aim and Objectives

This study aims to investigate the salinity reduction in brackish peat water for domestic consumption in coastal rural areas of Sarawak by utilizing continuous electrocoagulation treatment system with aluminium electrodes. In accordance with the aim of this study, the objectives of this study are devised as follows:

i. To conduct experimental study of salinity reduction in brackish peat water with continuous electrocoagulation treatment, particularly at varied seawater percentage, electric current, and flow rate.

ii. To formulate adsorption kinetic models and conduct electrocoagulation flocs analysis.

iii. To develop statistical model with response surface methodology for electrocoagulation treatment optimization.

1.5 Research Scopes

The following scopes have been devised in order to achieve the aim and objectives of this study.

i. The study only focuses on salinity reduction in brackish peat water from Kampung Metang Terap, Lundu, Kuching, Sarawak by utilizing continuous electrocoagulation treatment with aluminium electrodes.

ii. This study investigates the effect of seawater percentage (0% to 90%), electric current (1 A to 5 A), and flow rate (0.4 L/min to 2.0 L/min) on salinity reduction efficiency.

iii. A water quality analysis between untreated and treated salinity levels in brackish peat water is compared to the National Water Quality Standards (NWQS) as classified by the Department of Environment in Malaysia.

iv. In order to evaluate the energy operating cost, this study utilizes Faraday law equations to calculate the specific electrical energy consumption (SEEC) and electrode material consumption (EMC).

v. The formulation of Langmuir, Freundlich, and pseudo-first-order kinetic models is conducted to investigate the adsorption mechanism for salinity reduction.

vi. The mineral compositions on electrocoagulation flocs are also determined with Energy Dispersive X-ray (EDX).

vii. The statistical model is developed with central composite design and analysis of variance (ANOVA).

1.6 Significances of the Study

This study provides new insights into the emerging application of continuous electrocoagulation treatment, especially to reduce the salinity levels in brackish peat water sources for domestic consumption in Sarawak coastal rural areas. This study also promotes the utilization of continuous electrocoagulation treatment for salinity reduction that requires zero addition of chemical coagulants. The electrocoagulation treatment produces in-situ aluminium hydroxide coagulants which subsequently removes some salinity from brackish peat water in the form of flocs. The statistical analysis done in this study could be utilized for further study, especially in exploring the application of continuous electrocoagulation treatment as a full-scale standalone water treatment system in Sarawak coastal rural areas.

CHAPTER 2

LITERATURE REVIEW

2.1 Introduction

The literature review describes and discusses published studies on electrocoagulation treatment process. Correspondingly, this chapter describes the characteristics of brackish peat water sources and several conventional treatment processes that are associated with this water source. The chapter also includes a discussion on electrocoagulation operating parameters and their application to various types of water sources. The scheme to conduct adsorption isotherm and kinetic modeling as well as statistical model analysis with response surface methodology (RSM) is also discussed in this chapter.

2.2 Brackish Peat Water in Sarawak

Sarawak is endowed with an abundance of brackish peat water, particularly in some coastal rural areas that experience clean water supply issues. However, this water source is currently underutilized as a source of clean water supply due to its high salinity levels (Wildayana, 2017). According to Grzegorzek & Majewska-Nowak (2017), brackish peat water is defined as a water source that contains both humic acid and salinity. In addition, brackish peat water is naturally formed due to seawater intrusion into the coastal peatlands region during high tide (Waller & Kirby, 2021).

2.2.1 Coastal Peatlands

Coastal peatlands features wetlands with thick sequences of organic matter deposits as well as rich in mineral sources (Koster et al., 2018). According to Moomaw

et al., (2018), coastal peatlands are strategic ecosystems that provide habitat for plants and animals, prevent flooding and sea storms, accumulate sediments, control erosion, and store earth carbon. In Sarawak, coastal peatlands cover approximately 1.7 million hectares of peat forests and 154,000 hectares of mangrove forests of the state land as shown in **Figure 2.1** (Department of Irrigation and Drainage Sarawak, 2020).

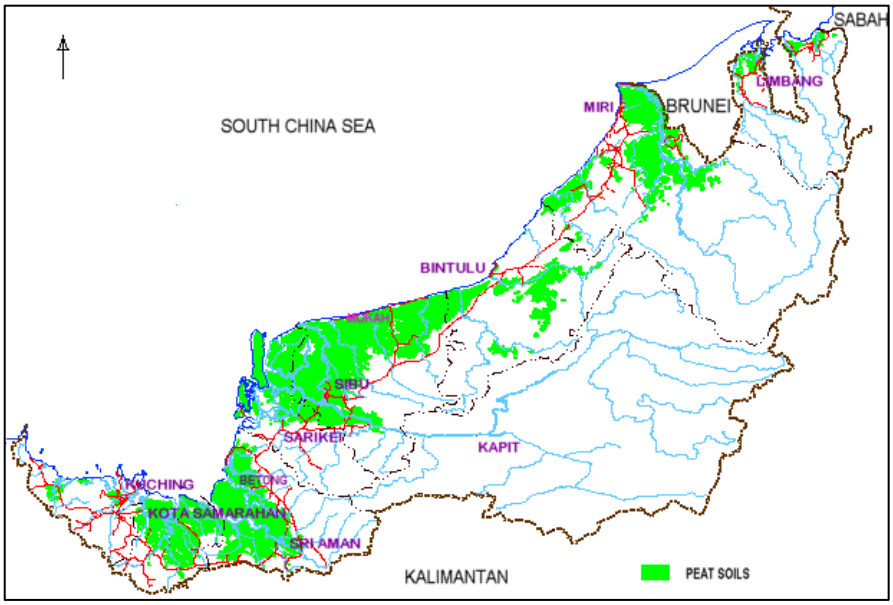

Figure 2.1: Distribution of Coastal Peatlands in Sarawak (Department of Irrigation & Drainage Sarawak, 2020)

Coastal peatlands in Sarawak could be found in river delta areas along the state coastline as illustrated in **Figure 2.1** (Department of Irrigation & Drainage Sarawak, 2020). According to Sangok et al. (2020), coastal peatlands in Sarawak have a vast accumulation of peat water which contains high acidity levels as well as dissolved organic compounds that derived from decayed plant residues. The coastal peatlands in Sarawak consist of peat deposits that are mostly found within interface of the river delta with the co-existence of natural seawater intrusion into such region during high tide (Waller & Kirby, 2021). Some coastal rural areas communities that reside within coastal peatlands in Sarawak have also utilized these lands for agriculture activities such as palm oil plantation, plants orchard, paddy rice, and poultry (Cole et al., 2021).

2.2.2 Coastal Rural Areas

The coastal rural areas in Sarawak coastal peatlands occupy about 60% of the state coastline that are found within several major divisions particularly in Kuching, Sri Aman, Sibu, and Limbang (Bakewell et al., 2017). In Sarawak, coastal rural areas are located within 1,035 km of the state shoreline starting from Telok Melano in the southern region (Vogelgesang et al., 2018). Moreover, some coastal rural areas in southern Sarawak are renowned for peat swamps regions that are co-existed with extensive sandy beaches particularly from Tanjung Datu to the mouth of Batang Kayan river in Lundu district (Kuok et al., 2021a). The coastal region geography in southern Sarawak is also enriched with low-lying flat grounds covered in swamp and wet watery environments (Teepol et al., 2021).

2.2.3 Water Supply Issues

Some coastal rural areas in Sarawak have lack access to freshwater supply owing to the inaccessible location. According to Baradey et al. (2018), several coastal rural areas in Sarawak have been installed with saltwater desalination system that aims to provide treatment for salty water through an alternative water supply programme. However, this treatment system could not be fully utilized by the coastal rural areas communities particularly in Beladin, Kampung Batang Maro, Telok Melano, Kampung Punang in Lawas, Kampung Bruit, Kampung Penipah, Kampung Lanjong, and Lubok Samsu due to the malfunctioned issues that required RM 5 million to repair such treatment system (Bujang, 2018).

In Sarawak coastal peatlands, some places are also suffering from poor water quality especially during drought season (Prasanna et al., 2019). Although such regions have some groundwater catchment areas, the occurrence of seawater intrusion has

lessened the ability of these catchment areas to provide fresh drinking water for coastal rural areas communities (Department of Irrigation and Drainage Sarawak, 2022). In order to mitigate this issue, Jabatan Bekalan Air Luar Bandar (JBALB) has daily provided truck water tankers to these affected areas as temporary solutions, despite the fact that they are costly (New Sarawak Tribune, 2019).

In Sarawak rural coastal regions, some communities also used rainwater harvesting systems by temporarily storing excess rainfall for non-potable water use (Kuok et al., 2021b). However, this rainwater could not be fully utilized for domestic consumption because its levels of content, particularly turbidity, lead, and total coliform, exceeded World Health Organization (WHO) limits (Lani et al., 2018). Instead of relying on a faulty saltwater desalination system, contaminated groundwater, and rainwater harvesting method, it is critical to investigate the potential of underutilized water sources in coastal peatlands areas for domestic consumption.

2.2.4 Characteristics of Peat Water

Peat water is defined as surface water that contains organic substances, specifically humic acid which is found primarily in peatland areas (Alif et al., 2018). According to Wenten et al. (2020), peat water could be an alternative water source especially for those residing in peatland areas. This water source is commonly found in Sarawak coastal areas particularly in southern and central parts of the state, and it is reported that some rural communities in those areas rely excessively on peat water and rainwater for domestic consumption (Rahman et al., 2020a). A study conducted by Ali et al. (2021) reported that direct consumption of peat water could lead to severe diseases due to this water containing high levels of acid and organic substances. A similar observation had been informed by Elma et al. (2022) that found peat water has high

acidity levels due to the high organic matter content, particularly dissolved organic carbon (DOC), which has a bad smell and also corrosive to water distribution networks. In addition, some peat water also contains salt ions that are naturally derived from the seawater intrusion into coastal peatlands areas during high tide (Gutekunst et al., 2022).

2.2.5 Brackish Peat Water

Brackish peat water is categorized as a peat water source that contains both humic acid and salinity levels that ranged from 1,000 mg/L to 15,000 mg/L (Grzegorzek & Majewska-Nowak, 2017). According to Gosch et al. (2018), brackish peat water in coastal peatlands is naturally formed due to seawater intrusion into peat water sources during high tides. Martin et al. (2018) reported that the southern Sarawak region particularly in Lundu and Sematan constitutes natural catchment areas that contained both peat water and brackish water. The study conducted by Martin et al. (2018) also informed that such regions also contained a high proportion of minerals and dissolved organic carbon which indicated the existence of brackish peat water in these regions. In terms of physical appearance, brackish peat water contains a complex mixture of yellowish-brown to black-coloured amorphous organic matter that is mostly found in estuaries regions. The seawater intrusion into peat water sources which usually occurs within marginal areas of peatlands will produce brackish peat water as depicted in **Figure 2.2** (Takahashi et al., 2021). In Sarawak, brackish peat water sources could be found mostly in lowland peatlands areas that have a high accumulation of organic soil materials along the coastal areas (Omar et al., 2022).

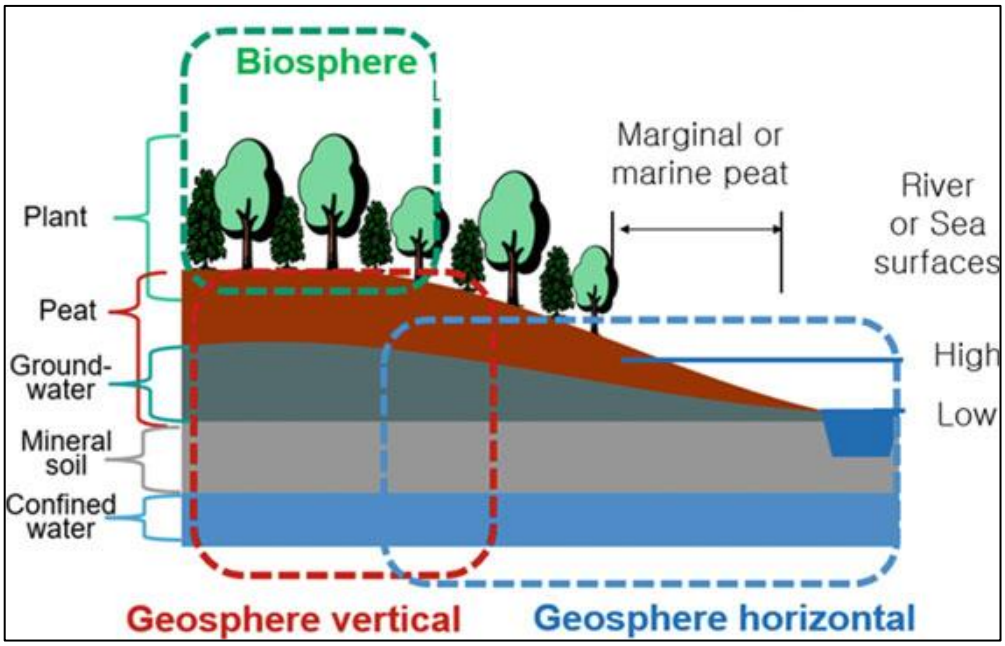

Figure 2.2: Estuaries Environment in Coastal Peatlands (Takahashi et al., 2021)

2.3 Brackish Peat Water Treatment

Despite brackish peat water is available abundantly in some coastal rural areas, this water is currently underutilized for domestic consumption due to excessive salinity levels (Wildayana et al., 2017). Brackish peat water also contains a peculiar smell and taste that may harm human health due to the availability of humic acid and salinity in such water (Sharip et al., 2019). Several treatment systems that are possible to treat brackish peat water especially to reduce salinity levels and separate dissolved humic substances from such water sources have been reported in several published studies in the literature which are as follow.

2.3.1 Chemical Coagulation

Chemical coagulation is a viable option to treat peatland-derived runoff water as reported by Sutapa et al. (2020). The study found that chemical coagulation could be utilized to reduce 95% of colour, 99% of turbidity, and 100% of chemical oxygen demand

in which the treated water being comparable to water standard in Indonesia. Despite chemical coagulation is effective on natural organic matter reduction, the ability of this treatment system for salinity reduction in brackish peat water is not reported by Sutapa et al. (2020). A study conducted by Elma et al. (2020) also used chemical coagulation treatment to treat brackish peat water. The study found that 83.5% of natural organic matter had been removed in the form of flocs by using 30 g/L of aluminium sulphate coagulants. Moreover, the study noticed that chemical coagulation treatment is only suitable for water pre-treatment because it could not remove conductivity and total dissolved solids from brackish peat water (Elma et al., 2020).

Although chemical coagulation treatment could remove natural organic matters from brackish peat water sources (Sutapa et al., 2020; Elma et al., 2020), the issue that concerns sludge generation is yet to be considered by these studies. Padmaja et al. (2020) indicated that chemical coagulation treatment is expensive and labor-intensive process because such treatment requires various additives and chemical reagents in order to attain efficient pollutant removal. In order to achieve high-quality of treated water, post-treatment is necessary for chemical coagulation because it could not completely reduce pollutant levels as a standalone water treatment system (Swain et al., 2020). Chemical coagulation treatment also generates many sludges which poses severe problems such as extensive sludge management and disposal issues (Zhang et al., 2020). The main drawback of chemical coagulation treatment also poses toxic sludge generation. As informed by Bahrodin et al. (2021), toxic sludge is also produced in chemical coagulation treatment due to excessive dosages of chemical additives. In order to mitigate this issue, an extensive post-treatment system is necessary after chemical coagulation in order to obtain potable treated water (Al Umairi et al., 2021).

2.3.2 Membrane-Related Process

The membrane-related process is an advanced filtration process that separates salts from water sources through microscopic porous membranes derived from polymeric or inorganic films. In terms of brackish peat water treatment, Aryanti et al. (2018) found that an ultrafiltration treatment system could be effectively utilized to remove 84% of humic acid from brackish peat water sources. However, the study reported that ultrafiltration treatment system is only suitable at low levels of natural organic materials content in order to prevent membrane degradation issues. According to Qasim et al. (2019), the membrane fouling issue needs to be considered in implementing reverse osmosis due to fast degradation of membranes when the treated water sources contain a large number of chlorides. Rahma et al. (2019) also noticed that membrane filtration through pervaporation treatment system could be utilized to reduce 81.8% of natural organic matter (NOM) and 40% of conductivity from brackish peat water. The study conducted by Rahma et al. (2019) had proposed to treat these water sources with chemical coagulation prior to pervaporation treatment in order to achieve 87% of NOM and 99.9% of salinity reduction. This signifies that pervaporation treatment system requires high-quality water feed to ensure complete salinity reduction in brackish peat water sources (Wilson & George, 2020).

Although membrane-related processes have shown excellent performance through high salt rejection, several conducted studies have indicated issues with membrane fouling and membrane degradation (Qasim et al., 2019; Wilson & George, 2020). As reported by Hailemariam et al. (2020), the drawbacks of utilizing membrane-related processes, especially for salts-containing solutions are membrane fouling and degradation in which these occurrences could be detected when salt rejection is less than 90%. Verbeke et al. (2020) informed that membrane degradation refers to damage

acquired upon chloride exposure and subsequently caused a sudden increase in water flux and reduction in salt retention. Membrane fouling also occurs when the pores of the membrane start to narrow due to the deposition of sludge flocs on its surfaces and eventually reduces permeating flux and water productivity (Du et al., 2020). These studies have reported that membrane-related processes possess disadvantages in terms of membrane fouling and degradation as well as could only be mitigated through cleaning and replacing membranes at high maintenance costs.

2.4 Electrocoagulation Treatment

Electrocoagulation is an electrochemical water treatment process that integrates both coagulation and flotation processes to generate in-situ chemical coagulants upon connection with electric current (Hakizimana et al., 2017). This treatment system is also an effective method to remove various types of pollutants in contaminated water sources at high efficiency without secondary waste generation (Moussa et al., 2017).

2.4.1 Fundamentals of Electrocoagulation

According to Garcia-Segura et al. (2017), electrocoagulation is an electrochemical process that utilized electric current to destabilize the charges of pollutants that caused electrode dissolution and subsequently trapped pollutants in the forms of electrocoagulation flocs. Tahreen et al. (2020) found that electrocoagulation is an effective water treatment system since it uses an adsorption mechanism to remove most pollutants in water sources. Electrocoagulation treatment in continuous mode could also remove various types of pollutants from water sources efficiently at a reasonable flow rate and electric current (López-Guzmán et al., 2021). In

electrocoagulation, the in-situ aluminium hydroxide coagulants are being produced through dissolution of sacrificial anodes upon connection of direct current (Ashraf et al et al., 2021).

2.4.2 Mechanism of Electrocoagulation

Electrocoagulation works based on the principles of electrochemistry in which metal ions are oxidized from anode electrodes whereas hydroxide ions are reduced from cathode electrodes (Moussa et al., 2017). Electrocoagulation treatment produces metal hydroxide coagulants that act as the neutralizer as well as agglomerate and coagulate suspended particles in the forms of electrocoagulation flocs (Bassyouni et al., 2017). As stated in Derjagun-Landua-Verwey-Overbeek (DLVO) theory, the stability of colloidal particles in water sources could be achieved by balancing both positive and negative charges which subsequently lead to effective adsorption of pollutants on coagulants surfaces (Moussa et al., 2017).

The utilization of copper metal electrodes in electrocoagulation could lead to secondary pollution due to the formation of green compounds caused by further oxidation of copper ions (Linares Hernández et al., 2017). Despite iron electrodes are effective materials in electrocoagulation, the dissolution of iron ions in water sources only favours low alkaline conditions (Moussa et al., 2017). A study conducted by Yavuz & Ögütveren (2018) also reported that iron metal could dissolve into several forms particularly divalent (Fe^{2+}) and trivalent (Fe^{3+}). A similar study performed by Ni et al. (2020) also found that the oxidation of divalent Fe^{2+} is inefficient at pH levels being less than five and this indicates that iron metal only favours neutral water conditions. In 2018, a study done by Zarei et al. (2018) used aluminium electrodes in electrocoagulation treatment. The study effectively reduced 90.2% of silica from

brackish water whereas iron electrodes could remove only 37.8% of silica. This is possibly due to aluminium ions having higher adsorption capacity as compared to iron. A similar study conducted by Al-Raad et al. (2019) also informed that aluminium electrodes could reduce 91% of total dissolved solids, 93% of chloride, 92% of bromide, and 90% of sulphate from saline water when electrocoagulation treatment is utilized. This observation is also similar to a study performed by Rusdianasari et al. (2019) which reported that aluminium metals served best as anode electrodes because they could reduce 42.09% of total dissolved solids, 34.36% of biological oxygen demand, and 88.89% of chemical oxygen demands from peat water sources with electrocoagulation. Based on these findings, it is observed that effective pollutants removal in various water sources is due to an effective redox reaction when electrocoagulation treatment system is equipped with aluminium metals electrodes as shown in **Equation 2.1**, **Equation 2.2**, and **Equation 2.3** (Garcia-Segura et al., 2017; Rusdianasari et al., 2019; Rahman et al., 2020a).

Anode Oxidation: $$Al \rightarrow Al^{3+}_{(aq)} + 3e^{-} \quad \textbf{(2.1)}$$

Cathode Reduction: $$3H_2O + 3e^{-} \rightarrow \frac{3}{2}H_{2(g)} + OH^{-} \quad \textbf{(2.2)}$$

Formation of Aluminium Hydroxides: $$Al^{3+}_{aq} + 3H_2O \rightarrow Al(OH)_3 + 3H^{+} \quad \textbf{(2.3)}$$

The formation of aluminium electrodes upon dissociation of aluminium ions from anode electrodes has exhibited the adsorption ability to separate various types of pollutants without any secondary pollution (Rahman et al., 2020a). Aluminium electrodes could also produce different hydroxo complexes including monomers and polymers such as $Al(OH)^{2+}$, $Al_2(OH)^{4+}_2$, $Al_3(OH)^{5+}_4$, $Al_6(OH)^{3+}_{15}$, $Al_7(OH)^{4+}_{17}$, $Al(OH)^{7+}_{20}$, $Al_{13}O_4(OH)^{7+}_{24}$, and $Al_{13}(OH)^{5+}_{34}$ (Kessentini et al., 2019; Akhtar et al., 2020). The

formation of different hydroxo complexes compounds with aluminium electrodes also indicates that aluminium ions react with water to form anionic, cationic, and neutral complexes in electrocoagulation (El-Ashtoukhy et al., 2020). As compared to aluminium and iron electrodes, copper electrodes are very expensive at market price. The cost price for one kilogram of copper metal is RM 25.74 (Rahman et al., 2020b), whereas iron is RM 7.50 per kilogram (Rahman et al., 2020c) and aluminium is RM 8.95 per kilogram (Rahman et al., 2020a). Despite the fact that aluminium price is slightly higher than iron metals, aluminium ions have high valence electrons charge as well as exhibit amphoteric properties (Moradi et al., 2021).

2.5 Operating Parameters

According to Bajpai et al. (2020) and López-Guzmán et al. (2022), the effectiveness of continuous electrocoagulation treatment could be determined by adjusting the main operating parameters which are (i) electric current, (ii) seawater percentage, and (iii) flow rate.

2.5.1 Electric Current

Electric current is the main operating parameter in electrocoagulation treatment. According to Shamaei et al. (2018), electric current regulates the electrocoagulation reactions particularly for dissolution of aluminium ions from anode electrodes. This parameter is also important because it controls the production of aluminium hydroxide coagulants that subsequently bind with pollutants to produce electrocoagulation flocs. The formation of metal coagulants with electrocoagulation is often associated with the value of electric current. As reported by Ghernaout (2019), the dissociation of metal ions from anode electrodes is directly proportional to the electric current.

The effect of electric current is reportedly essential in peat water treatment with electrocoagulation. According to Rahman et al. (2020a), a high electric current could lead to an effective pollutant reduction from peat water sources. The study reported that 5 A of electric current had removed 88.22% of total organic carbon (TOC), 89.90% of chemical oxygen demand (COD), and 87.50% of total suspended solids (TSS) (Rahman et al., 2020a). When the electric current is reduced to 1 A, the study conducted by Rahman et al. (2020a) found that electrocoagulation treatment had reduced only 72.09% of TOC, 43.55% of COD, and 62.50% of TSS. As informed by Nidheesh et al. (2020), a high electric current generates an adequate amount of aluminium hydroxide coagulants that aid in pollutant separation from water sources in the form of flocs.

2.5.2 Seawater Percentage

In electrocoagulation, the hydrolysis of aluminium ions species with chloride ions could lead to the precipitation of $Al(OH)Cl_2$ in the form of electrocoagulation flocs (Graça et al., 2019). This signifies that electrocoagulation treatment could reduce excessive levels of chloride ions in the form of electrocoagulation flocs with the aid of in-situ aluminium hydroxide coagulants. In 2019, a study attempted by Al-Raad et al. (2019) found that electrocoagulation treatment could reduce 93% of chloride ions from saline lake water that contains 8,498 mg/L of chlorides. A study performed by El-Ashtoukhy et al. (2020) reported that the presence of sodium chloride could also enhance the high production of aluminium hydroxide coagulants and had removed most heavy metals from water sources. The study conducted by El-Ashtoukhy et al. (2020) noticed that 2,000 mg/L of sodium chlorides could remove 100% of copper whereas 500 mg/L only reduced 94% of copper metal in water source (El-Ashtoukhy et al., 2020).

Bendaia et al. (2021) also reported that excessive amounts of sodium chloride in water sources could transform aluminium hydroxide coagulants into transitory

compounds. Due to further oxidation, some aluminium hydroxides coagulants will dissolve into $AlCl_4^-$ and eventually reduce the number of aluminium hydroxide coagulants that are supposed to adsorb pollutants from water sources. This observation occurred in a study conducted by Rafiee et al. (2020) which reported that the amount of $Al(OH)_3$ could possibly lessen due to excessive levels of sodium chloride. The study conducted by Rafiee et al. (2020) also indicated that excessive chloride ions could cause the transition of aluminium hydroxides coagulants into soluble transitory compounds such as $Al(OH)_3Cl$, $Al(OH)Cl_3$, and $AlCl_3$. As reported in several works of literature studies, electrocoagulation treatment could be utilized to reduce salinity levels, particularly chloride ions from water sources in the form of electrocoagulation flocs (Al-Raad et al., 2019). Even though electrocoagulation could reduce salinity from saline water and seawater, its application on brackish peat water with varying seawater percentages is unknown.

2.5.3 Flow Rate

Flow rate is defined as the volume of water that enters electrocoagulation treatment system at a given time (Nguyen et al., 2017). According to Nugroho et al. (2021), the study suggested that continuous electrocoagulation treatment could be employed to treat water sources that contain high concentrations of colloids, organic compounds, and suspended solids. This is due to the fact that continuous flow rate could simultaneously aid in water transportation as well as accelerate the formation of aluminium hydroxide coagulants with in-situ mixing process (Nugroho et al., 2021). In certain cases, both high and low flow rates could not promote high colour reduction efficiency when the study conducted by Wu et al. (2021) obtained an optimal water flow rate of 1.0 L/min to achieve 99.23% of colour reduction efficiency. This observation is dissimilar to a study conducted by Al-Raad and Hanafiah (2021) when the study

observed low chemical oxygen demand reduction at 1.0 L/min of flow rate due to inadequate time for the emitted ions from sacrificial anode to form aluminium hydroxides flocs.

Several conducted studies have also reported that an effective continuous electrocoagulation treatment could be attained at high flow rate. Ayyappa et al. (2021) informed that high flow rate is applicable with high electric current to achieve high pollutants reduction efficiency. The study conducted by Ayyappa et al. (2021) observed that 95.49% of chemical oxygen demands in water sources could be effectively removed at both high flow rate and electric current due excessive generations of coagulants within short time. As reported by Muniasamy et al. (2022), electrocoagulation treatment could generate high formation of aluminium hydroxide coagulants at high flow rate and high electric current simultaneously. The study observed that the treated chemical oxygen demand levels are lower than 10 mg/L due to high dissolution rate of sacrificial anode to form electrocoagulation flocs (Muniasamy et al., 2022). A study conducted by Bun et al. (2022) reported that electrocoagulation treatment could also effectively reduce 92% of turbidity and 95% of colour with flow rate that ranged from 1 L/min to 2 L/min. The study noticed that these flow rates could provide an adequate time for adsorption process between coagulants and pollutants in electrocoagulation treatment system (Bun et al., 2022).

2.6 Past Studies on Electrocoagulation

Electrocoagulation treatment is an alternative undertaken in water processing due to its simplicity as a standalone water treatment system (Ghernaout, 2019; Ayyappa et al., 2021). In accordance with this statement, several conducted studies have attempted to treat various types of water sources, particularly peat water, brackish water, and seawater by utilizing electrocoagulation treatment.

2.6.1 Peat Water

According to Rusdianasari et al. (2019), peat bog drainage water that contains humic acid could be treated with electrocoagulation treatment. The study reported that electrocoagulation treatment could reduce 42% of total dissolved solids, 34% of biological oxygen demands, 89% of chemical oxygen demand, 55% of iron, and 90% of manganese from peat water. An electrocoagulation treatment system could also be utilized to remove 100% of colour, 93.35% of turbidity, 89.90% of chemical oxygen demands, 88.22% of total organic content, and 87.50% of total suspended solids (Rahman et al., 2020a). The study conducted by Rahman et al. (2020a) also reported that electrocoagulation treatment could achieve high pollutants removal efficiency at high electric current due to high generation of in-situ aluminum hydroxide coagulants. Another study performed by Rahman et al. (2020b) also found that continuous electrocoagulation treatment could be used to treat peat water. The study found that such treatment could also remove 100% of turbidity, 82% of total suspended solids, 81% of chemical oxygen demand, 97% of total organic carbon, and 100% of colour from peat water sources. Moreover, the study also noticed that high removal efficiency of pollutants is attainable at long treatment times. This is possibly due to such conditions providing an adequate time for the separation of pollutants from water sources with the aid of adsorption process (Rahman et al., 2020b).

A study attempted by Rahman et al. (2020c) also suggested that electrocoagulation treatment of peat water needs to be implemented with a reliable filtration system. The study reported that such conditions could effectively reduce 98% of chemical oxygen demand, 92% of total organic carbon, 97% of turbidity, and 99% of colour from peat water (Rahman et al., 2020c). In 2021, a study performed by Rahman et al. (2021) observed that electrocoagulation treatment system with solar-powered

energy could be installed for peat water treatment. The study reported the installation of solar-powered energy on batch and continuous electrocoagulation treatment system could effectively reduce 19% and 46% of water turbidity respectively (Rahman et al., 2021b).

2.6.2 Seawater

Seawater is generally known as a complex water solution that covers 70% of the earth surface (Abujazar et al., 2017). According to Ishika et al. (2018), seawater is also known as a water source that has salinity levels being more than 35,000 mg/L which is primarily constituted of sodium and chloride ions. To date, several published studies in the literature had treated seawater sources with electrocoagulation treatment. A study conducted by Al-Raad et al. (2019) found that electrocoagulation could reduce 91% of total dissolved solids, 93% of chloride, 92% of bromide, and 90% of sulphate from saline water. The study also reported that such efficiencies could only be attained with pH levels that ranged from 5 to 9 due to disintegration of aluminimum hydroxide coagulants at pH of 10 (Al-Raad et al., 2019).

A similar observation had been reported by Zhang et al. (2019) when the study employed electrocoagulation treatment on seawater. The study observed that this treatment system could effectively reduce 60.7% of silica from seawater with a salinity level of 34,000 mg/L. This also indicates that electrocoagulation could be utilized as pretreatment prior to the reverse osmosis system especially reducing the effects of silica on membrane fouling issues (Zhang et al., 2019). Despite seawater being considered the most corrosive natural environment, electrocoagulation could be utilized to reduce water hardness particularly magnesium and calcium (Abdulkarem et al., 2017), salts ions (Al-Raad et al., 2019), and silica (Zhang et al., 2019) in the forms of electrocoagulation flocs. Furthermore, electrocoagulation could also be integrated with

reverse osmosis system for the abatement of membrane fouling issues (Hakizimana et al., 2017; Zhang et al., 2019; Dayarathne et al., 2020).

2.6.3 Brackish Water

Brackish water is known as a water source that constitutes salinity levels between fresh and marine water that is commonly found within estuaries regions (Agha et al., 2018). Brackish water could also be found as groundwater sources which are formed in deep aquifers and also contain high levels of minerals (Honarparvar et al., 2019). In 2019, Zhang et al. (2019) had utilized electrocoagulation treatment in order to treat brackish water with 11,333 mg/L of salinity levels. The study found that electrocoagulation treatment could effectively reduce 90.2% of silica from brackish water. Additionally, the study observed high reduction efficiency of silica in alkaline brackish water, and this is due to the high dissolution of aluminium ions from anode electrodes that subsequently bind to hydroxides ions to form high yield of aluminium hydroxides coagulants (Ghernaout, 2019). The reduction of silica from brackish water sources signified that electrocoagulation treatment could be utilized as pre-treatment prior to the reverse osmosis system in order to prevent membrane fouling issues (Zhang et al., 2019).

2.7 Water Quality Analysis

Malaysia Environmental Quality Act (EQA) 1974 aims for the prevention, abatement, control of pollution, and enhancement of the environment in the country (Department of Environment, 2017; Economic Planning Unit, 2018). Under this legislation, any water treatment process needs to abide by the National Water Quality Standard (NWQS) in Malaysia as imposed by the Department of Environment Malaysia (Praveena et al., 2018). Several studies related to electrocoagulation treatment had

conducted water quality analysis by comparing investigated water parameters to the National Water Quality Standard (NWQS) in Malaysia as shown by **Table 2.1**.

Table 2.1: National Water Quality Standards (NWQS) in Malaysia (Department of Environment, 2020)

Parameter	Unit	Class					
		I	IIA	IIB	III	IV	V
Ammoniacal Nitrogen	mg/L	0.1	0.3	0.3	0.9	2.7	>2.7
Biochemical Oxygen Demand	mg/L	1	3	3	6	12	>12
Chemical Oxygen Demand	mg/L	10	25	25	50	100	>100
Dissolved Oxygen	mg/L	7	5-7	5-7	3-5	<3	<1
pH	-	6.5-8.5	6-9	6-9	5-9	5-9	-
Colour	TCU	15	150	150	-	-	-
Electrical Conductivity	S/cm	1,000	1,000	-	-	6,000	-
Floatable	-	N	N	N	-	-	-
Odour	-	N	N	N	-	-	-
Salinity	mg/L	500	1,000	-	-	2,000	-
Taste	-	N	N	N	-	-	-
Total Dissolved Solids	mg/L	500	1,000	-	-	4,000	-
Total Suspended Solids	mg/L	25	50	50	150	300	300
Temperature	^{o}C	-	Normal + 2°C	-	Normal + 2°C	-	-
Turbidity	NTU	5	50	50	-	-	-
Faecal Coliform**	count/100mL	10	100	400	5000 (20000)a	500 (2000)a	-
Total Coliform	count/100mL	100	5,000	5,000	50,000	50,000	>50,000
Iron	mg/L	<1	1	1	1	>1	>1

Notes:
N: No visible floatable materials or debris, no objectional odour or no objectional taste
*: Related parameters, only one recommended for use
**: Geometric mean
a: Maximum not to be exceeded

The main water parameters which had been investigated with electrocoagulation treatment are turbidity, colour, total suspended solids, chemical oxygen demands, and heavy metals, particularly iron, lead, and cadmium. A study performed by Kasmuri et al. (2021) effectively utilized electrocoagulation treatment in order to remove iron content from surface water. When electrocoagulation treatment is employed, the treated iron levels reduced from 2.75 mg/L to 0.92 mg/L and the treated surface water was deemed suitable for domestic consumption in terms of iron levels

only as shown in **Table 2.1**. Rahman et al. (2020a) also attempted to treat peat water sources in Sarawak which was applicable for domestic consumption in Malaysia by utilizing batch electrocoagulation treatment. The study conducted by Rahman et al. (2020a) effectively obtained 1 NTU of turbidity, 5 mg/L of chemical oxygen demand (COD), 0 TCU of colour, pH of 7, and 1 mg/L of total suspended solids (TSS) as well as found that the treated peat water has meet Malaysian Class I standard in NWQS.

Rahman et al. (2020b) also found that continuous electrocoagulation treatment of peat water could achieve 0 NTU, 2 mg/L of TSS, 12 mg/L of COD, 0 TCU of colour, and a pH of 7. The study reported that the treated peat water complied with the Malaysian Class I standard in NWQS (Rahman et al., 2020b). The combination of electrocoagulation and filtration system also effectively from peat water sources by attaining 1 NTU of turbidity, 1 mg/L of COD, 1 TCU of colour, and 0.001 mg/L of iron as informed by Rahman et al. (2020c). The study also observed that the treated peat water complied with Malaysian Class I standards in NWQS and was suitable for domestic consumption as in **Table 2.2**.

Table 2.2: Water Classifications (Department of Environment, 2020)

Class	Uses
Class I	Conservation of natural environment. Water Supply 1 – Practically no treatment is necessary Fishery I – Very sensitive aquatic species
Class IIA	Water Supply II – Conventional treatment required. Fishery II – Sensitive aquatic species
Class IIB	Recreational use with body contact
Class III	Water Supply III – Extensive treatment required. Fishery III – Common of economic value and tolerant species particularly livestock drinking
Class IV	Irrigation
Class V	None of the above

Water classification in NWQS is categorized into several classes particularly Class I, Class II A, Class II B, Class III, Class IV, and Class V as shown in **Table 2.2**. The water classification that falls under Class I is deemed suitable for domestic

consumption in Malaysia because this water will no longer require further treatment and could be utilized for a clean water supply. As reported by Rahman et al. (2020a), Rahman et al. (2020b), and Rahman et al. (2020d), electrocoagulation treatment could also be utilized to treat peat water which is considered suitable for domestic consumption in Malaysia.

2.8 Energy Operating Cost Analysis

Energy operating cost is defined as the evaluation of electrocoagulation's viability in terms of energy consumption in water treatment (Garcia-Segura et al., 2017). In electrocoagulation, the amount of electrical energy consumed per cubic meter of treated water also defined as specific electrical energy consumed *(SEEC)* in electrocoagulation and is calculated by using **Equation 2.4** (Rahman et al., 2020a).

$$SEEC(kWh/m^3) = \frac{VIT}{Q} \quad \textbf{(2.4)}$$

Where *SEEC* refers to specific electrical energy consumption (kWh/m^3), *V* refers to voltage, *I* refers to the electric current (A), *T* refers to residence time (hours), and *Q* refers to volume (m^3). As shown by **Equation 2.4**, it is found that SEEC is directly proportional to the electric current and residence time in electrocoagulation. According to Shahedi et al. (2020), electrocoagulation obtained high SEEC is due to the high electric current as well as high residence time. The energy operating cost in electrocoagulation treatment is also associated with electrode material consumption *(EMC)* (El-Ashtoukhy et al., 2020) as shown in **Equation 2.5**.

$$EMC(kg/m^3) = \frac{ItM}{zF} \quad \textbf{(2.5)}$$

Where *EMC* refers to electrode material consumption (kg/m^3), *I* refers to electric current (A), *t* refers to residence time (s), *M* refers to the molecular weight of

metal (g/mol), Z refers to the number of electrons involved in the oxidation reaction, and F refers to Faraday's constant that valued at 96,485 C/mol. **Equation 2.5** shows that *EMC* is directly proportional to the electric current and residence time in electrocoagulation. As informed by Khorram and Fallah (2020), high electrode material consumption *(EMC)* could be attained at high electric current and residence time lead to high dissociation of metal ions from the sacrificial anode. The overall energy operating cost with electrocoagulation is calculated by utilizing **Equation 2.6** as adopted by Hashim et al. (2020).

$$EOC(RM / m^3) = a(SEEC) \times b(EMC) \quad \textbf{(2.6)}$$

Where *EOC* refers to energy operating cost (RM/m^3), a refers to the domestic electricity price (RM/kWh), *SEEC* refers to specific electrical energy consumed (kWh/m^3), b refers to the price of aluminium electrode material (RM/kg), and *EMC* refers to electrode material consumption (kg/m^3). Hashim et al. (2020) informed that energy operating cost evaluation with Faraday's law is necessary in order to determine its practicality in terms of energy consumption as well as coagulant delivery.

2.9 Adsorption Mechanisms in Electrocoagulation

This section aims to discuss the application of adsorption and kinetic modelling which are pertinent to electrocoagulation treatment system. The characteristics of electrocoagulation flocs that are essential in the confirmation of adsorption phenomenon with electrocoagulation treatment system is also presented in this section.

2.9.1 Adsorption Isotherm Model

The adsorption isotherm theorem is a model that evaluates the adsorption capacity of an adsorbent (Nakama, 2017). According to Al-Ghouti and Da'ana (2020), adsorption process is a phenomenon in which a multi-component fluid mixture is

attracted to the solid surface of the adsorbent through chemical or physical bonds. The Langmuir and Freundlich isotherm models are used in most adsorption isotherm theorem analyses because these models exhibit real adsorption of molecules and ions on the solid surface of metallic coagulants which is commonly limited to layers adsorption (Rasmey et al., 2018; Ezzati, 2020; Budhiary & Sumantri, 2021).

2.9.2 Langmuir Adsorption Isotherm

Langmuir adsorption theorem describes the equilibrium behaviours between adsorbate and adsorbent in which the adsorption phenomena are limited only to single molecular layer (Liu et al., 2019). There are several assumptions for the formulation of Langmuir isotherm models particularly (i) molecules bind to the adsorbent's surface with separate active sites, (ii) each site only adsorbs one molecule, (iii) uniform adsorbing surfaces, and (iv) no interaction between adsorbed molecules (Sahu & Singh, 2019). As informed by Al-Ghoutti and Da'ana (2020), Langmuir adsorption theorem is formulated by utilizing the general equation as adopted by several studies as shown by **Equation 2.7**.

$$q_e = \frac{q_{\max} K_L C_e}{1 + K_L C_e} \quad \textbf{(2.7)}$$

Where q_e refers to the equilibrium adsorption capacity (mg/g), K_L refers to the Langmuir constant that is related to the adsorption capacity (L/g), C_e refers to the concentration at equilibrium point (mg/g), and $q_{\max}$ refers to the maximum adsorption capacity of an adsorbent (mg/g). The Langmuir constant denotes as K_L refers to adsorption capacity (L/g) is be calculated to determine the separation factor in the

adsorption process as shown in **Equation 2.8** (Al-Ghoutti & Da'ana, 2020; Kalam et al., 2021).

$$R_L = \frac{1}{1 + K_L C_o} \quad \textbf{(2.8)}$$

Where R_L refers to the Langmuir separation factor, K_L refers to the Langmuir adsorption capacity (L/g), and C_o refers to the initial concentration of pollutants levels (mg/L). The Langmuir separation factor R_L is crucial in formulation of isotherm adsorption theorem to evaluate the adsorption capacity and theoretically predicts the adsorbent surface areas as well as the pore volume (Hu et al., 2018; Sahu & Singh, 2019; Akrawi et al., 2021). As reported by Upadhyay et al. (2021) and Al-Ghouti and Da'ana (2020), the Langmuir separation factor which denotes as R_L represents the shape of isotherms to be either unfavourable ($R_L > 1$), linear ($R_L = 1$), irreversible ($R_L = 0$), or favourable ($0 < R_L < 1$).

The Langmuir isotherm adsorption theorem model also possesses several advantages as reported by several studies in the literature. Kecili and Hussain (2018) in their study found the main advantage of Langmuir isotherm adsorption theorem model is to describe the monolayer adsorption between absorbate and adsorbents. Liu et al. (2019) also found that the Langmuir adsorption isotherm describes the equilibrium between an adsorbate and an adsorbent system in which adsorbate adsorption is limited to one molecular layer at or before a uniform equilibrium concentration is achieved. Even though the Langmuir adsorption theorem model is effective to describe adsorption phenomenon, several studies have also found some disadvantages with such model. Azizian and Eris (2021) reported that most

assumptions that underlie in Langmuir adsorption isotherm model seldom exist in real adsorption system.

2.9.3 Freundlich Adsorption Isotherm

Freundlich adsorption isotherm is a model that describes multilayer adsorption of molecules onto the adsorbent surfaces (Adeogun & Balakrishnan, 2017). The Freundlich model expression shows the heterogeneity of the molecule surface in terms of exponential distribution of active sites and their energies (Mu & Sun, 2019). The multilayer layer adsorption described by the Freundlich adsorption isotherm model also signifies a non-uniform distribution and affinity of molecules towards the heterogenous surface of the adsorbent (Kalam et al., 2021). In order to formulate Freundlich adsorption isotherm models, several studies have adopted **Equation 2.9** in order to describe the occurrence of multilayer adsorption (Adeogun & Balakrishnan, 2017; Ayub et al., 2020; Laskar & Hashisho, 2020).

$$q_e = K_f C_e^{\frac{1}{n_f}} \tag{2.9}$$

Where q_e refers to the amount of the solute adsorbed per unit weight of adsorbent (mg/g), C_e refers to the concentration of solute in bulk solution (mg/L), and K_f refers to the Freundlich constant that measures the adsorption capacity of the adsorbent (L/mg), and n_f refers to the empirical constant related to the heterogeneity of the adsorbent surface. The constant empirical particularly K_f and n_f are calculated from the slope and the intercept of the plot $\ln q_e$ against $\ln C_e$ as shown in **Equation 2.10** (Ayub et al., 2020).

$$\ln q_e = \ln K_f + \frac{1}{n_f} \ln C_e \tag{2.10}$$

The values of $\frac{1}{n_f}$ describes the adsorption process either favourable ($0.1 < \frac{1}{n_f} < 0.5$) or unfavourable when $\frac{1}{n_f}$ being more than two (Adeogun & Balakrishnan, 2017; Ehiomogue et al., 2022). Laskar and Hashisho (2020) informed that the Freundlich adsorption isotherm model also possesses several advantages and disadvantages. Unlike Langmuir, which is developed theoretically, Freundlich isotherm is categorized as an empirical model that is formulated based on the adsorption process that occurs in a real application derived from several experimental data (Ashoor et al., 2019; Laskar & Hashisho, 2020). Freundlich equations are frequently used in many industrial processes due to such model could represent nonlinear adsorption in a small range of adsorbate concentrations, have a straightforward mathematical application, and could describe the adsorption process on energetically heterogeneous surface adsorption sites (López-Luna et al., 2019). Although Freundlich adsorption isotherm is formulated based on an empirical model, this model also possesses drawbacks in terms of adsorbate concentration limitations. The Freundlich equation is limited only to a certain concentration due to such model could not predict the adsorption behaviour at high range of concentration. This observation has been discovered experimentally that the adsorption capacity varies with the amount of equilibrium adsorbate concentration as well as varies with concentration raised to the power $\frac{1}{n_f}$ until saturation point is reached (Mboyi et al., 2021).

2.9.4 Application of Langmuir and Freundlich Isotherm Models in Electrocoagulation

Several conducted studies in the literature have formulated both Langmuir and Freundlich Adsorption Isotherm Models in order to determine the adsorption mechanism for pollutants removal with electrocoagulation treatment as shown in **Table 2.3**.

Table 2.3: Application of Langmuir and Freundlich Adsorption Isotherm Models in Electrocoagulation Treatment

No.	Parameter	Langmuir			Freundlich			Remarks	References
		K_L (L/mg)	q_{max} (mg/g)	R^2	K_F (mg/g)	n	R^2		
1.	Lead	0.25	39.21	0.97	354.82	0.17	0.77	Monolayer adsorption	AlJaberi & Mohammed (2018)
2.	Total Nitrogen	0.00012	45,997	0.82	0.177	0.652	0.95	Multilayer Adsorption	Mohammadi et al. (2019)
3.	Fluoride	0.20	4,761	0.99	0.0012	0.62	0.95	Multilayer Adsorption	Chibani et al. (2019)
4.	Colour	0.02	1,000	0.99	22.80	1.04	0.99	Not limited monolayer adsorption	Bendaia et al. (2021)
5.	Colour	0.21	454.54	0.81	145.70	2.87	0.92	Multilayer Adsorption	Houssini et al. (2020)
6.	Colour	0.034	68.03	0.98	1.07	0.66	0.99	Not limited monolayer adsorption	Shaker et al. (2020)
7.	Colour	0.19	2,996	0.77	2,469	34.98	0.92	Multilayer Adsorption	Abdul Jalal (2022)
8.	Turbidity	0.86	49.40	0.83	28.62	5.31	0.92	Multilayer Adsorption	Abdul Jalal (2022)
9.	Chemical Oxygen Demand	0.40	291.6	0.80	170	8.01	0.92	Multilayer Adsorption	Abdul Jalal (2022)

2.10 Kinetic Modeling

The adsorption kinetic model is formulated to study details on adsorption rate as well as mass transfer mechanism. In order to evaluate and explain adsorption mechanism, several studies have utilized pseudo-first-order model to formulate kinetic datasets for a wide range of adsorption systems particularly from biomass to

nanomaterials as adsorbents whereas contaminants as the adsorbates (Revellame et al., 2020).

2.10.1 Pseudo-First Order Kinetic Model

According to Pooresmaeil and Namazi (2020), the pseudo-first-order model is known as the Lagrange rate equation. In this model, the rate of adsorption is calculated by plotting the difference between the amount of adsorbed adsorbate molecules on the adsorbents against the equilibrium residence time (Pooresmaeil & Namazi, 2020). As added by Lima et al. (2021), the pseudo-first-order model could be formulated with two forms particularly linear form and non-linear form to describe the adsorption of solutes on adsorbent following first-order mechanism as shown in **Equation 2.11**.

$$\frac{dq_t}{dt} = k_1(q_e - q_t) \qquad \textbf{(2.11)}$$

Where q_e refers to equilibrium adsorption capacity (mg/g), q_t refers to the adsorbate adsorbed onto adsorbent at time (mg/g), and k_1 refers to the rate constant per minute (min^{-1}).

2.10.2 Linear Pseudo-First Order Kinetic Model

The linear pseudo-first-order model is the main approach in order to determine kinetic parameters in adsorption process (Kajjumba et al., 2018). This model is formulated by plotting $log[q_e - q_t]$ against t in order to attain a linearized form (Ayub et al., 2020) as shown in **Equation 2.12**.

$$log[q_e - q_t] = -k_1 t + log\, q_e \qquad \textbf{(2.12)}$$

Where q_e refers to the amount of adsorbate adsorbed at equilibrium (mg/g), q_t refers to the amount of adsorbate adsorbed at a given time (mg/g), k_1 refers to the

reaction rate constant (min^{-1}), and t refers to time (min). These kinetic parameters are estimated based on the intercept of the best fit of the line particularly m = slope, b = intercept, k_1 = -m, and q_e = exp (b) (Simonič et al., 2020). In the linear form of the pseudo-first-order model, the left hands side of **Equation 2.12** becomes undefined once the equilibrium capacity q_e has been achieved with time being higher than zero (Kul et al., 2021).

2.10.3 Non-Linear Pseudo-First Order Kinetic Model

As compared to linear model, the non-linear pseudo first order model possesses better adequacy and accuracy to achieve realistic kinetics parameters (Marasović et al., 2017). According to Tan and Hameed (2017), non-linear modelling does not require an initial estimation of initial kinetic parameters because it could provide an accurate comparative assessment to determine the model that fits given kinetics datasets. As suggested by Revellame et al. (2020), the general objective function is defined as the sum of the squares of the differences between the experimental and predicted values of the response variables as shown in **Equation 2.13.**

$$\textit{Objective Function } (OF) = \sum_{i=1}^{n} \left(y_i - \hat{y}_i \right)^2 \qquad \textbf{(2.13)}$$

Where y_i refers to the experimental response for i^{th} observation, $\hat{y}_i$ refers to the predicted value of y_i, and n refers to the total number of data points. Wang and Guo (2020) reported that a perfectly fitted model to datasets would attain an objective function that equals zero and this indicates the kinetics parameters as equated in **Equation 2.14** are estimated through minimization of least square regression.

$$q_t = q_e (1 - \exp^{-k_t t}) \qquad \textbf{(2.14)}$$

Where q_e refers to measured values of equilibrium adsorbate concentration in the solids phase (mg/g), q_t refers to the amount of dye adsorbed (mg/g) at a time, k_1 refers to the rate constant of the pseudo-first-order kinetics (min^{-1}), and t refers to time (min). The non-linear pseudo first order models could provide an accurate estimation of kinetic model parameters due to the fact that such model able to describe the whole adsorption process instead of modelling the initial stage of adsorption (Jasper et al., 2020)

2.10.4 Evaluation of Model Validity

Model validation is an evaluation step to determine the accuracy of formulated models in representing an adsorption process (Muttakin et al., 2018). The validity of the formulated adsorption model could be assessed based on the error function (Davoodi et al., 2019). The coefficient of determination (R^2) test is performed to assess the suitability of formulated adsorption models with various forms as shown in **Equation 2.15** (Ayub et al., 2020; Wang & Guo, 2020).

$$R^2 = \frac{\left(q_{e,\exp} - q_{e,model}\right)^2}{\sum\left(q_{e,\exp} - \overline{q_{e,model}}\right) + \sum\left(q_{e,\exp} - q_{e,model}\right)^2} \quad \textbf{(2.15)}$$

Where R^2 refers to the regression coefficients, $q_{e,\exp}$ refers to the experimental values of adsorbate concentration at equilibrium (mg/g), $q_{e,model}$ refers to the modelled values of adsorbate concentration at equilibrium. As informed by Delgado et al. (2019)**,** the R^2 test is conducted in adsorption modelling studies that compare both q_e parameters for experimental and modelled data. Some studies in published literature suggested that the values of R^2 being less than 0.5 indicate a weak relation between

the independent variable and response variable, whereas $0.5 < R^2 < 0.75$ signifies an inaccuracy of formulated model (Ayub et al., 2020; Revellame et al., 2020). The formulated adsorption model is valid when the values of R^2 are higher than 0.75 which signifies a good fit between experimental and modelled data (Rahman et al., 2020d).

2.10.5 Application of Pseudo-First Order Kinetic Model in Electrocoagulation

The pseudo-first-order model could be formulated to determine the reaction rate constant for pollutants reduction from water sources. A study conducted by El-Hosiny et al. (2018) found that a pseudo-first-order kinetic model is formulated to evaluate the reaction rate constant for the reduction of colour with electrocoagulation from water source valued at 0.09 min^{-1}. The study also found that formulated kinetic model correlated well with the experimental data and this is due to the regression value being higher than 0.93. This signifies that colour reduction follows a pseudo-first-order kinetic model as well as the adsorption follows both physical and chemical adsorption (El-Hosiny et al., 2018). A similar study conducted by Abakedi et al. (2019) also discovered that the reduction of colour from experimental data could be fitted well with pseudo-first-order model with high regression value of 0.99. From the formulated kinetic model, the study attained a rate constant at 0.71 min^{-1} with an adsorption capacity of 14.04 mg/g to reduce colour levels from water sources (Abakedi et al., 2019). In the formulation of pseudo-first order kinetic models, these studies emphasized model validation in terms regression coefficient to obtain an accurate estimation of reaction rate constant in electrocoagulation treatment (Chen et al., 2018; El-Hosiny et al., 2018; Abakedi et al., 2019).

2.11 Electrocoagulation Flocs Analysis

In accordance with the adsorption mechanism in electrocoagulation treatment, electrocoagulation flocs analysis needs to be conducted to confirm the occurrence of such phenomenon. This section describes and explains the main approach to execute electrocoagulation flocs analysis.

2.11.1 Electrocoagulation Flocs

Electrocoagulation flocs are generated due to redox reaction between sacrificial anode and cathode electrodes as depicted in **Figure 2.3**. In addition, electrocoagulation flocs are formed spontaneously during redox reactions (Liu et al., 2018). According to Yu et al. (2018), electrocoagulation flocs have compact amorphous shapes and weak crystalline structure.

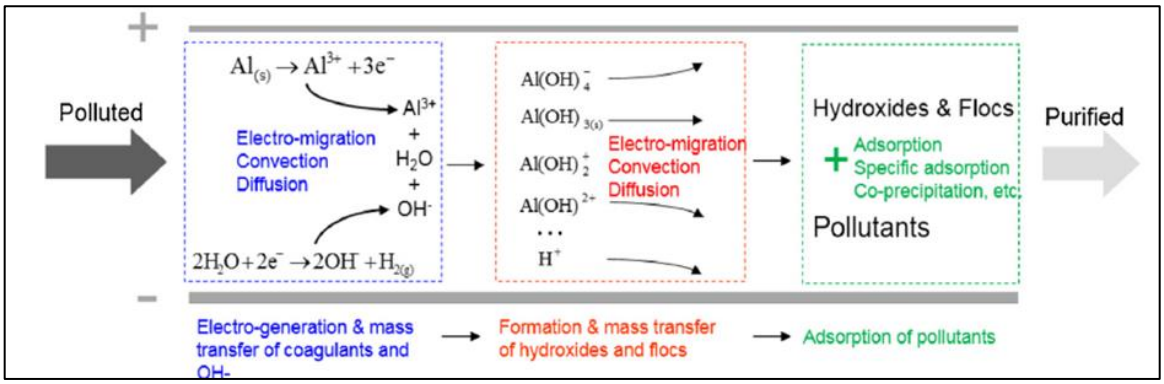

Figure 2.3: Formation of Electrocoagulation Flocs (Liu et al., 2018)

As added by Ghernaout (2019), electrocoagulation flocs are microscopic coagulants that have high adsorption capacity owing to large surface areas could provide easy targets for the adsorption of pollutants in water sources. The nature of electrocoagulation flocs includes formation of nanocrystalline structures that are porous and fragile and evolving into different forms to achieve high adsorption capacity (Chan et al., 2019). As reported by Shahedi et al. (2020), the mass transfer of flocs in electrocoagulation is primarily governed by hydrolysis reaction that generates bubbles

which subsequently aids in the precipitation of flocs and suspended pollutants in water sources.

2.11.2 Electrocoagulation Flocs Analysis with Energy Dispersive X-Ray

Energy Dispersive X-Ray (EDX) is an analytical method that is adopted to perform chemical characterization by focusing a beam of high-energy charged particles on electrocoagulation flocs shown in **Figure 2.4** (Colpan et al., 2018).

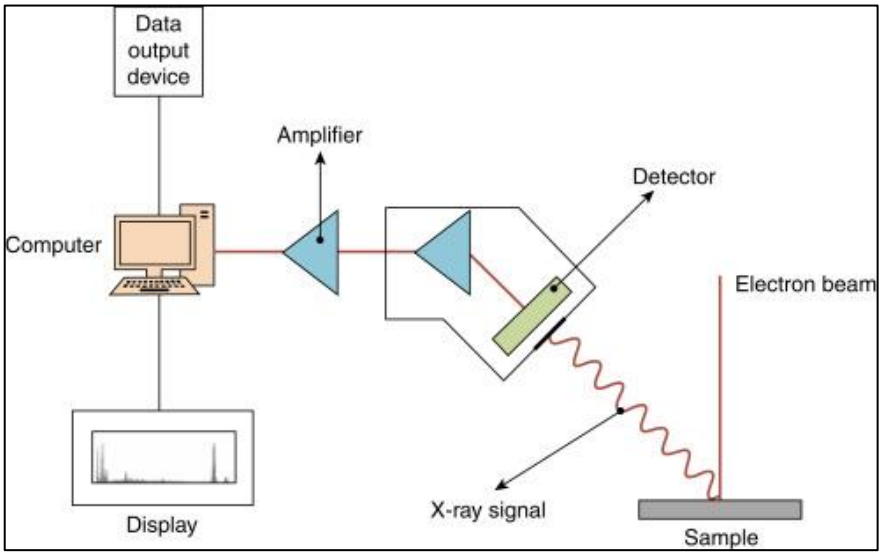

Figure 2.4: Energy Dispersive X-Ray Spectroscopy (Colpan et al., 2018)

In EDX analysis, a high-energy beam of charged particles such as electrons, protons, or an X-Ray beam is directed into the electrocoagulation flocs samples in order to induce the emissions (Gniadek & Dąbrowska, 2019). According to Palanisamy et al. (2020), the EDX analysis is a reliable method in determining the correlation between compositions of electrocoagulation flocs with pollutants reduction efficiency. The study conducted by Palanisamy et al. (2020) also discovered that electrocoagulation treatment could reduce 97% of colour and 72% of chemical oxygen demand from water sources containing triazine-substituted reactive dyes. The detection of various minerals on samples is due to the energy differential between higher and lower energy shells are then emitted as an X-Ray (Torres-Rivero et al., 2021).

2.12 Statistical Model

Statistical analysis is a technique that examines data information in order to derive useful insights based on statistical concepts (Karimifard & Alavi, 2018). According to Mishra et al. (2019), statistical analysis is critical for acquiring reliable information which is practically based on assumptions and method constraints. Statistical analysis is carried out in order to identify data trends through mathematical correlations by adopting response surface methodology with a central composite design approach (AlJaberi, 2019). As reported by Tones et al. (2020), design studies and research interpretations could utilize the statistical analysis method because such method defines the correlation of variables with the analysis of variance. This method includes the elimination of bias occurrence since most of the collected data are analyzed through numerical analysis and subsequently derived in the form of regression model equations (Oden, 2020). The conclusions obtained from statistical analysis are also important in facilitating decision-making as well as formulating recommendations based on the collected data (Follmann et al., 2020). Several terms that pertinent for statistical model analysis are shown in **Table 2.4**.

Table 2.4: Key Terms in Statistical Analysis

No.	Terms	Definition	References
1.	Experimental Domain	An experimental field is defined by the minimum and maximum limits of the variables being investigated in experiments.	Manilal & Soloman (2020)
2.	Experimental Design	It is a collection of experiments defined by a matrix comprised of various levels of investigated variables. Additionally, this design also defines specific set of investigated variables need to be executed experimentally in order to obtain real responses.	Selmane et al. (2020)
3.	Independent Variables	Experimental variables that could be manipulated independently of each other.	Abbasi et al. (2020)
4.	Levels of Variables	This refers to different levels of a variable at which the experiment needs to be conducted.	Hamid et al. (2020)
5.	Dependent Variables	This refers to the measured values of responses from conducted experiments.	Apshankar & Goel (2020)
6.	Residual	This refers to the difference between the modelled and experimental results in which low residual indicates good mathematical which fitted to experimental data.	Pandey & Thakur (2020)

There are six key terms particularly experimental domain, experimental design, independent variable, levels of variables, dependent variables, and residual which constituted in development of a statistical analysis model. In order to examine the correlation between variables, it is utilized develop response surface methodology to develop a statistical model that has high adequacy and accuracy for optimization (Bajpai et al., 2020).

2.12.1 Response Surface Methodology

Response Surface Methodology (RSM) is a collection of mathematical and statistical methods that design and develop experimental models based on the interactions of parameters for optimizations (Acharya et al., 2018). There are six consecutive steps for response surface methodology to develop and formulate statistical models which are (i) screening and selection of independent factors and responses, (ii) experimental design strategy, (iii) running the experiments and obtaining results, (iv) experimental data fitting to the mathematical model, and (v) model validation, and (vi) model optimization (Anfar et al., 2020).

2.12.2 Screening and Selection of Independent Factors and Responses

It is practically impossible to examine numerous variables in a single process due to such application could negatively affect the outcomes of studied responses (Yolmeh & Jafari, 2017). As reported by Bhatti et al. (2017), the development of statistical model with response surface methodology is done by selecting both dependent and independent variables that have significant effects on each other. It is also necessary to conduct a preliminary screening of experiments with literature review so that the major variables are well identified in order to obtain a reliable statistical

model (Bhatti et al., 2017). The ranges of selected factors should be selected reasonably and this is due to a random selection of variables that could result in uninformative and unreliable outcomes (Karimifard & Alavi, 2018).

2.12.3 Experimental Design Strategy

The next step in developing a statistical analysis model is to obtain the possible response outcomes through an experimental design strategy. The CCD model provides similar information to three-level fractional factorial design (FFD) that only requires minimal number of experimental runs as well as obtains high accuracy of formulated polynomial equations (Yolmeh & Jafari, 2017). To develop a statistical model with CCD, three types of points need to be considered which are center points, axial points, and cube points. These points are crucial to determining the total number of experiments needed as shown by **Equation 2.16** (Ferreira et al., 2018).

$$\textit{Total Number of Experiments} = 2^k + 2k + C_o \qquad \textbf{(2.16)}$$

Where k refers to the number of factors, 2^k refers to cubic run, $2k$ refers to the axial runs, and C_o refers to the center point runs. In this case, the values that are attributed to each variable need to be assigned properly with five levels ($-\alpha$, -1, 0, +1, $+\alpha$) and could be obtained by conducting preliminary experiments, literature reviews, or consideration of the acquired equipment limitation (Ferreira et al., 2018; Politis et al., 2017). The accuracy of the fitted quadratic model with central composite design is also dependent on the five levels of variables that are efficient in the estimation of first and second-order terms (Hakizimana et al., 2017; Karimifard & Alavi, 2018). As reported by Karimifard and Alavi (2018), α in CCD model indicates the number of variables in a study is calculated by using **Equation 2.17**.

$$\alpha = 2^{(k-p)/4} \quad \textbf{(2.17)}$$

The values of α in CDD could be automatically generated in Design Expert software in which two variables are defined at 1.41, three variables are 1.68, and four variables are 2.00 (Karimifard & Alavi, 2018). Several conducted studies in published literature adopted the CCD model to optimize several process variables by formulating a second-order polynomial regression equation (Khorram & Fallah, 2018; Murdani et al., 2018; Oden, 2020) as shown by **Equation 2.18.**

$$S = \alpha_o + \sum_{i=1}^{k} \alpha_i x_i + \sum_{i=1}^{k} \alpha_{ii} x_i^2 + \sum_{i.j=1, j \neq i}^{k} \alpha_{ij} x_i x_j \quad \textbf{(2.18)}$$

Where S refers to response, α_o refers to the average of responses, α_i, α_{ii}, and α_{ij} refers to coefficient. The second term, $\sum_{i=1}^{k} \alpha_i x_i$ refers to linear interaction effect, the third term, $\sum_{i=1}^{k} \alpha_{ii} x_i^2$ refers to higher order interaction, and the fourth term, $\sum_{i.j=1, j \neq i}^{k} \alpha_{ij} x_i x_j$ refers to dual interaction effects. These quadratic terms are also essential in polynomial functions to determine a critical point (maximum, minimum, or saddle) (Roy et al., 2018). All the studied variables are carried out at three-factor levels to attain an accurate quadratic term in the polynomial model (Azizi et al., 2021).

2.12.4 Running the Experiments and Obtaining Results

Design Expert software is used to generate the number of required experiments runs. This stage is usually conducted after selecting the right experimental design as well as confirming the variables constraint values (Yolmeh & Jafari, 2017). The mathematical models should also fit actual experimental data (Karimifard & Alavi,

2018). It is necessary to fit in the actual experimental results in order to attain high validity of the developed statistical model (Murdani et al., 2018).

2.12.5 Experimental Data Fitting to the Mathematical Model

There are two steps in fitting the obtained experimental data to the mathematical models which are (i) coding of experimental data and (ii) determination of regression coefficient. These steps are important to evaluate the deviation between the experimental and mathematical models with a maximum percentage difference at 10% (Acharya et al., 2018). As added by Yu et al. (2018), coding of experimental data consists of transforming each real value onto coordinates inside a scale with dimensionless values particularly -1, 0, and +1 to ensure proportional localization within the experimental space. The coded data will be fitted into the mathematical model by adopting least squares methods in which the equations for experimental designs are mostly incorporated in Design Expert software (Perperoglou et al., 2019).

In evaluating a mathematical model, a study could not solely depend on R^2 values to determine the validity of the formulated quadratic model. The R^2 values should be evaluated along with the residual plots to determine whether the formulated mathematical is biased or unbiased towards the experimental data (Igwegbe et al., 2019). The adjusted R^2 is usually lower than the actual R^2 due to the comparative explanatory power of mathematical models that acquires reduction of variables (Piepho, 2019). In validation of mathematical models, the regression values need to be reported in terms of actual R^2, adjusted R^2, and predicted R^2 and these values are assumed to be valid when the R^2 being higher than 0.75 (Rahman et al., 2020d).

2.12.6 Model Validation

The evaluation of data variation in ANOVA is conducted by investigating the mean dispersion as described in deviation evaluation (d_i) that each observation (y_{ij}) is noted with the square deviation (Anders, 2017) as shown in **Equation 2.19**.

$$d_i^2 = \left(y_{ij} - \overline{y}\right)^2 \tag{2.19}$$

The sum of the squares for all deviation observed with the responses is known as the total sum of squares *(SS_{tot})*. The total sum of squares, as in **Equation 2.20**, is the combination of both sum of squares regression *(SS_{reg})* and the sum of squares due to residuals *(SS_{res})* (Shamaei et al., 2018).

$$SS_{tot} = SS_{reg} + SS_{res} \tag{2.20}$$

The sum of squares due to residuals also constituted a total addition of both sums of squares due to pure error *(SS_{pe})* and the sum of squares due to the lack of fit *(SS_{lof})* as shown in **Equation 2.21** (Hendaoui et al., 2018). Afterward, the mathematical model is further validated in terms of media of the squares as shown in **Table 2.5**.

$$SS_{res} = SS_{pe} + SS_{lof} \tag{2.21}$$

Table 2.5: Mathematical Model Validation Source (Acharya et al., 2018; Hendaoui et al., 2018; Shamaei et al., 2018)

Variation Source	Sum of Squares	Degree of Freedom	Media of the Squares
Regression	$SS_{reg} = \sum_i^m \sum_j^{n_i} \left(\hat{y}_i - \bar{y}\right)^2$	$p-1$	$MS_{reg} = \frac{SS_{reg}}{p-1}$
Residuals	$SS_{res} = \sum_i^m \sum_j^{n_i} \left(\hat{y}_{ij} - \hat{y}_i\right)^2$	$n-p$	$MS_{res} = \frac{SS_{res}}{n-p}$
Lack of fit	$SS_{lof} = \sum_i^m \sum_j^{n_i} \left(\hat{y}_i - \bar{y}_i\right)^2$	$m-p$	$MS_{lof} = \frac{SS_{lof}}{m-p}$
Pure Error	$SS_{pe} = \sum_i^m \sum_j^{n_i} \left(y_{ij} - \bar{y}_i\right)^2$	$n-m$	$MS_{pe} = \frac{SS_{pe}}{n-m}$
Total	$SS_{tot} = \sum_i^m \sum_j^{n_i} \left(y_{ij} - \bar{y}\right)^2$	$n-1$	-

Where n_i refers to the number of observations, m refers to the total number of levels in the design, p refers to the number of model parameters, $\hat{y}_i$ refers to an estimated value by the model for level I, $\overline{y}$ refers to an overall media, y_{ij} refers to replicates performed in each level, $\overline{y_i}$ refers to media of replicates performed in the same set of experimental conditions. As tabulated in the third column of **Table 2.5,** the number of degrees of freedom for the sources of variations based on the p refers to the number of coefficients of the mathematical model, n represents the number of total observations, and m refers to the numbers of levels being used for the study.

Alenyorege et al. (2020) in their study reported that the formulated mathematical model is defined as well-fitted to the experimental data when it shows a significant regression and non-significant lack of fit. The mathematical model needs to be examined in terms of the F-value coefficient which is calculated as the quotient of the mean square and residual mean square. Bajpai et al. (2020) also reported that F-value is an essential term that determined the probability of p-value. As added by Bajpai et al. (2020), p-value is defined as the level of marginal significance within a statistical hypothesis test. This value also represents the occurrence probability of a given event in which the p-value being less than 0.05 indicates the formulated mathematical model is statistically significant in the study (Thakur, 2020).

2.12.7 Model Optimization

Model optimization is the final stage in RSM which involves the adjustment of independent variables in order to determine the suitable factor levels that lead to the most desired outcomes (Balaram & Chennakeshava, 2018). It is crucial to validate the formulated mathematical model in RSM before confirming the optimal conditions with numerical optimization approach (Zaied et al., 2020). The outcomes from the

mathematical model prediction were compared to the actual experimental data under optimized conditions (Igwegbe et al., 2021). In generating the surface response with Design Expert, the critical point of the graph is characterized as maximum, minimum, or saddle point and could be calculated with differentiation of polynomial mathematical models and equates it in terms of zero value (Li et al., 2021).

2.13 Summary

Coastal peatland in Sarawak is endowed with vast availability of brackish peat water sources. Although brackish peat water is abundantly available in some rural coastal areas, this water source is currently underutilized as a clean water supply owing to excessive salinity levels. It is reported that electrocoagulation treatment system possesses several advantages such as zero chemical addition, low operating cost, easy maintenance, high pollutants reduction efficiency, and the treated water sources are comparable to the water standards. This treatment system also produces in-situ aluminium hydroxide coagulants which subsequently aid in the pollutants reduction in water sources with an adsorption process. Furthermore, the adsorption process with electrocoagulation treatment system is effective for high pollutants reduction owing to the in-situ coagulants having high adsorption capacity as well as generating insoluble flocs. The application of electrocoagulation on brackish peat water treatment is unknown despite the system is effective on peat water, brackish water, and seawater sources. This literature review reported that there is lack of study in investigating the salinity reduction of brackish peat water with adsorption process in electrocoagulation treatment system.

CHAPTER 3

RESEARCH METHODOLOGY

3.1 Introduction

This chapter presents and discusses stages of methodology in order to achieve the aim and objectives of this study, as depicted in **Figure 3.1**.

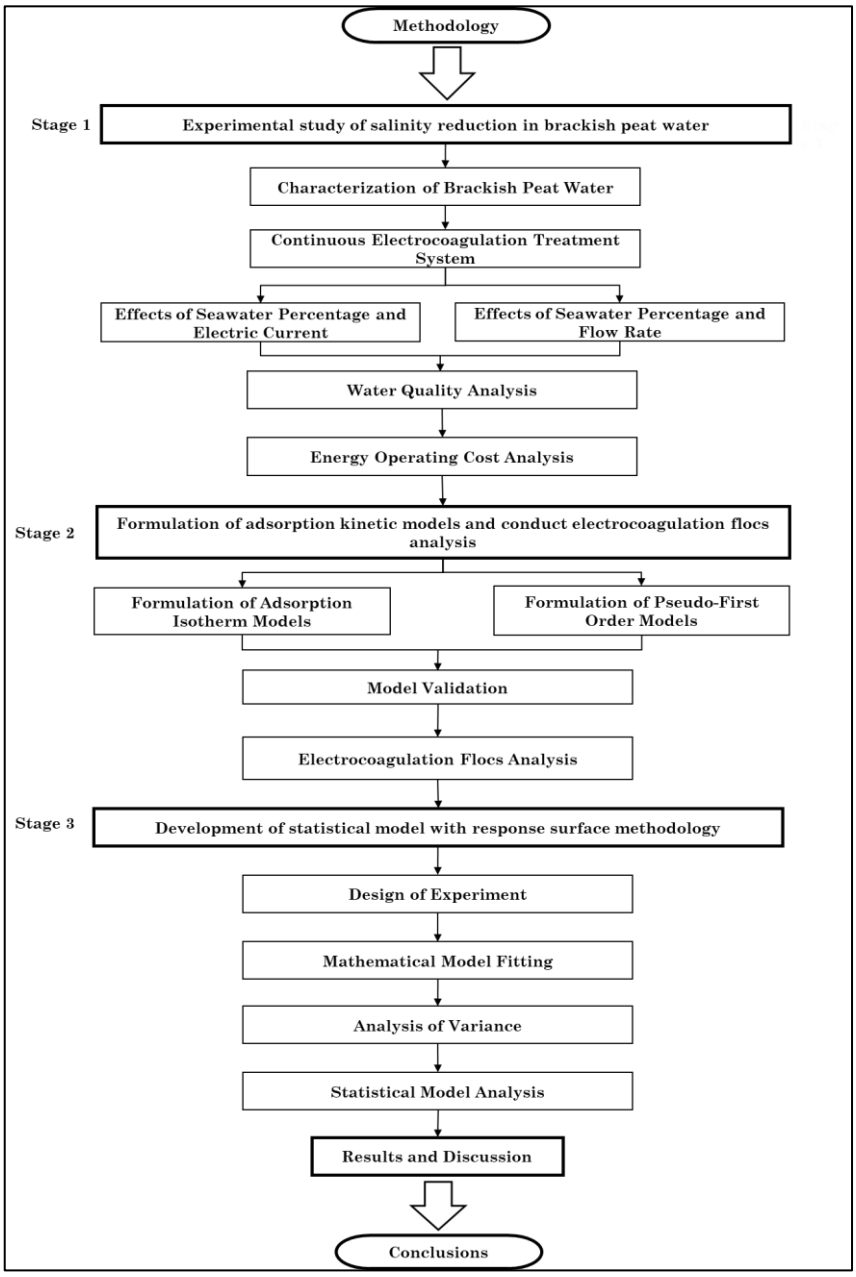

Figure 3.1: Stages in Research Methodology

This study devised three main stages of methodology which were aligned to the objectives as stated in **Chapter 1**. The first stage associated with Objective 1 involved the analysis of salinity reduction in brackish peat water with continuous electrocoagulation treatment. The experimental works included brackish peat water characterization, investigated the effects of seawater percentage, electric current, and flow rate on salinity reduction efficiency, water quality analysis, and energy operating cost evaluation with Faraday's law. The second stage that linked to Objective 2 was executed to formulate adsorption isotherm and kinetic order models as well as to conduct electrocoagulation flocs analysis. Moreover, this stage calculated the maximum adsorption capacity and adsorption rate constant that were related to salinity reduction in brackish peat water. The third stage that referred to Objective 3 was performed to develop statistical model with response surface methodology (RSM). A detailed discussion for each respective stage was presented as follows.

3.2 Stage 1: Experimental Study of Salinity Reduction in Brackish Peat Water

This section aims to present and discuss the practicality of utilizing a continuous electrocoagulation system to reduce salinity levels in brackish peat water. Initially, brackish peat water samples were collected from an identified location in Sarawak coastal rural areas. Then, the samples were subjected to continuous electrocoagulation treatment to study the effects of seawater percentage, electric current, and flow rate on salinity reduction efficiency. Next, the study compared the water quality of untreated and treated brackish peat water to the National Water Quality Standard (NWQS) as classified by the Department of Environment in Malaysia. This study evaluated the effects of electric current and water flow rate on energy operating cost with Faraday law equations.

3.2.1 Characterization of Brackish Peat Water

The brackish peat water samples in this study were collected from Kampung Metang Terap, Lundu, Kuching, Sarawak, Malaysia. The study location was known as coastal rural areas due to such region constituted by peat swamps and a coastline environment. Kampung Metang Terap is located 8.0 km away from the mouth of Batang Kayan River as well as surrounded with low-lying peatlands as depicted in **Figure 3.2**.

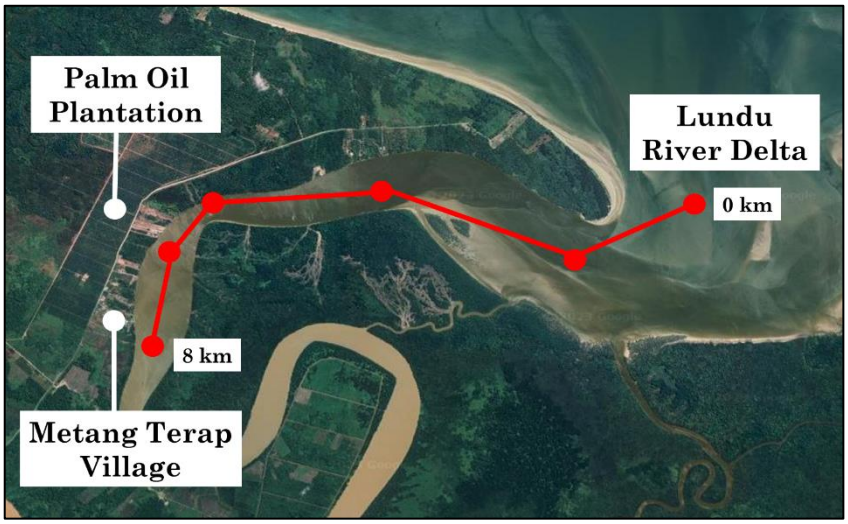

Figure 3.2: Kampung Metang Terap in Lundu district (Google Map, 2022).

Kampung Metang in Lundu district located within coastal peatlands areas near to river delta between 1° 41' 18.33" N latitude and 109° 52' 51.6864"E longitude. As reported by Edward (2020), some residents in Metang Terap village were cultivating palm oil plantations because this region has vast availability of peat soil. To date, Kampung Metang Terap has experienced water supply issues, owing to its location in rural areas far from Lundu town. The Sarawak state government launched the Sarawak Alternative Water Supply (SAWAS) programme to temporarily mitigate water supply issues. Some coastal rural areas in Lundu were supplied with gravity feed and rainwater harvesting systems and this is due to such methods being known to be preferable for scattering populations in coastal rural areas (Jabatan Bekalan Air Luar

Bandar, 2022). A study visit conducted in Kampung Metang Terap found vast availability of brackish peat water sources that contained complex mixture of yellowish-brown to black colored compounds as shown in **Figure 3.3**.

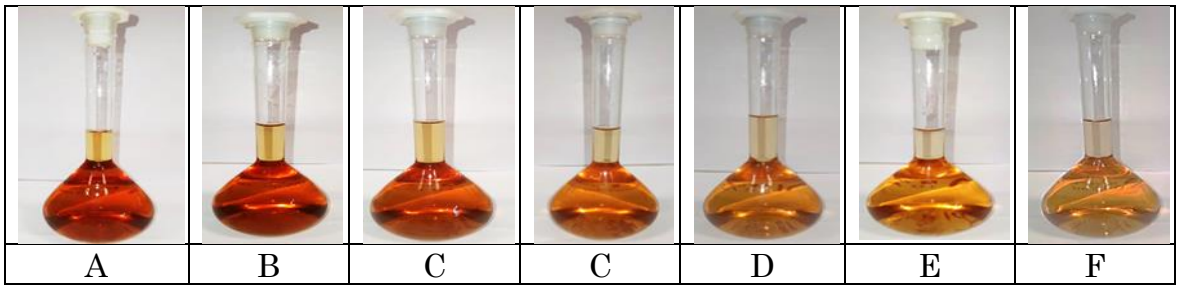

Figure 3.3: Brackish peat water from Kampung Metang Terap in Lundu at Varied Seawater Percentage (A) 0%, (B) 10%, (C) 30%, (D) 50%, (E) 70%, (F) 80%, and (G) 90%.

The seawater percentage in brackish peat water was determined based on mixing volume of seawater and peat water sources as shown in **Table 3.1**. The source of seawater was also collected within the vicinity of Kampung Metang Terap. Brackish peat water samples were collected for laboratory analysis in order to analyze the salinity levels with Hanzhan EZ-9910 salinity meter. In this study, 50 mL of brackish peat water samples were filled into a small beaker prior to salinity level analysis with salinity meter. An average reading was taken as result by conducting five readings for each sample. The salinity meter electrodes were washed with distilled water in order to remove impurities. In this study, the salinity levels were measured according to the American Public Health Association (APHA) 2520 that specifically aim for examination of water and wastewater (Sonda et al., 2022). This standard outlined salinity measurement based on electrical conductivity and water density with electrometric method.

Table 3.1: Formation of Brackish Peat Water from Intrusion of Seawater into Peat Water Sources

No.	Volume of Peat Water (mL)	Volume of Seawater (mL)	Volume of Brackish Peat Water (mL)	Seawater Percentage in Brackish Peat Water (%)	Salinity Levels (mg/L)
1.	1,000	0	1,000	0	317
2.	900	100	1,000	10	2,430
3.	700	300	1,000	30	4,507
4.	500	500	1,000	50	6,877
5.	300	700	1,000	70	9,650
6.	200	800	1,000	80	10,703
7.	100	900	1,000	90	14,967
8.	0	1,000	1,000	100	16,000

3.2.2 Continuous Electrocoagulation Treatment System

Continuous electrocoagulation treatment was designed and fabricated in order to allow brackish peat water flow through raw water chamber, electrocoagulation reaction chamber, filtration chamber, and treated water chamber with the aid of pump equipment. This study utilized continuous electrocoagulation treatment system in order to reduce the salinity levels in brackish peat water as shown in **Figure 3.4**.

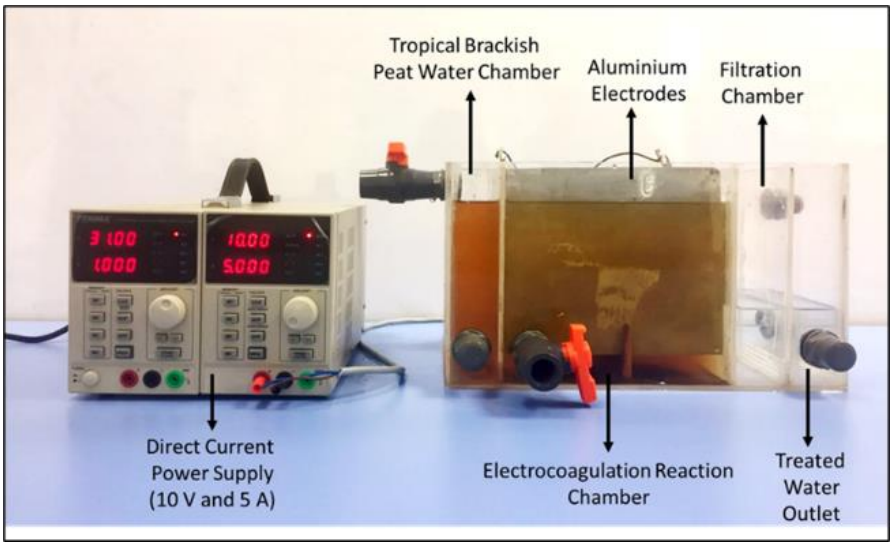

Figure 3.4: Continuous Electrocoagulation Treatment System

The continuous electrocoagulation treatment system with a dimension of 36 cm (length) × 20 cm (width) × 20 cm (height) was segmented into four main chambers which are (i) brackish peat water chamber, (ii) electrocoagulation reaction chamber,

(iii) filtration chamber, and (iv) treated water outlet. The overall maximum volume capacity of the fabricated continuous electrocoagulation treatment was 7 litres. The design for this electrocoagulation treatment system was based on the criteria set in several studies for laboratory desktop scale (Rahman et al., 2020a; Rahman et al., 2020b, Rahman et al., 2020c). These studies designed the electrocoagulation treatment system by considering several criteria particularly an easy fabrication, low maintenance, low cost, and the materials are available locally (Garcia-Segura et al., 2017; Ghernaout, 2019; Rahman et al., 2021a). The continuous electrocoagulation treatment system was also segmented into a filtration chamber in which the filter medium is constructed with filter wool (12 cm × 100 cm) that is purchased locally. This design was developed by a study conducted by Rahman et al. (2020c) which suggested utilizing filtration system in order to separate electrocoagulation flocs from the treated peat water sources.

3.2.3 Effects of Seawater Percentage and Electric Current on Salinity Reduction in Brackish Peat Water

Electric current regulated the dissolution of aluminium ions from anode electrodes in order to produce aluminium hydroxides which subsequently bind with pollutants to produce flocs (Mena et al., 2019). Several conducted studies had utilized electrocoagulation treatment system to treat several water sources with an electric current that ranges between 1 A to 5 A (Rahman et al., 2020a; Rahman et al., 2020b; Rahman et al., 2020c; Rahman et., 2020d). These studies found that an optimum electric current to achieve maximum pollutants reduction is equivalent to 5 A. In comparison to past studies, this study aims to investigate the effect of electric current on salinity reduction in brackish peat water with electric current that ranged between

1 A and 5 A. The effects of both parameters on salinity reduction in brackish peat water were not clarified despite some studies have investigated the effect of current (Al-Raad et al., 2019; Rahman et al., 2020a) and seawater percentage (Wellner et al., 2018; El-Ashtouky et al., 2020). This study investigated the effects of seawater percentage and electric current on salinity reduction in brackish peat water as tabulated in **Table 3.2**.

Table 3.2: List of Variables for Experimental Study for The Effects of Seawater Percentage and Electric Current on Salinity Reduction in Brackish Peat Water

Constant Variables	
Number of electrodes	10 electrodes (20 cm × 15 cm × 0.1 cm of aluminium plates)
Water Flow Rate	0.8 L/min
Inter-electrode distance	1 cm
Varied Variables	
Seawater Percentage in Brackish Peat Water (%)	0% interval up to 90%
Electric Current	1 A interval up to 5 A

The constant variable in this study was ten electrodes with an inter-electrode distance of one centimeter. The salinity reduction efficiency in brackish peat water was also examined by varying the electric current from 1 A to 5 A and the seawater percentage from 0% to 90%. The changes in salinity level of untreated and treated brackish peat water were evaluated by using **Equation 3.1** (Hakizimana et al., 2017; Al-Raad et al., 2019; Zhang et al., 2019).

$$Salinity\ Reduction\ Efficiency\,(\%) = \frac{C_t - C_o}{C_o} \times 100\% \qquad \textbf{(3.1)}$$

Where C_t refers to the final salinity level at a time (mg/L) and C_o refers to the initial salinity level of brackish peat water (mg/L).

3.2.4 Effects of Seawater Percentage and Flow Rate on Salinity Reduction in Brackish Peat Water

Flow rate was defined as the amount of water that enters electrocoagulation treatment at a given time (Nawarka & Salkar, 2019). Several studies had investigated

the effect of flow rate on numerous pollutants reduction particularly ionic compounds (Nguyen et al., 2017), colour (Wu et al., 2021), chemical oxygen demand (Ayyappan et al., 2021; Al-Raad & Hanafiah, 2021), and turbidity (Bun et al., 2022). However, these studies only investigated the effect of flow rate with constant salinity concentration of water sources. Accordingly, this study analyzed the effects of seawater percentage and flow rate on salinity reduction in brackish peat water. As shown in **Table 3.3**, this study examined the effect of seawater percentage (0% to 90%) and flow rate (0.4 L/min to 2.0 L/min) on the salinity reduction efficiency in brackish peat water. In this study, the range of flow rates were specified based on published studies in literature (Wu et al., 2021; Al-Raad & Hanafiah, 2021; Bun et al., 2022). The optimal flow rates to treat water sources with electrocoagulation treatment was typically between 1 to 2 L/min as reported by these studies.

Table 3.3: List of Variables for Experimental Study for The Effects of Seawater Percentage and Flow Rate on Salinity Reduction in Brackish Peat Water

Constant Variables	
Number of electrodes	10 electrodes (20 cm × 15 cm × 0.1 cm of aluminium plates)
Electric Current	5 A
Inter-electrode distance	1 cm
Varied Variables	
Seawater Percentage in Brackish Peat Water	0% interval up to 90%
Flow Rate	0.4 L/min interval up to 2.0 L/min

3.2.5 Water Quality Analysis

Water quality analysis referred to the evaluation of required water parameters in compliance with the national water quality standard (Roy, 2019). Several conducted studies performed water quality analysis in order to evaluate the quality of treated water from electrocoagulation treatment (Rahman et al., 2020a; Rahman et al., 2020b; Rahman et al., 2020c; Rahman et al., 2020d; Kasmuri et al., 2021). These studies compared the water quality between untreated and treated water sources to the

National Water Quality Standard (NWQS) in Malaysia. These studies also investigated that the applicability of the treated water sources with electrocoagulation treatment suitable for domestic consumption in Malaysia. Accordingly, this study conducted water quality analysis by comparing the quality of untreated and treated salinity levels in brackish peat water from electrocoagulation treatment to the National Water Quality Standard in Malaysia as tabulated in **Table 3.4**. The salinity levels in water sources were classified into several classes. The quality of the treated water sources that fall under Class I standard in NWQS was suitable for domestic consumption when the salinity levels being less than 500 mg/L (Department of Environment, 2020). This indicated that the treated water source is safe for clean water supply, fishery, and agricultural activities in terms of salinity levels only.

Table 3.4: National Water Quality Standards (NWQS) in Malaysia (Department of Environment, 2020)

Parameter	**Unit**	**Class**					
		I	**IIA**	**IIB**	**III**	**IV**	**V**
Salinity	mg/L	500	1,000	-	-	2,000	-
Water classification and uses							
Class I		Conservation of natural environment. Water Supply 1 – Practically no treatment is necessary Fishery 1 – Very sensitive aquatic species					
Class IIA		Water Supply II – Conventional treatment required. Fishery II – Sensitive aquatic species					
Class IIB		Recreational use with body contact					
Class III		Water Supply III – Extensive treatment required. Fishery III – Common of economic value and tolerant species; livestock drinking					
Class IV		Irrigation					
Class V		None of the above					

3.2.6 Energy Operating Cost Analysis for the Treatment of Brackish Peat Water with Electrocoagulation

Energy operating cost analysis referred to the evaluation of electrocoagulation viability in terms of energy consumption (Garcia-Segura et al., 2017). The performance of electrocoagulation in terms of energy operating cost had been reported in several conducted studies in literature in which the system had high commercialization

potential (Al-Raad et al., 2019; Rahman et al., 2020a; Rahman et al., 2020b; Rahman et al., 2020c; Rahman et al., 2020d). These studies also evaluated the specific electrical energy consumed (SEEC) which referred to the amount of electrical energy consumed per cubic meter as in **Equation 3.2.**

$$SEEC(kWh/m^3) = \frac{VIT}{Q} \quad \textbf{(3.2)}$$

Where *SEEC* referred to the specific electrical energy consumption (kWh/m^3), *V* referred to voltage, *I* referred to electric current (A), *T* referred to time (hours), and *Q* referred to volume (m^3). The SEEC values were dependent on the electric current, voltage, treatment time, and volume of the treated water sources. The energy operating cost analysis also included the electrode material consumption (EMC) as stated in Faraday's law (Al-Raad et al., 2019) and formulated in **Equation 3.3**.

$$EMC(kg/m^3) = \frac{ItM}{zF} \quad \textbf{(3.3)}$$

Where *EMC* referred to electrode material consumption (kg/m^3), *I* referred to electric current (A), *t* referred to time (s), *M* referred to the molecular weight of metal (g/mol), *Z* referred to the number of electrons involved in the oxidation or reduction reaction, and *F* referred to Faraday's constant (96,485 C/mol). Electrode material consumption (EMC) referred to the number of metal ions that are dissociated from the sacrificial anode electrodes (Papadopoulus et al., 2019). In addition, electrode material consumption was dependent on the electric current and treatment time in electrocoagulation. In order to evaluate the overall energy operating cost, **Equation 3.2** and **Equation 3.3** were combined to form **Equation 3.4** (Hashim et al., 2020).

$$EOC(RM/m^3) = a(SEEC) + b(EMC) \quad \textbf{(3.4)}$$

Where *EOC* referred to energy operating cost (RM/m^3), *a* referred to domestic electricity price (RM 0.18/kWh), *SEEC* referred to the specific electrical energy consumed (kWh/m^3), *b* referred to the price of aluminium electrode materials (RM 8.95/kg), and *EMC* referred to electrode material consumption (kg/m^3). The overall energy operating cost in electrocoagulation treatment was calculated in terms of specific electrical energy consumption (RM/m^3) and electrode material consumption (kg/m^3). In this study, the domestic electricity price was based on the Sarawak electricity tariff as applied by Sarawak Energy whereas the price of aluminium electrode materials was approximately equivalent to RM 8.95 per kilogram (Rahman et al., 2020a).

3.3 Stage 2: Formulation of Adsorption Kinetic Models and Conduct Electrocoagulation Flocs Analysis

This stage aims to formulate adsorption isotherm and kinetic order models as well as to conduct electrocoagulation flocs analysis with Energy Dispersive X-Ray. The following sequence was devised in order to develop these models by following guidelines from various published literature (Mena et al., 2019; Graça et al., 2019; Rahman et al., 2020d).

i. A literature review was conducted to understand the adsorption and kinetic rate equations of salinity adsorption with continuous electrocoagulation treatment.
ii. Scopes of investigation were established that focus on salinity reduction efficiency.
iii. The collated results undergo data fitting for validation of the adsorption theorem and rate kinetic constant.

iv. The compositions of elements on electrocoagulation flocs were examined with Energy Dispersive X-RAY (EDX) analysis.

3.3.1 Formulation of Adsorption Isotherm Models

The following were the procedures taken to formulate the adsorption model and identify the salinity reduction behaviour in electrocoagulation. In this study, the Langmuir and Freundlich isotherm models were utilized in this study owing to such models exhibit real adsorption of molecules and ions on the solid surface of metallic coagulants that are commonly limited to layers adsorption (Rasmey et al., 2018; Budhiary & Sumantri, 2021; Ezzati, 2020). A comparative study to select the suitable adsorption theorem between Langmuir and Freundlich models was also conducted in this study. This undertaken was adopted from several literature published studies (AlJaberi & Mohammed, 2018; Mohammadi et al., 2019; Chibani et al., 2019; Houssini et al., 2020; Shaker et al., 2020; Bendaia et al., 2021; Abdul Jalal, 2022).

i. Langmuir Isotherm Model

Langmuir adsorption model described the equilibrium behaviours between adsorbate and adsorbent in which the adsorption phenomena were limited only to single molecular layer (Liu et al., 2019; Swenson & Stadie, 2019). This model was formulated to determine the maximum salinity adsorption capacity (q_m) and constant rate for Langmuir adsorption (K_L) as shown in **Equation 3.5** (Al-Ghoutti & Da'ana, 2020; Kalam et al., 2021).

$$q_e = \frac{q_m K_L C_e}{1 + K_L C_e} \quad \textbf{(3.5)}$$

Where q_e referred to the adsorption capacity at equilibrium (mg/g), C_e referred to final salinity levels in brackish peat water at equilibrium (mg/L), q_m referred to maximum adsorption capacity, and K_L referred to Langmuir constant rate (L/mg). The Langmuir constant, K_L which referred to the maximum adsorption capacity of adsorbent was calculated in order to determine the separation factor in adsorption process as shown by **Equation 3.6**.

$$R_L = \frac{1}{1 + K_L C_o} \tag{3.6}$$

Where R_L referred to the Langmuir separation factor, K_L referred to Langmuir adsorption capacity (L/g), and C_o referred to the initial salinity levels in brackish peat water (mg/L). The Langmuir separation factor, R_L, was used to determine the adsorption phenomenon in electrocoagulation treatment system. It was informed that the Langmuir separation factor represented the shape of isotherms to be either unfavourable (R_L> 1), linear (R_L= 1), irreversible (R_L= 0), or favourable (0 < R_L<1) (Al-Ghoutti & Da'ana, 2020; Upadhyay et al., 2021).

ii. Freundlich Isotherm Model

Freundlich adsorption isotherm was formulated to determine the maximum salinity adsorption rate (q_e) and constant rate for Freundlich adsorption (K_F). The non-linear form for the Freundlich isotherm model as shown by **Equation 3.7** (Ayub et al., 2020; Laskar & Hahisho, 2020).

$$q_e = K_F C_e^{1/n_f} \tag{3.7}$$

Where q_e referred to the adsorption capacity at equilibrium, C_e referred to the final salinity levels in brackish peat water at equilibrium (mg/L), K_F referred to Freundlich constant rate, and n_f referred to Freundlich exponent constant. The values of $\frac{1}{n_f}$ described the adsorption process either favourable ($0.1 < \frac{1}{n_f} < 0.5$) or unfavourable when $\frac{1}{n_f}$ being more than two (Ayub et al., 2020; Ehiomogue et al., 2022).

3.3.2 Formulation of Pseudo–First Order Kinetic Models

Pseudo-first-order model was utilized to calculate the adsorption rate constant by plotting equilibrium adsorption capacity against residence time (Pooresmaeil & Namazi, 2020; Revellame et al., 2020). The pseudo-first-order model was derived from **Equation 3.8** to formulate this model in terms of linear and non-linear form (Lima et al., 2021).

$$\frac{dq_t}{dt} = k_1(q_e - q_t) \quad \textbf{(3.8)}$$

Where q_e referred to equilibrium adsorption capacity (mg/g), q_t referred to the adsorbate adsorbed onto adsorbent at time (mg/g), and k_1 referred to the rate constant per minute (min^{-1}).

i. Linear Pseudo-First Order Kinetic Model

The linear pseudo first order kinetic model was formulated by plotting $log[q_e - q_t]$ against t in order to achieve linearized form (Ayub et al., 2020) as shown in **Equation 3.9**.

$$log[q_e - q_t] = log(q_e) - \frac{-k_1 t}{2.303} \quad \textbf{(3.9)}$$

Where q_e referred to the amount of adsorbate adsorbed at equilibrium (mg/L), q_t referred to the amount of adsorbate adsorbed at a given time (mg/g), k_1 referred to reaction rate constant (min^{-1}), and t referred to time (min). These kinetic parameters were estimated based on the intercept of the best fit of line which is as follow: m = slope, b = intercept, k_1 = -m, and q_e = exp (b) (Simonič et al., 2020).

ii. Non-Linear Pseudo First Order Kinetic Model

The non-linear pseudo first-order kinetic model was plotted between q_e against t as shown in **Equation 3.10** (Wang & Guo, 2020; Jasper et al., 2020; Revellame et al., 2020).

$$q_e = \frac{q_t}{(1 - \exp^{-k_1 t})} \quad \textbf{(3.10)}$$

Where q_e referred to the experimental values of equilibrium treated salinity level (mg/g), q_t referred to the amount of adsorbed salinity at a time (mg/g), t referred to time (min), and k_1 referred to rate constant for pseudo-first-order (min^{-1}).

iii. Model Validation

Model validation was an assessment step that determined the adequacy and accuracy of formulated models in representing an adsorption process. A comparative study was done by fitting the modelled data to the actual experimental data in order to obtain the determination of coefficient (R^2) as shown in **Equation 3.11** (Ayub et al., 2020; Wang & Guo, 2020).

$$R^2 = \frac{\left(q_{e,exp} - q_{e,model}\right)^2}{\sum\left(q_{e,exp} - \overline{q_{e,model}}\right)^2 + \left(q_{e,exp} - q_{e,model}\right)^2} \quad \textbf{(3.11)}$$

Where R^2 referred to the regression coefficients, $q_{e,\exp}$ referred to the experimental values of equilibrium adsorption capacity (mg/g), $q_{e,model}$ referred to the modelled values of equilibrium capacity (mg/g). The R^2 was calculated to evaluate the regression between both experimental and modelled adsorption capacity values (Delgado et al., 2019). This method was adopted by several published studies in the literature in order to evaluate the data fitness that was close to unity (Ersan et al., 2019; Guo & Wang, 2019; Khan et al., 2019; Sabarinathan et al., 2019; Revellame et al., 2020). These studies suggested the value of R^2 being less than 0.5 indicated a weak relation between the independent variable and response variable, whereas $0.5 < R^2 < 0.75$ signified an inaccuracy of formulated model (Ayub et al., 2020; Revellame et al., 2020; Mehri et al., 2021). The formulated adsorption model was valid when the values of R^2 being higher than 0.75 which signifies a good fit between experimental and modelled data (Rahman et al., 2020d).

3.3.3 Electrocoagulation Flocs Analysis

Electrocoagulation flocs analysis referred to the characterization of flocs that indicated the occurrence of an adsorption process. This study investigated the minerals compositions that were available on electrocoagulation flocs by conducting Energy Dispersive X-Ray (EDX) analysis with energy dispersive spectroscopy. Prior to the EDX analysis, electrocoagulation flocs were collected from the electrocoagulation reaction chamber with skimming method and then dried to remove the moisture content. Then, the dried flocs underwent elemental analysis with Energy Dispersive X-Ray (EDX)

detector model Bruker Nano GmbH. In this study, the accuracy of EDX results was presented in terms of absolute error which also indicates the deviation of the measured value and expected value. This method was adopted from Scimeca et al. (2018) who stated that absolute error in EDX indicates the error in the weight percent concentration at one sigma level. In addition, the EDX only required 10,000 number of counts in order to satisfy the needed 1% deviation with 68% confidence levels (Scimeca et al., 2018). The Electron Dispersive X-Ray analysis for electrocoagulation flocs was conducted according to the American Society for Testing Materials (ASTM) E2015-04 (2014) which outlined the electron microscopy testing procedure (Khui et al., 2021).

3.4 Stage 3: Development of Statistical Model with Response Surface Methodology

The statistical model analysis was a technique that examined data information in order to derive useful insight based on statistical concepts (Karimifard & Alavi, 2018). This study developed a statistical model to study the relationship between salinity reduction efficiency and energy operating cost for brackish peat water treatment with electrocoagulation. The study also formulated quadratic equations which represent salinity reduction efficiency and energy operating cost. This method was performed by adopting the design of experiment (DOE).

3.4.1 Design of Experiment

The design of experiment (DoE) was a statistical method that systematically and structurally developed to investigate the relationship between input factors and responses through variation of means. In this study, the statistical technique method of response surface methodology by using central composite design (CCD) in a

statistical mathematical software (Design Expert 13 Trial Version) was performed to develop response surface for both salinity reduction efficiency and energy operating cost. This study utilized a central composite design (CCD) due to such model requiring only minimal experimental runs as well as achieving high accuracy of the formulated polynomial equations (Yolmeh & Jafari, 2017). The total experiment runs which developed with central composite design were calculated by utilizing **Equation 3.12** (Ferreira et al., 2018).

$$\textit{Total Number of Experiments} = 2^k + 2k + C_o \quad \textbf{(3.12)}$$

Where k referred to the number of factors, 2^k referred to cubic run, $2k$ referred to the axial runs, and C_o referred to the center point runs. The values that were attributed to each variables need to be assigned properly with five levels (-α , -1, 0, +1, +α).

3.4.2 Mathematical Model Fitting

According to Khorram and Fallah (2018), response surface methodology (RSM) referred to a collection of mathematical and statistical methods that was essential in designing and developing experimental models. RSM was constituted by several mathematical terms particularly linear, square, and polynomial functions that fit experimental results as well as validated with statistical techniques (Murdani et al., 2018; Acharya et al., 2018; Oden, 2020) as shown in **Equation 3.13.**

$$S = \alpha_o + \sum_{i=1}^{k} \alpha_i x_i + \sum_{i=1}^{k} \alpha_{ii} x_i^2 + \sum_{i.j=1, j \neq i}^{k} \alpha_{ij} x_i x_j \quad \textbf{(3.13)}$$

Where S referred to response, α_o referred to the average of responses, α_i, α_{ii}, and α_{ij} referred to a coefficient that is associated with the experiments. The second

term, $\sum_{i=1}^{k} \alpha_i x_i$ referred to linear interaction effect, the third term, $\sum_{i=1}^{k} \alpha_{ii} x_i^2$ referred to higher order interaction, and the fourth term, $\sum_{i.j=1, j \neq i}^{k} \alpha_{ij} x_i x_j$ referred to dual interaction effects. These quadratic terms were also essential in polynomial functions in order to determine a critical point either maximum, minimum, or saddle as reported by a study conducted by Roy et al. (2018). The coding of experimental data in this study was employed by transforming each real value onto coordinates inside a scale with dimensional values as shown in **Table 3.5**.

Table 3.5: Experimental Design of Actual and Coded Values of Independent Variables

Variable	Symbol	Real Values of Coded Levels				
		-α[a]	**-1**	**0**	**+1**	**+ α[a]**
Seawater Percentage (%)	X_1	0	0	50	90	90
Electric Current (A)	X_2	1	1	3	5	5
Flow Rate (L/min)	X_3	0.4	0.4	1.2	2.0	2.0

[a] α = 1 (axial point for orthogonal CCD in the case of 3 independent variables)

This study investigated the effects of three variables particularly seawater percentage, electric current, and flow rate on salinity reduction efficiency and energy operating cost as shown by **Table 3.5**. The deviation values between the experimental and mathematical model were determined to ensure the accuracy of formulated model should less than 10% (Acharya et al., 2018). This study also assessed the coefficient of determination (R^2) of formulated mathematical models with experimental data fitting. This method was implemented by Acharya et al. (2019), Igwegbe et al. (2019), Steyerberg (2019), Piepho (2019), and Haas (2020). These studies reported that regression analysis should be reported in terms of actual R^2, adjusted R^2, and predicted R^2. The mathematical model was considered valid when the R^2 values being higher than 0.75 owing to the well-fitted data (Rahman et al., 2020d).

3.4.3 Analysis of Variance

Analysis of variance (ANOVA) showed the comparison of variance due to the adjustment in the combination of variable levels as resulting from the random errors that owing to the generated responses (Kim, 2017). The accuracy of the developed models was determined in terms of sum of squares, degree of freedom (df), and mean squares by adopting method from a study performed by Acharya et al. (2018), Hendaoui et al. (2018), and Shamaei et al. (2018). In ANOVA, the formulated mathematical models were examined in terms of p-value. As informed by Bajpai et al. (2020), p-value defined the level of marginal significance within statistical hypothesis test and this value should be less than 0.05 to show that the formulated mathematical models were statistically significant.

3.4.4 Statistical Model Analysis

Statistical model analysis was the final stage in RSM that generated contour plots in three-dimensional (3D) diagram. RSM was employed in order to investigate the relationship between salinity reduction efficiency in brackish peat water and energy operating cost with electrocoagulation treatment as shown by **Table 3.6**.

Table 3.6: Statistical Goals, Limits, Weights, and Importance for The Treatment of Brackish Peat Water with Continuous Electrocoagulation Treatment

Item	Parameters	Goal	Lower Limit	Upper Limit	Lower Weight	Upper Weight	Importance
Variables	Seawater Percentage	In range	0	90	1	1	3
	Electric Current (A)	In range	1	5	1	1	3
	Flow Rate (L/min)	In range	0.4	2.0	1	1	3
Responses	Salinity Reduction Efficiency (%)	Maximize	-	-	1	1	3
	Energy Operating Cost (RM/m^3)	Minimize	-	-	1	1	3

The upper and lower weight are equivalent to one which indicated equal importance on desired targets and constraints of study (Taheri, 2022). The importance of mathematical model in Design Expert software was assigned at three to ensure all the variables were being equally analyzed with RSM (Design Expert, 2022).

CHAPTER 4

RESULTS AND DISCUSSION

4.1 Introduction

This chapter presents and discusses the major findings which are pertinent to the aim and objectives of this study. The results and discussion sections in this chapter are divided into three main stages which correspond to the devised objectives as depicted by **Figure 3.1** in **Chapter 3**.

4.2 Stage 1: Salinity Reduction of Brackish Peat Water with Electrocoagulation Treatment

This study investigates the effects of seawater percentage, electric current, and flow rate on salinity reduction efficiency in brackish peat water and compares the water quality of untreated and treated salinity levels of brackish peat water from electrocoagulation process to the National Water Quality Standard (NWQS) in Malaysia. In order to evaluate energy consumption in electrocoagulation treatment, this study conducts energy operating cost analysis with Faraday's laws equations.

4.2.1 Salinity Reduction of Brackish Peat Water with Varied Seawater Percentage and Electric Current

An experimental study to analyze salinity reduction in brackish peat water treatment with varied seawater percentage and electric current with continuous electrocoagulation treatment is shown in **Figure 4.1** and **Figure 4.2** respectively. The effects of both seawater percentage and electric current on salinity reduction efficiency are also illustrated in the surface plot as in **Figure 4.3**.

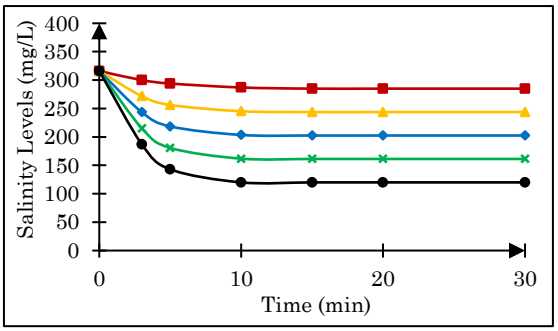

(A) Brackish Peat Water with 0% of Seawater Percentage

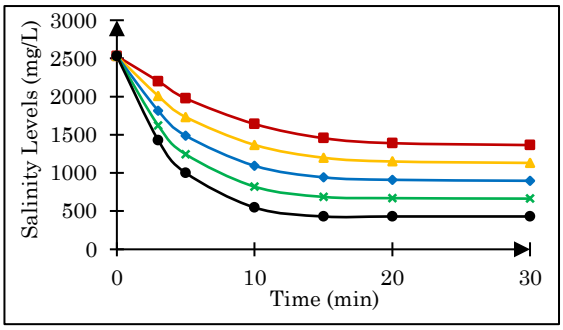

(B) Brackish Peat Water with 10% of Seawater Percentage

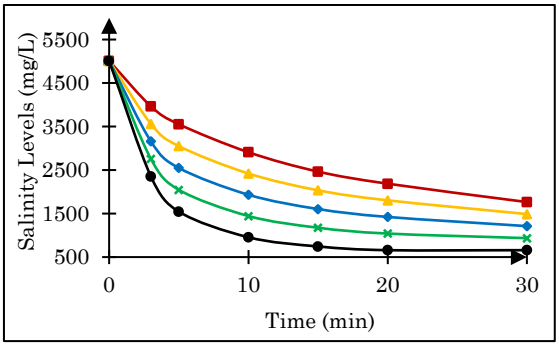

(C) Brackish Peat Water with 30% of Seawater Percentage

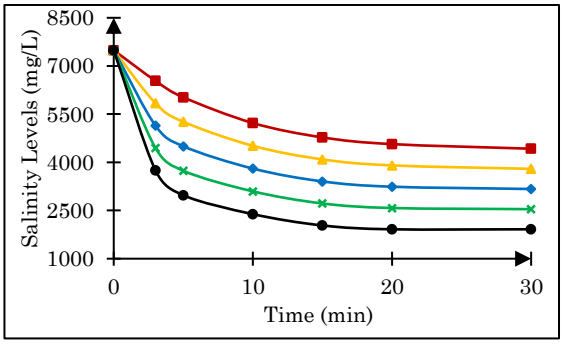

(D) Brackish Peat Water with 50% of Seawater Percentage

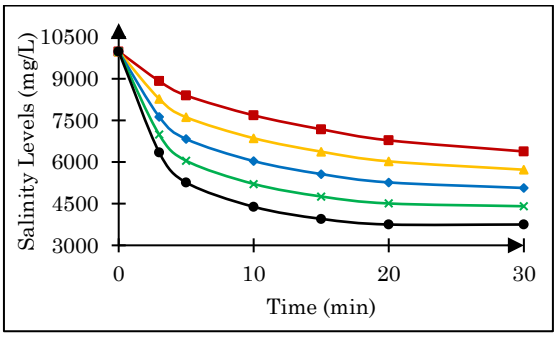

(E) Brackish Peat Water with 70% of Seawater Percentage

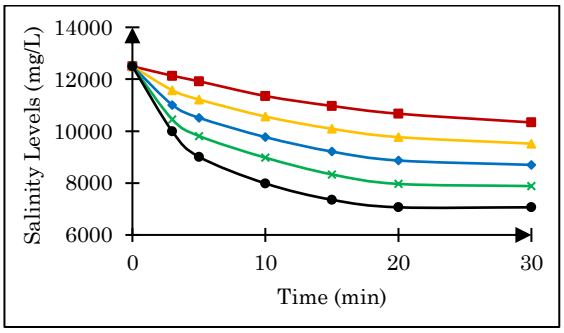

(F) Brackish Peat Water with 80% of Seawater Percentage

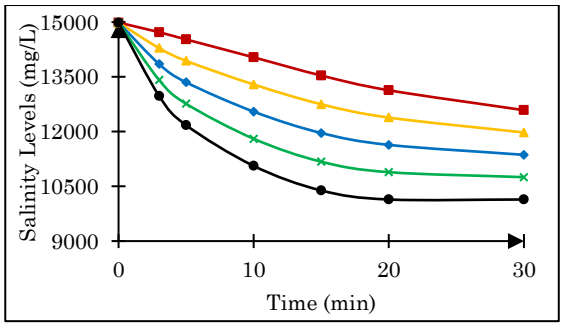

(G) Brackish Peat Water with 90% of Seawater Percentage

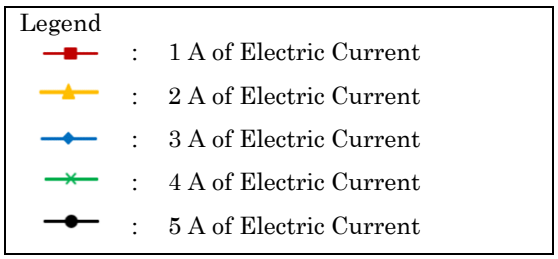

Figure 4.1: Effect of Electric Current on Salinity Levels Changes with Varied Seawater Percentage and Time

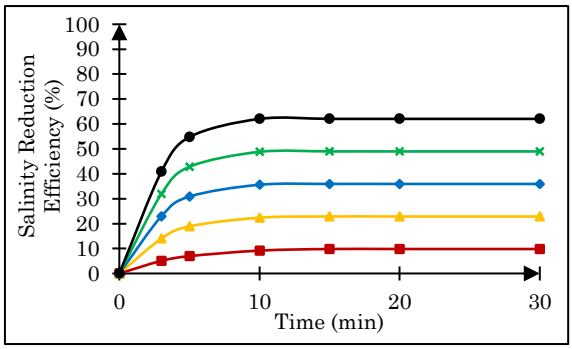

(A) Brackish Peat Water with 0% of Seawater Percentage

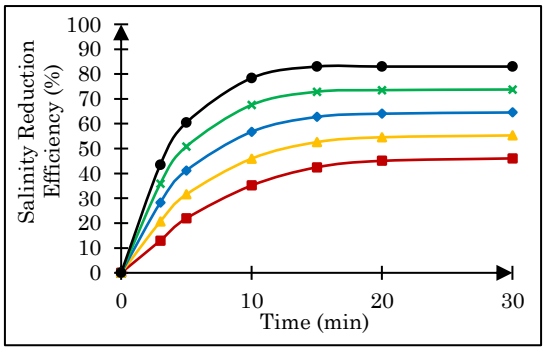

(B) Brackish Peat Water with 10% of Seawater Percentage

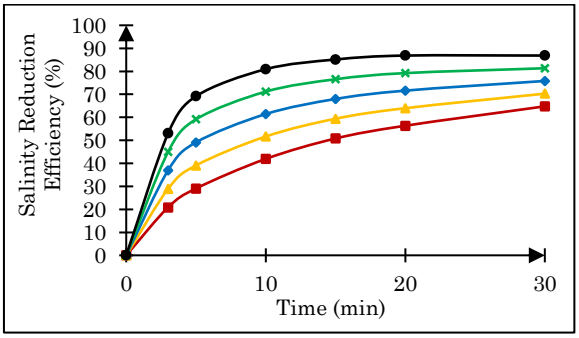

(C) Brackish Peat Water with 30% of Seawater Percentage

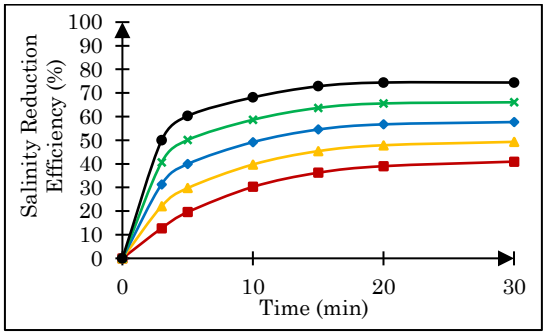

(D) Brackish Peat Water with 50% of Seawater Percentage

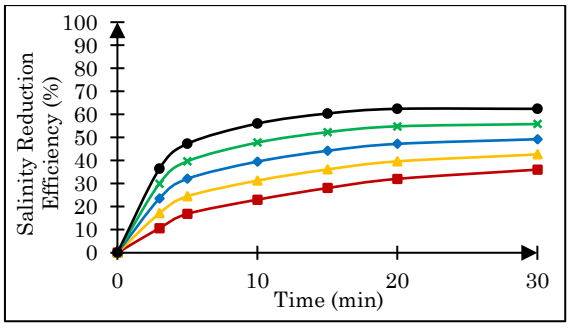

(E) Brackish Peat Water with 70% of Seawater Percentage

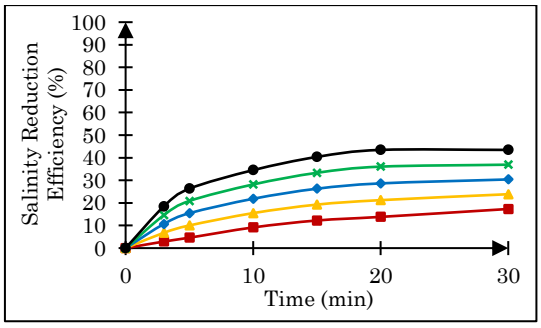

(F) Brackish Peat Water with 80% of Seawater Percentage

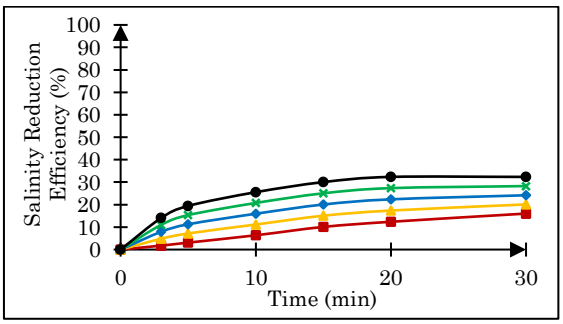

(G) Brackish Peat Water with 90% of Seawater Percentage

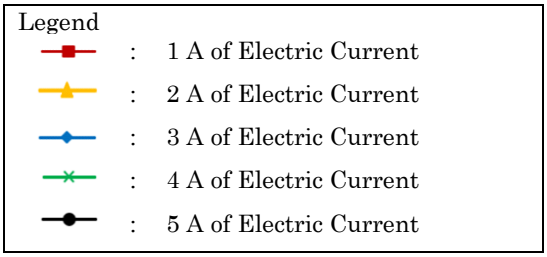

Figure 4.2: Effect of Electric Current on Salinity Reduction Efficiency with Varied Seawater Percentage and Time

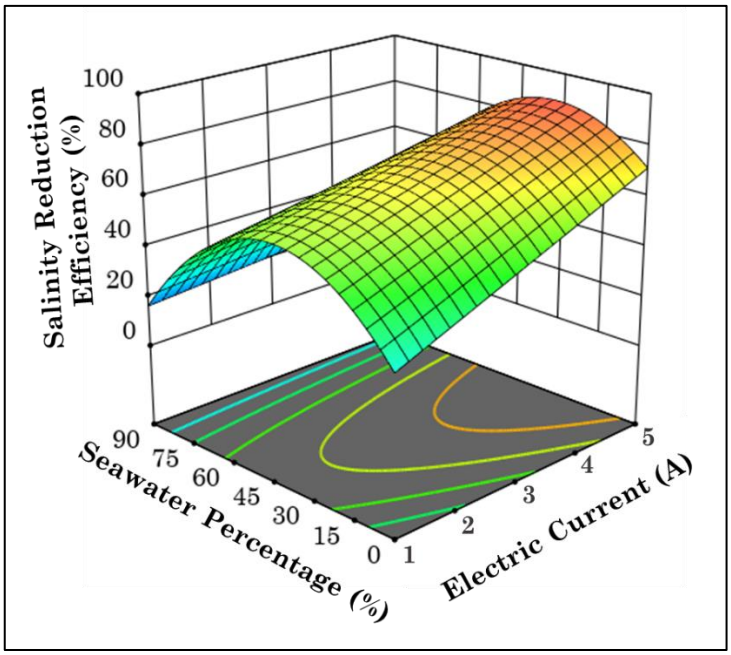

Figure 4.3: Effects of Seawater Percentage and Electric Current on Salinity Reduction Efficiency in Brackish Peat Water

A constant flow rate of 0.8 L/min is used to study the effects of electric current and seawater percentage on salinity reduction efficiency in brackish peat water. After electrocoagulation treatment, the salinity levels in brackish peat water had reduced significantly as depicted from **Figure 4.1(A**) to **Figure 4.1(G)**. At 0% of seawater percentage, this study has observed the highest salinity reduction could be achieved at 5 A of electric current whereas the lowest is attained at 1 A. This is due to high electric current could possibly lead to high generation of aluminium hydroxide coagulant to separate salinity from brackish peat water source. The rate of electron transfer between the electrodes and water solution increase at high current density, leading to an efficient redox reaction and formation of large and stable aluminium hydroxide flocs in electrocoagulation (Hu et al., 2023).

The salinity level in this brackish peat water source has also reduced from 316 mg/L to 108 mg/L with 65.98% of salinity reduction efficiency at 5 A of electric current which is shown by **Figure 4.2(A)**. When the electric current is reduced to 1 A, this

study has noticed that the salinity level in brackish peat water with 0% of seawater percentage only decreased from 316 mg/L to 285 mg/L with 10% of salinity reduction efficiency. This signifies that high salinity reduction efficiency in brackish peat water could be achieved at 5 A of maximum electric current. High electric current could remove salinity ions from water sources through electrostatic attraction, chemical precipitation, and adsorption onto aluminium hydroxide coagulants (Zaied et al., 2020). A similar observation is found in the treatment of brackish peat water with a seawater percentage that ranges from 10% to 90% which indicates that salinity reduction efficiency is directly proportional to electric current. It is also noticed that a high electric current could lead to high salinity reduction efficiency owing to an effective redox reaction. A high electric current ensures an effective redox reaction especially in terms of the formation of in-situ aluminium hydroxide coagulants that lead to salinity reduction in brackish peat water sources. Applying electrocoagulation at high electric current could accelerate the oxidation and reduction reactions at the electrode surfaces, eventually increasing the availability of electrons at interface layers to promote more stable aluminium hydroxide coagulants (Ingelsson et al., 2020). A study conducted by Rahman et al. (2020a) also reported that high electric current could lead to an effective pollution reduction in peat water sources. The study conducted by Rahman et al. (2020a) also observed that 5 A of electric current effectively reduced 88% of total organic carbon, 89.90% of chemical oxygen demand, and 87.50% of total suspended solids when electrocoagulation treatment is utilized. A high electric current also accelerates the redox reaction process and provides an adequate amount of aluminium hydroxide coagulants for an effective salts reduction in water sources (Al-Raad & Hanafiah, 2021).

Although high electric current is effective for brackish peat water treatment, this study has discovered that high seawater percentage in source water sources has

an inverse effect on salinity reduction efficiency. At 5 A of electric current, it is found that the salinity reduction efficiency has increased from 65.98% to 86.85% when the seawater percentage in brackish peat water rises from 0% to 30%. When the seawater percentage continually increased from 30% to 90%, the salinity reduction efficiency reduced from 86.85% to 32.34%. This shows that the highest salinity reduction efficiency could be attained at 30% of the seawater percentage in brackish peat water. At 30% of seawater percentage, the salinity levels in brackish peat water have dropped from 5,010 mg/L to 659 mg/L with 86.85% of salinity reduction efficiency. This study has also noticed that electrocoagulation treatment could be used to treat brackish peat water with a seawater percentage lower than 30%. This is due to such conditions favours high salinity reduction efficiency as well as attaining low levels of treated salinity as depicted in **Figure 4.2(C)**. Low salinity levels in treated brackish peat water with a 30% seawater percentage indicate effective adsorption of chloride ions on aluminium hydroxide coagulants. At 30% of seawater percentage, the available sodium and chloride ions can provide an optimal balance of water conductivity and minimize further dissociation of aluminium hydroxide coagulants (Alam et al., 2022). A study attempted by Graça et al. (2019) also reported that electrocoagulation treatment with the aid of in-situ aluminium hydroxide coagulants could reduce some chloride ions in the form of electrocoagulation flocs. A similar finding had been informed by Al-Raad et al. (2019) in which electrocoagulation treatment could be utilized to reduce 93.00% of chloride ions from saline lake water that contains 8,498 mg/L of chloride ions. The studies signified that electrocoagulation treatment could be employed to reduce salinity levels in saline water sources with the aid of in-situ aluminium hydroxide coagulants.

This study has also observed that the salinity reduction efficiency started to decrease when the seawater percentage in brackish peat water being more than 30%

as illustrated in **Figure 4.3**. The lowest salinity reduction efficiency has been observed for brackish peat water with a 90% of seawater percentage. The salinity level in brackish peat water with 90% of seawater percentage only reduce from 14,987 mg/L to 10,140 mg/L with 32.34% of salinity reduction efficiency. Even though the treatment of brackish peat water source has been conducted at high electric current, this study has found that such condition is not applicable at high seawater percentage. This is possibly due to an inadequate amount of in-situ aluminium hydroxides being produced when the seawater percentage is more than 30%. The high conductivity of water sources could increase the rate of ion exchange and migration between electrodes, subsequently increasing the production of hydrogen gas at the cathode and oxygen gas at the anode. This phenomenon decreases the available surface areas of the anode electrode to produce aluminium ions (Kobya et al., 2020). The conductivity levels in brackish peat water increase at high seawater percentages, which could cause competition between ions for the available binding sites on the aluminium hydroxide coagulants. In this case, the salinity reduction efficiency decreases due to inadequate binding sites to attach the flocs (Al-Raad & Hanafiah, 2020). A similar study conducted by Hakizimana et al. (2017) informed that poor salinity reduction efficiency with electrocoagulation treatment could be observed at high salinity levels due to secondary reactions that occur simultaneously with the anodic dissolution of metal. The secondary reactions that particularly involve oxygen evolution and formation of hypochlorite ions from anodic oxidation of chloride ions could prevent the formation of in-situ aluminium hydroxide coagulants. Bendaia et al. (2021) reported that the presence of sodium chloride in water sources will dissolve some aluminium hydroxides into transitory compounds, thus, reducing the number of coagulants in electrocoagulation treatment.

4.2.2 Salinity Reduction of Brackish Peat Water with Varied Seawater Percentage and Flow Rate

This study has investigated the effects of seawater percentage and flow rate on salinity reduction in brackish peat water with electrocoagulation treatment. As depicted in **Figure 4.4** and **Figure 4.5**, this study has analyzed the effect of flow rates that ranges from 0.4 L/min to 2.0 L/min with a constant electric current of 5 A on salinity reduction in brackish peat water. In electrocoagulation treatment, the brackish peat water samples with varied seawater percentages that ranged from 0% to 90% are subjected to electrocoagulation reaction chamber at several flow rates as illustrated in **Figure 4.6**. The salinity reduction in brackish peat water with electrocoagulation treatment is dependent on seawater percentage and flow rates.

From conducted experimental study, the highest salinity reduction efficiency in brackish peat water could be achieved at 30% of seawater percentage and 1.2 L/min of flow rate. Under these conditions, the salinity level has reduced from 5,010 mg/L to 412 mg/L with 91.28% of salinity reduction efficiency as shown by **Figure 4.4(C)** and **Figure 4.4(D)** respectively. Increasing the flow rate could enhance the mixing and contact rate between water and aluminium electrodes. This condition improves the dispersion and distribution of aluminium hydroxide flocs, which allows effective adsorption for salinity reduction (AlJaberi et al., 2022). This is possibly due to such flow rate aids ensuring an effective mixing process between aluminium and hydroxide ions which subsequently formed white gelatinous aluminium hydroxide coagulants. A study attempted by Nugroho et al. (2021) also reported that an optimal flow rate in electrocoagulation treatment could accelerate the formation of aluminium hydroxide coagulants due to the in-situ mixing process.

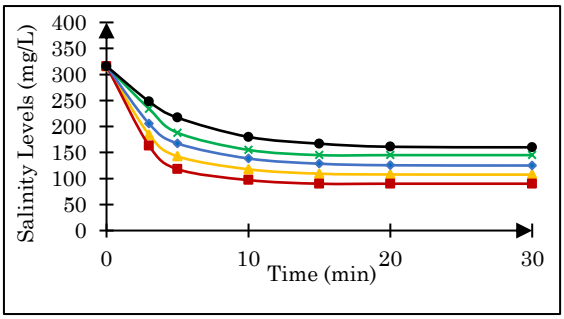

(A) Brackish Peat Water with 0% of Seawater Percentage

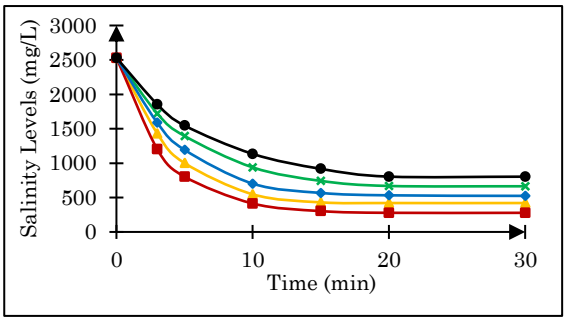

(B) Brackish Peat Water with 10% of Seawater Percentage

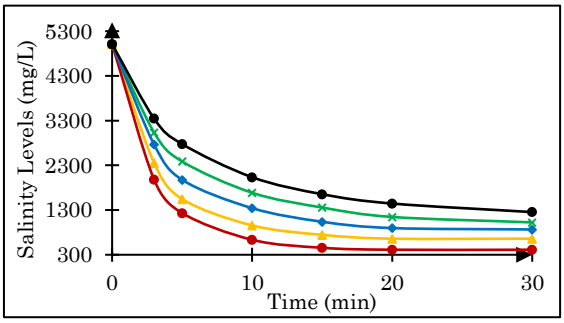

(C) Brackish Peat Water with 30% of Seawater Percentage

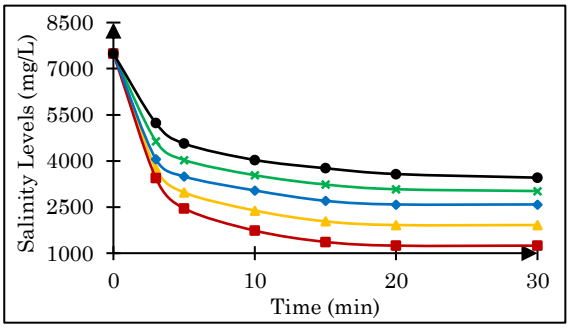

(D) Brackish Peat Water with 50% of Seawater Percentage

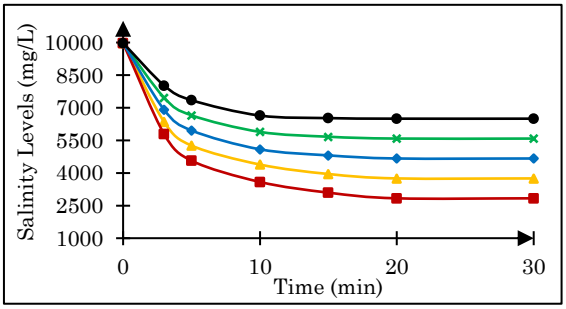

(E) Brackish Peat Water with 70% of Seawater Percentage

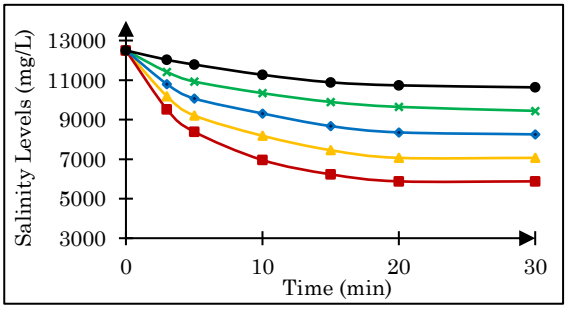

(F) Brackish Peat Water with 80% of Seawater Percentage

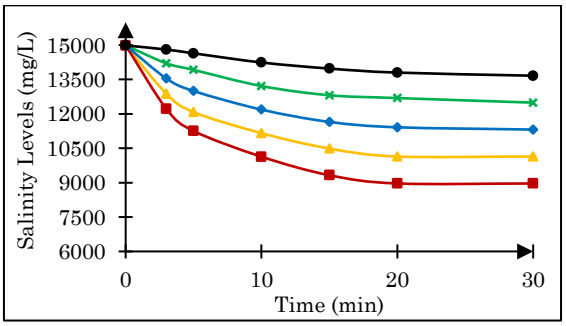

(G) Brackish Peat Water with 90% of Seawater Percentage

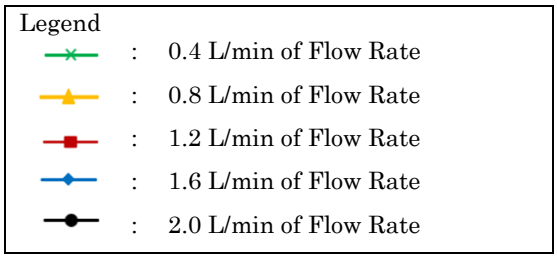

Figure 4.4: Effect of Flow Rate on Salinity Levels Changes with Varied Seawater Percentage and Time

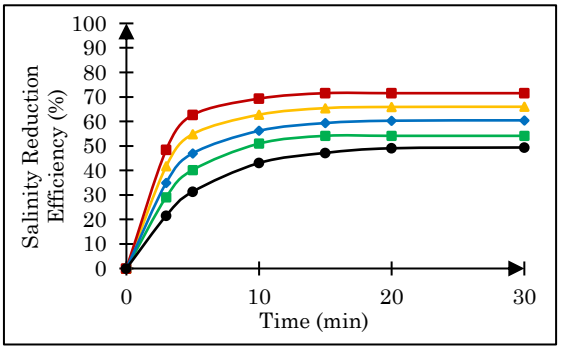

(A) Brackish Peat Water with 0% of Seawater Percentage

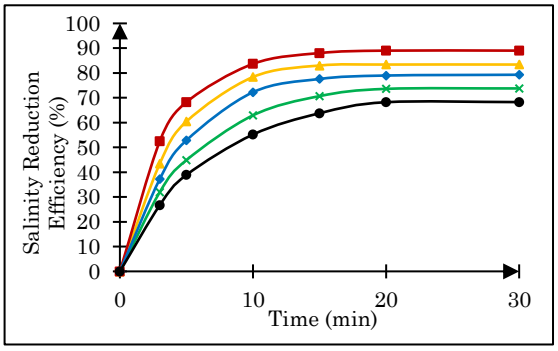

(B) Brackish Peat Water with 10% of Seawater Percentage

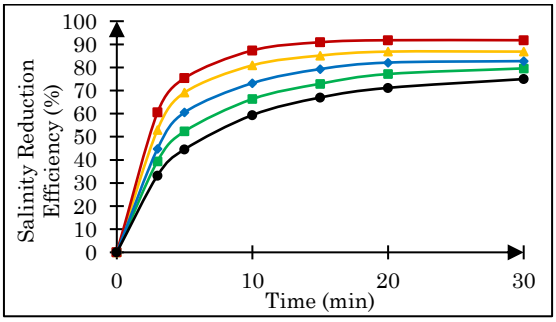

(C) Brackish Peat Water with 30% of Seawater Percentage

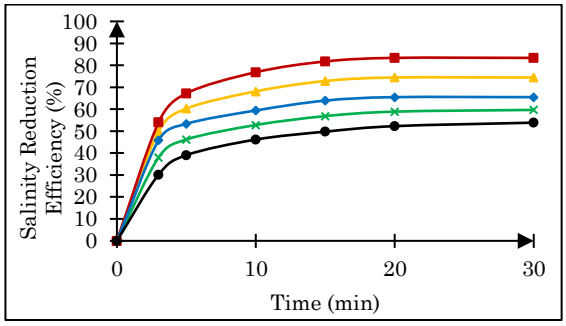

(D) Brackish Peat Water with 50% of Seawater Percentage

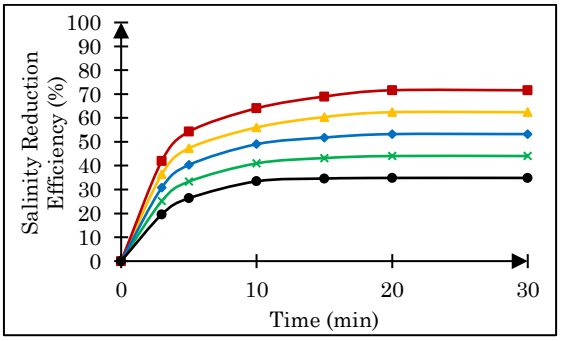

(E) Brackish Peat Water with 70% of Seawater Percentage

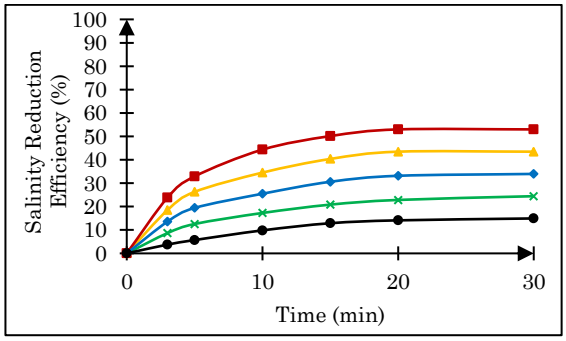

(F) Brackish Peat Water with 80% of Seawater Percentage

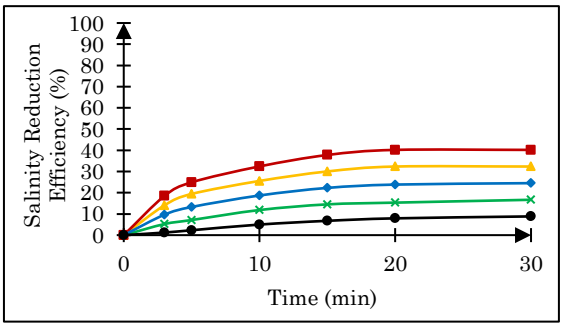

(G) Brackish Peat Water with 90% of Seawater Percentage

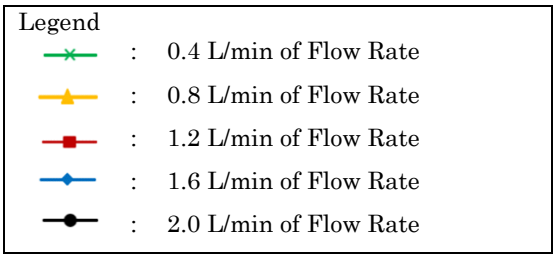

Figure 4.5: Effect of Flow Rate on Salinity Reduction Efficiency with Varied Seawater Percentage and Time

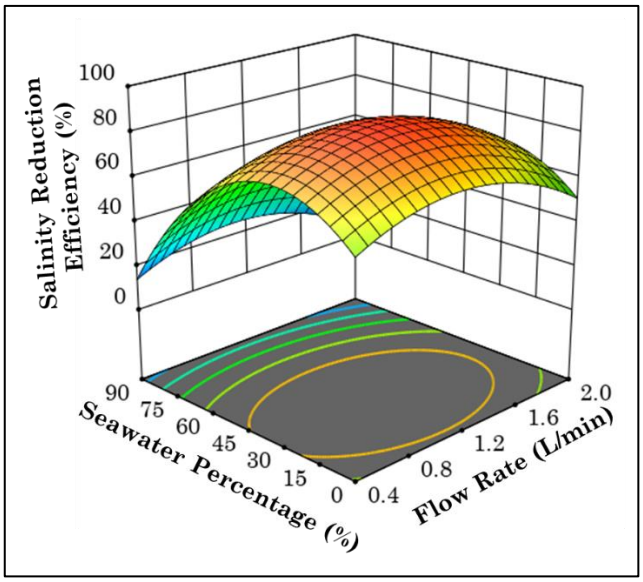

Figure 4.6: Effect of Seawater Percentage and Flow Rate on Salinity Reduction Efficiency in Brackish Peat Water

This study has noticed that the lowest (0.4 L/min) and highest (2.0 L/min) of flow rates unfavoured high salinity reduction efficiency in electrocoagulation treatment as shown in **Figure 4.6**. At 0.4 L/min of flow rate, electrocoagulation treatment has recorded 79.58% of salinity reduction efficiency in which the salinity levels reduced from 5,010 mg/L to 1,023 mg/L only. At a low flow rate, the electrocoagulation system works with a long residence time which causes an excessive formation and build-up of aluminium hydroxide coagulants on the electrodes. Electrode fouling could reduce the available surface areas and limit the number of binding sites available for ions to attach to the flocs (Ashraf et al., 2021). When the flow rate is increased to 2.0 L/min, the salinity level in brackish peat water with a seawater percentage of 30% has only decreased from 5,010 mg/L to 1,254 mg/L with 74.97% of salinity reduction efficiency. The electrocoagulation system operates at a short residence time due to a high flow rate. This circumstance reduces the contact time between the water and aluminium electrodes, thus limiting the formation and growth of aluminium hydroxide coagulants to small and less stable flocs (Betancor-Abreu et al., 2019). These observations indicate

that the salinity reduction in brackish peat water is not applicable at both low and high flow rate due to an ineffective adsorption process between in-situ aluminium hydroxide coagulants and salt elements. A study conducted by Wu et al. (2021) also informed that both high and low flow rates could not promote high pollutants reduction efficiency due to an ineffective adsorption process in electrocoagulation treatment. As reported by Al-Raad and Hanafiah (2021), a high flow rate could lead to an inadequate time for the emitted ions from sacrificial anode to form aluminium hydroxide coagulants.

As illustrated in **Figure 4.6**, this study has also observed that the seawater percentage in brackish peat water significantly affects the salinity reduction efficiency. At a constant flow rate of 1.2 L/min, it is noticed that the salinity reduction efficiency has increased from 71.52% to 91.78% when the seawater percentage rises from 0% to 30%. The salinity reduction efficiency has also reduced from 91.78% to 40% when the seawater percentage of brackish peat water increased from 30% to 90%. This signifies that high salinity reduction efficiency could only be attained in brackish peat water with seawater percentage being less than 30%. A similar study attempted by Bendaia et al. (2021) also found that excessive levels of salinity in water sources could cause the transition of aluminium hydroxides compounds into transitory compounds such as $Al(OH)_3Cl$, $Al(OH)Cl_3$, and $AlCl_3$ which are soluble in water sources. The dissolution of aluminium hydroxides into transitory compounds could also lead to less formation of coagulants that are supposed to absorb pollutants from water sources in the form of electrocoagulation flocs (Al-Raad et al. 2019).

The highest salinity reduction efficiency of 91.78% could be attained in brackish peat water with a seawater percentage of 30% at 1.2 L/min of flow rate. This is due to such conditions ensuring high formation of in-situ aluminium hydroxide coagulants owing to high mixing rate and adequate time for the adsorption process (Nugroho et al.,

2021). When the seawater percentage and flow rate being more than 30% and 1.2 L/min respectively, this study found that the salinity reduction efficiency in brackish peat water significantly decreased which is possibly due to further oxidation of aluminium hydroxides into transitory compounds (Rafiee et al., 2020).

4.2.3 Comparison of Untreated and Treated Brackish Peat Water to the National Water Quality Standards in Malaysia

Water quality analysis is conducted in this study to compare the levels of untreated and treated salinity levels in brackish peat water to the National Water Quality Standards (NWQS) as implemented by the Department of Environment in Malaysia. In order to evaluate the changes in salinity levels, this study has adopted the laboratory electrometric method by using Hanzhan 9910 salinity meter. The quality of untreated and treated salinity levels in brackish peat water is compared by conducting continuous electrocoagulation treatment at 5 A of electric current, 1.2 L/min of flow rate and 30% of seawater percentage as shown in **Figure 4.7**.

The salinity levels of untreated brackish peat water do not meet any water classification standard in NWQS when the seawater percentage of such water being more than 10%. This is due to the initial salinity levels of untreated brackish peat water sources being higher than the minimum NWQS limit of 2,000 mg/L. Wildayana et al. (2017) also reported similar observations in which excessive salinity levels in brackish peat water could harm human health if consumed directly. According to the Department of Environment (2020), water sources with salinity level being more than 2,000 mg/L are unsafe for any application and should undergo water treatment process such as reverse osmosis.

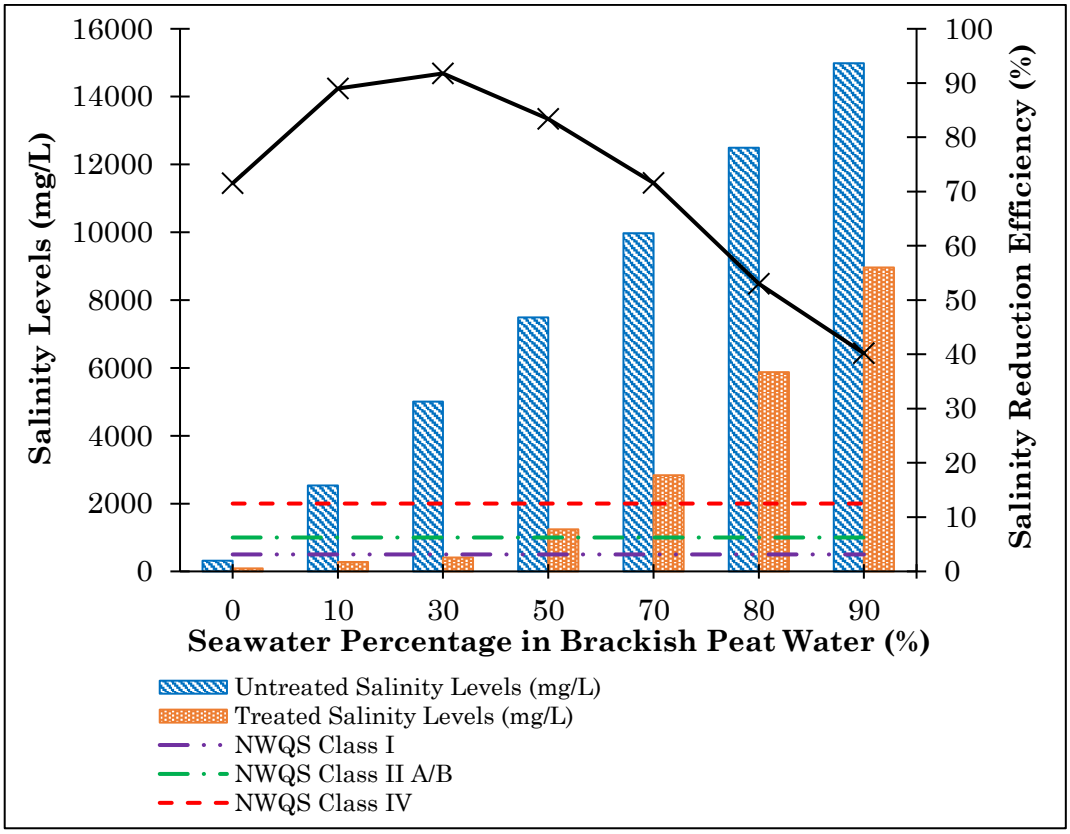

Figure 4.7: Comparison of Untreated and Treated Salinity Levels in Brackish Peat Water to the National Water Quality Standards in Malaysia at 5 A of Electric Current, 1.2 L/min of Flow Rate, and 30% of Seawater Percentage

In order to reduce the salinity levels in brackish peat water, this study has employed a continuous electrocoagulation treatment system with 5 A of electric current and 1.2 L/min of flow rate. This study has observed that the treated salinity levels in brackish peat water met Malaysian Class I standards in NWQS when the seawater percentage of such water is less than 30%. The treated brackish peat water could be used for domestic consumption in Malaysia due to the treated salinity levels being less than 500 mg/L (Department of Environment, 2020). In addition, this study has also noticed that brackish peat water with a seawater percentage of 30% achieved maximum salinity reduction efficiency at 91.78%. This signifies that electrocoagulation treatment could be utilized to reduce salinity levels in brackish peat water which is found to be suitable for domestic consumption in Sarawak. In 2020, several conducted studies have

found that electrocoagulation treatment of peat water could be utilized for domestic consumption especially in rural areas in southern and central Sarawak (Rahman et al., 2020a; Rahman et al., 2020b; Rahman et al., 2020c; Rahman et al., 2020d).

Although electrocoagulation is effective to reduce salinity levels in brackish peat water with a seawater percentage being less than 30%, this study has found that the treated salinity levels do not meet Class I standard in NWQS when the seawater percentage being more than 30%. The electrocoagulation treatment system is not suitable for brackish peat water with seawater percentage being more than 30% due to the salinity reduction efficiency significantly decreasing as shown in **Figure 4.7**. This observation is also similar to a study attempted by Al-Raad et al. (2019) which reported that electrocoagulation treatment only reduces slight salinity levels in highly saline water sources.

4.2.4 Analysis of Energy Operating Cost for Brackish Peat Water Treatment with Continuous Electrocoagulation System

As discussed in **Section 4.1.5**, this study has observed that the treated brackish peat water could be consumed safely when the seawater percentage being less than 30%. In order to investigate the viability of electrocoagulation treatment system, this study investigates the effects of electric current and flow rate on energy operating costs.

i. Effects of Electric Current and Flow Rate on Energy Operating Cost in Electrocoagulation Treatment.

Previously, this study investigated the effects of electric current and flow rate on energy operating cost in continuous electrocoagulation treatment. In order to evaluate the energy operating cost with electrocoagulation, this study attempts to

identify the applicable electric current and flow rate for brackish peat water with a 30% of seawater percentage. This study has found that high energy operating costs could be attained at high electric current as shown in **Figure 4.8**. At 0.4 L/min of flow rate, the energy operating cost of electrocoagulation treatment at 1 A and 5 A of electric current cost only RM 0.22 per m^3 and RM 1.14 per m^3 respectively. This indicates that the energy operating cost is directly proportional to the electric current.

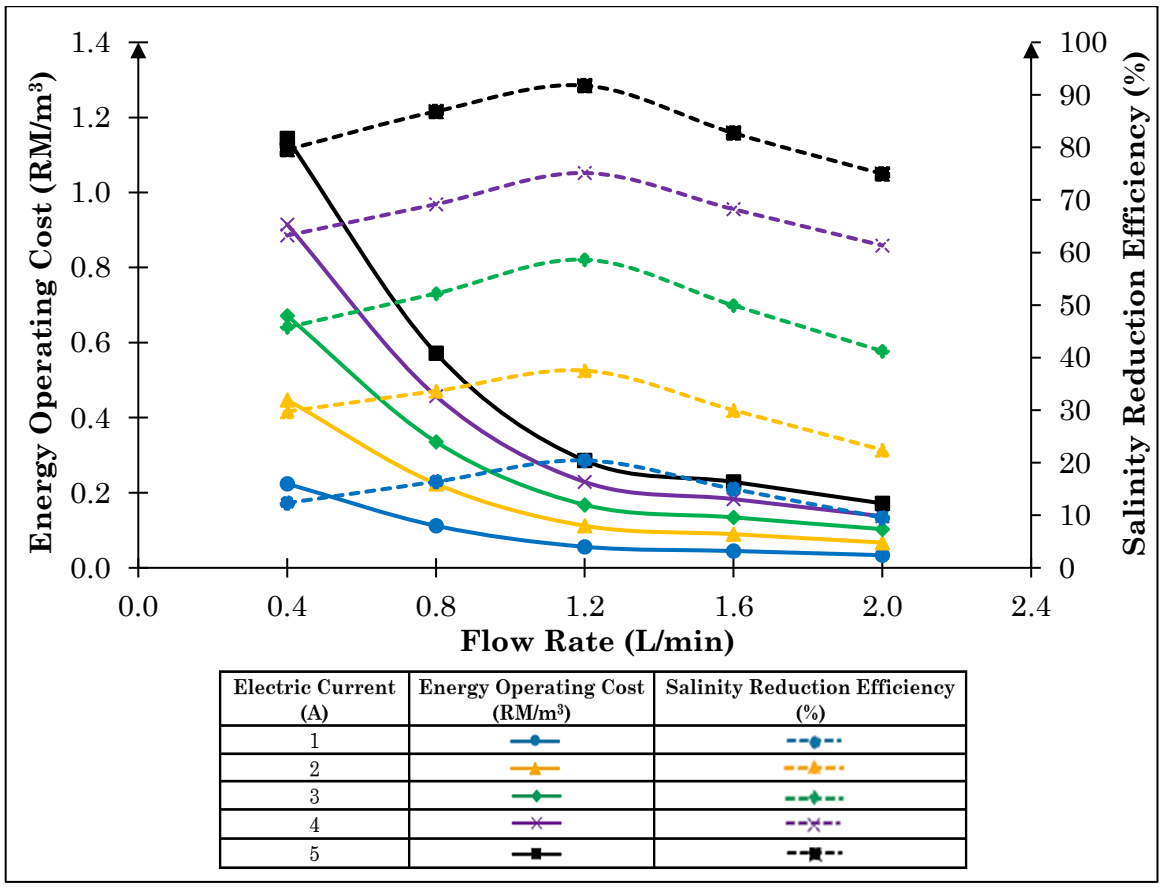

Figure 4.8: Effects of Electric Current and Flow Rate on Energy Operating Cost with Electrocoagulation Treatment of Brackish Peat Water with 30% of Seawater Percentage

A study conducted by Garcia-Segura et al. (2017) also reported that high electric current could lead to high energy operating costs owing to high specific electrical energy consumption with electrocoagulation treatment. Another factor that could lead to high energy operating costs is due to high electrode materials consumption owing to the high

dissociation of metal ions from sacrificial anodes (Papadopoulus et al., 2019). In order to reduce the energy operating cost, this study has increased the flow rate of brackish peat water in the continuous electrocoagulation treatment system. This study has noticed that the energy operating cost decreases when the flow rate increases in electrocoagulation treatment. When the flow rate is increased from 0.4 L/min to 2.0 L/min at 5 A of electric current, the energy operating cost is reduced from RM 1.14 per meter cubic to RM 0.17 per meter cubic. This signifies the energy operating cost is inversely proportional to flow rate in electrocoagulation treatment. This finding is similar to a study conducted by Ebba et al. (2022) which reported that high flow rate is associated with short residence time in electrocoagulation treatment. The study attempted by Ebba et al. (2022) found high residence time led to high energy operating costs as stated in Faraday law.

As shown in **Figure 4.8**, this study has also noticed that the highest salinity reduction efficiency of 91.78% in brackish peat water with 30% of seawater percentage could be attained at 5 A of electric current. Although electrocoagulation treatment is reasonable at high electric current, this study has found that the salinity reduction efficiency is low at both low and high flow rates. In this study, the salinity reduction efficiency in brackish peat water is achieved at 79.59% at 0.4 L/min and then increased to 91.78% when electrocoagulation treatment is applied with 1.2 L/min of flow rate. The salinity reduction efficiency has reduced to 74.97% of salinity reduction efficiency when the flow rate is increased to 2.0 L/min. This indicates that electrocoagulation treatment could achieve maximum salinity reduction efficiency of 91.78% in brackish peat water at 5 A of electric current and 1.2 L/min of flow rate. Under these conditions, this study found that the treatment of brackish peat water with a seawater percentage of 30% cost only RM 0.29 per meter cubic.

ii. Effect of Specific Electrical Energy Consumption (SEEC) on Energy Operating Cost in Electrocoagulation Treatment.

From the conducted energy operating cost analysis, the treatment of brackish peat water is optimum at 5 A of electric current. In order to investigate the effect of flow rate on specific electrical energy consumption, this study has evaluated the residence time and electrode materials consumption as shown in **Table 4.1**.

Table 4.1: Energy Operating Cost for The Treatment of Brackish Peat Water with Continuous Electrocoagulation Treatment at 5 A of Electric Current

Flow Rate (L/min)	Residence Time (min)	SEEC (kWh)	EMC (g $Al(OH)_3/m^3$)	EOC (RM/m^3)	EOC (RM/L)
0.4	20	2.40	80.0	1.14	0.0011
0.8	10	1.19	40.0	0.57	0.00057
1.2	5	0.60	20.0	0.29	0.00029
1.6	4	0.48	16.0	0.23	0.00023
2.0	3	0.36	12.0	0.17	0.00017

The flow rate has significantly affected the residence time, specific electrical energy consumption, electrode material consumption, and energy operating cost when continuous electrocoagulation is utilized on brackish peat water. This study has observed that the higher the flow rate, the lower the specific electrical energy consumption in electrocoagulation treatment. These conditions could lead to low energy operating costs as depicted in **Figure 4.9**. The specific electrical energy consumption (SEEC) decreases inversely to the flow rate in electrocoagulation treatment. In this study, it is noticed that the highest SEEC of 2.38 kWh/m^3 is attainable at 0.4 L/min of flow rate whereas the lowest SEEC of 0.36 kWh/m^3 is observed at 2.0 L/min of flow rate. Although electrocoagulation treatment could achieve low SEEC at 2.0 L/min of flow rate, this study has discovered that electrocoagulation treatment could achieve a maximum of 91.78% salinity reduction efficiency only at 1.2 L/min. When the flow rate is increased to 2.0 L/min, the salinity reduction efficiency has dropped to 74.97%. Wu et al. (2021) reported a similar finding that continuous flow rate of 1.0 L/min could

achieve 95% of decolorization rate fast and stable formation of electrocoagulation flocs. In addition, this flow rate leads to high formation of aluminium hydroxides in electrocoagulation treatment system (Nugroho et al., 2021).

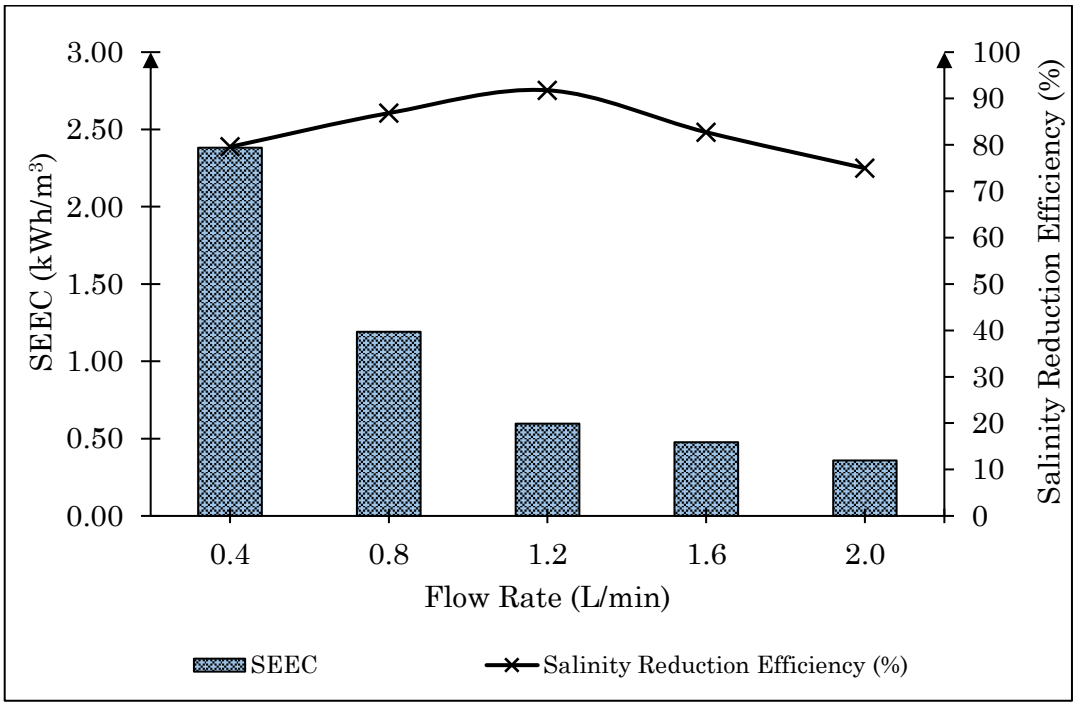

Figure 4.9: Effect of Flow Rate on Specific Electrical Energy Consumption (SEEC) with Electrocoagulation Treatment at 5 A of Electric Current in Brackish Peat Water with 30% of Seawater Percentage

iii. Comparison of Energy Operating Cost between Electrocoagulation and other Water Treatment Processes.

In electrocoagulation treatment, the energy operating cost is dependent on specific electrical energy consumption (SEEC) and electrode materials consumption (EMC) and this has been stated by Faraday's laws. This study has found that the treatment of brackish peat water with continuous electrocoagulation treatment costs only RM 0.29 per meter cubic which is comparable to other treatment processes as tabulated in **Table 4.2**.

Table 4.2: Comparison of Energy Operating Cost between Electrocoagulation and Other Water Treatment Processes

Treatment	Water Supply Agency/Water Sources	Energy Operating Cost (RM/m^3)	References
Electrocoagulation	Brackish Peat Water	0.29	This study
Chemical Coagulation (Fresh River Water)	Sibu Water Board (SWB)	0.43	SWB (2018)
	Jabatan Bekalan Air Luar Bandar (JBALB)	0.44	Petinggi (2022)
	Lembaga Air Kawasan Utara (LAKU)	0.60	National Audit Department (2022)
	Kuching Water Board	0.61	KWB (2018)
Membrane Related Process (Saline Water)	Reverse Osmosis	0.54 – 1.80	Al-Raad et al. (2019)

The energy operating cost with electrocoagulation treatment is much lower than chemical coagulation and membrane-related processes. In Sarawak, most water supply agencies are utilizing chemical coagulation treatment in order to treat fresh river water sources for domestic consumption with average energy operating cost of RM 0.52 per meter cubic (Sibu Water Board, 2018; Kuching Water Board, 2018; Petinggi, 2022; National Audit Department, 2022). Even though chemical coagulation treatment is effective on fresh river water sources in Sarawak, its application on brackish peat water is unknown. A study conducted by Elma et al. (2020) reported that chemical coagulation treatment could not be utilized to remove conductivity and total dissolved solids from saline water sources. This signifies that chemical coagulation treatment is not applicable for salinity reduction in saline water sources. The energy operating cost with chemical coagulation is higher than the electrocoagulation treatment. In this study, it is observed that the energy operating cost with electrocoagulation treatment is 44% less than chemical coagulation treatment in Sarawak. This is possibly due to chemical coagulation treatment requiring high energy and operating cost in order to attain high reduction efficiency. As reported by Kuching Water Board (2018), chemical coagulation treatment utilized numerous chemical additives substances particularly aluminium

sulphate, hydrated lime, liquid chlorine, anhydrous ammonia, sodium silicofluoride, sodium silica, sodium bicarbonate, polymer coagulants, polymer flocculants, aluminium chlorohydrate, and polyaluminium chlorides.

Several conducted studies had also reported that chemical coagulation treatment possesses drawbacks in terms of extensive sludge management due to toxic sludge generation (Sun et al., 2019; Zhang et al., 2020). A study conducted by Khor et al. (2020) has also informed that the energy operating cost in chemical coagulation treatment is usually higher than electrocoagulation treatment. This is possibly due to chemical coagulation treatment covering energy operating costs in terms of chemical and electrical consumption as well as energy of chemical production, transportation, and mixing of chemical coagulants (Gasmi et al., 2022). Even though reverse osmosis could completely remove salinity from saline water sources, this treatment system required a high energy operating cost. According to Al-Raad et al. (2019), the energy operating cost to desalinate saline water costs approximately RM 0.54 to RM 1.80 per meter cubic. In comparison to electrocoagulation treatment, this study has found that such a system could effectively reduce 91.78% of salinity in brackish peat water which is suitable for domestic consumption with energy consumption that costs only RM 0.29 per meter cubic. Membrane-related process, on the other hand, possesses several drawbacks in terms of membrane fouling and degradation issues due to exposure to attacking chloride ions in saline water sources (Wilson & George, 2020; Gürses et al., 2021).

4.3 Stage 2: Adsorption Kinetic Models and Analysis of Electrocoagulation Flocs

Electrocoagulation treatment produces gelatinous white aluminium hydroxides which reduce salinity levels in brackish peat water sources. In order to investigate the

occurrence of adsorption process in electrocoagulation treatment, this study has formulated adsorption isotherm and kinetic order models. This study also conducts electrocoagulation flocs analysis to determine the presence of sodium and chloride elements with Energy Dispersive X-Ray (EDX) analysis.

4.3.1 Langmuir and Freundlich Adsorption Isotherm Models

Continuous electrocoagulation treatment is utilized to reduce the salinity levels in brackish peat water at optimum 5 A of electric current and 1.2 L/min of flow rate. In electrocoagulation, the sacrificial anode electrodes release aluminium ions whereas the cathode electrodes generate hydroxide ions as illustrated in **Figure 4.10**.

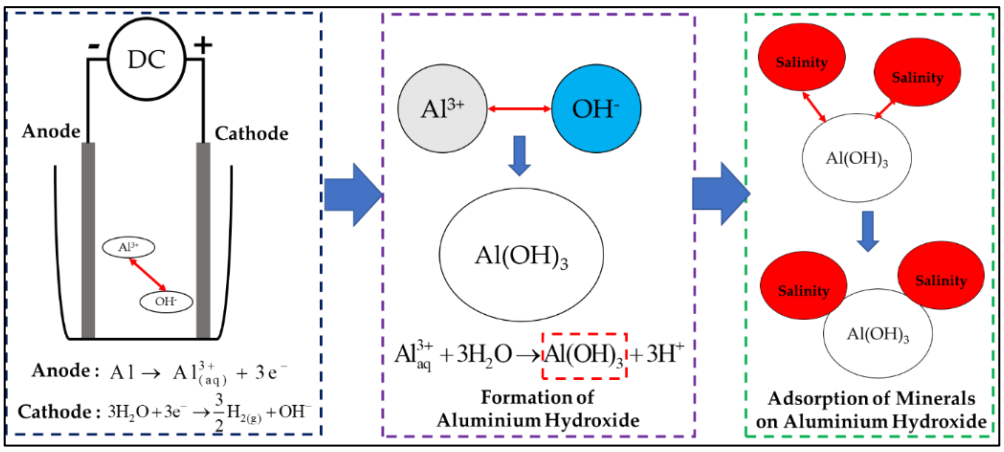

Figure 4.10: Illustration of Salinity Reduction with Adsorption Process in Continuous Electrocoagulation Treatment

The redox reaction between both aluminium and hydroxide ions is a precursor to formation of aluminium hydroxide coagulants. This study has noticed that aluminium hydroxide coagulants adsorb salinity from brackish peat water in the form of insoluble electrocoagulation flocs. The adsorption mechanism in electrocoagulation treatment of brackish peat water could be evaluated by formulating Langmuir and Freundlich adsorption isotherm models as shown in **Table 4.3.** The adsorption capacity for salinity reduction has increased from 79.10 mg/g to 2,499.70 mg/g when the seawater percentage is raised from 0% to 70%. When the seawater percentage being

more than 70%, this study has noticed that the adsorption capacity significantly decreased to 2,107.70 mg/g. This indicates that the maximum adsorption capacity with aluminum hydroxides could be obtained at 2,499.70 mg/g in brackish peat water with a 70% seawater percentage.

Table 4.3: Comparison of Adsorption Capacity (q_e) for Salinity Reduction in Brackish Peat Water with Langmuir and Freundlich Adsorption Isotherm Models

Seawater Percentage (%)	Salinity Reduction Efficiency (%)	Experimental adsorption capacity, q_e (mg/g)	Langmuir Adsorption Capacity		Freundlich Adsorption Capacity	
			q_L (mg/g)	Deviation (%)	q_F (mg/g)	Deviation (%)
0	71.52	79.10	71.47	10.67	74.15	6.67
10	89.01	788.20	771.87	2.11	754.26	4.50
30	91.78	1,609.30	1,678.89	4.14	1,675.10	3.93
50	83.38	2,185.75	2,151.75	1.58	2,335.30	6.40
70	71.59	2,499.70	2,414.05	3.54	2,541.50	1.64
80	52.98	2,317.35	2,447.11	5.30	2,435.35	4.84
90	40.18	2,107.70	2,445.04	13.80	2,218.31	4.99

The experimental data is well fitted with the Langmuir and Freundlich adsorption isotherm models. In this study, the deviation between experimental and modelled values is within the acceptable range of 10% particularly for Freundlich adsorption isotherm model. Although the deviation values for seawater percentage at 0% and 90% are more than 10%, the adsorption capacity for seawater percentage that ranges from 10% to 80% follows the Langmuir adsorption isotherm model. This signifies that the reduction of salinity levels in brackish peat water follows monolayer adsorption process (Liu et al., 2019). This study has analyzed several parameters in Langmuir and Freundlich isotherm model as tabulated in **Table 4.4.**

Table 4.4: Parameters for Adsorption Process for Salinity Reduction in Brackish Peat Water with Adsorption Isotherm Models

Isotherm Model	Parameters	Values
Langmuir Isotherms	q_m (mg/g)	2,500.00
	K_L (L/mg)	0.004
	R_L	0.03
	R^2	0.91
Freundlich Isotherm	K_F (L/g)	1,032.52
	$1/n_f$	0.11
	R^2	0.90

Table 4.4 shows the maximum adsorption capacity of aluminium hydroxides obtained from Langmuir adsorption isotherm model is equivalent to 2,500 mg/g. This observation is also similar to the adsorption capacity obtained from experimental data for brackish peat water with a seawater percentage of 70%. In addition, this study has noticed that the shape of Langmuir isotherm models favour monolayer adsorption process when the seawater percentage is less than 70%. This is due to the Langmuir separation factors, R_L, is less than one. As reported by Al-Ghoutti and Da'ana (2020), an adsorption process is favourable when the R_L is more than zero and less than one.

This phenomenon could also be confirmed by evaluating the regression coefficient (R^2) values. In this study, it is found that the R^2 for formulated Langmuir adsorption isotherm model is equivalent to 0.91 and this signifies that the model has high validity owing to a good correlation between experimental and modelled data (Rahman et al., 2020d). Moreover, this study also noticed that the salinity reduction in brackish peat water follows Freundlich adsorption isotherm models due to the R^2 being equal to 0.90. From the formulated Freundlich isotherm model, this study has also found that the salinity reduction in brackish peat water follows a multilayer adsorption process due to the value of $\frac{1}{n_f}$ is within the ranges of 0.1 and 0.5 (Ayub et al., 2020). This study has observed that the experimental data for salinity reduction is well fitted to both Langmuir and Freundlich adsorption isotherm model when the seawater percentage is less than 70% as shown by **Figure 4.11**. The adsorption of salinity on aluminium hydroxide coagulants is due to both monolayer and multilayer adsorption. According to Shaker et al. (2020), this type of adsorption occurs within microscopic structures of coagulants that are dominated by single monolayer adsorption.

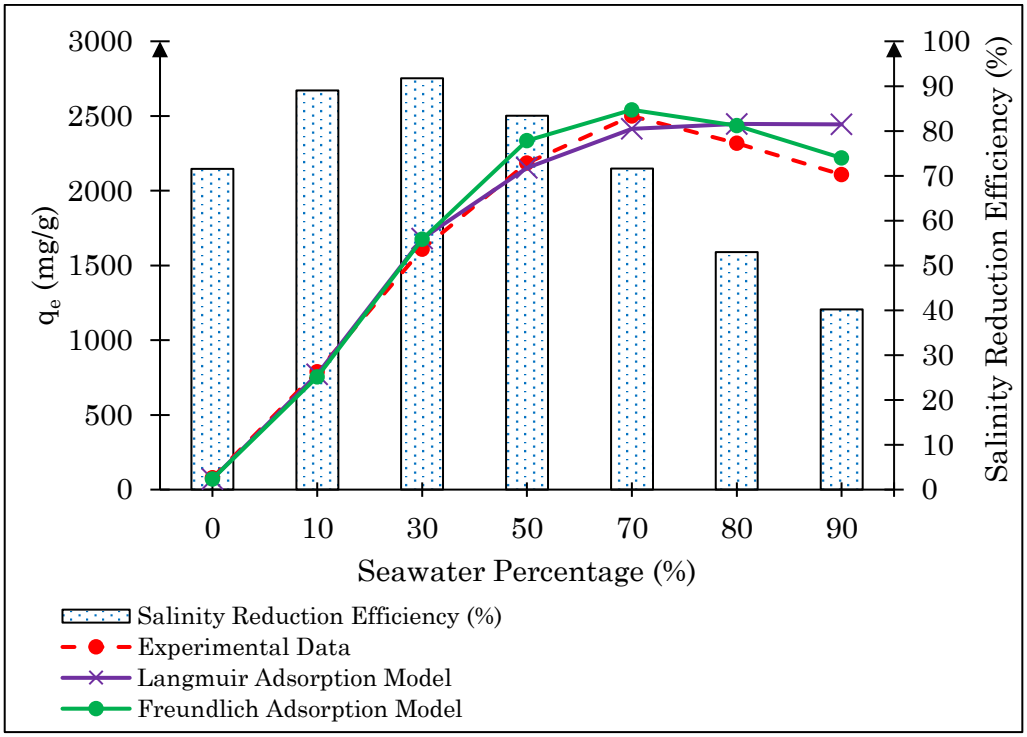

Figure 4.11: Experimental Data Fitting to Langmuir and Freundlich Adsorption Isotherm Models

This observation is also similar to a study conducted Bendaia et al. (2021) which reported that some heterogeneous adsorbents with multiple actives sites were not limited only to monolayer adsorption but also multilayer adsorption when the experimental data achieved well correlation with Langmuir and Freundlich adsorption isotherm models. This study has found that the salinity reduction efficiency increased from 71.52% to 91.78% when the seawater percentage was raised from 0% to 30% as depicted in **Figure 4.11**. Although the maximum adsorption capacity is achieved at 70% of seawater percentage, this study has observed that the salinity reduction efficiency is lower than brackish peat water with 30% of seawater percentage. This is possibly due to a less amount of aluminium hydroxides coagulants that are present in brackish peat water sources, thus reducing the salinity reduction efficiency (Guisela et al., 2022).

4.3.2 Linear and Non-Linear Pseudo-First Order Kinetic Models

Pseudo-first-order model is the Lagrange rate equation that calculates adsorption rate constant by plotting equilibrium adsorption capacity against residence time (Revellame et al., 2020). In order to determine the adsorption rate, this study has formulated pseudo first order model as tabulated in in **Table 4.5**.

Table 4.5: Pseudo-First Orders Kinetic Model Parameters for Salinity Reduction in Brackish Peat Water with Continuous Electrocoagulation Treatment

Seawater Percentage (%)	$q_{e,exp}$ (mg/g)	Pseudo-first order (Linear form)			Pseudo-first order (Non-linear form)		
		$q_{e,model}$ (mg/g)	K_1 (min^{-1})	R^2	$q_{e,model}$ (mg/g)	K_1 (min^{-1})	R^2
0	79.10	1.50	0.045	0.68	79.20	2.65	0.99
10	788.20	6.00	0.092	0.55	789.25	2.65	0.99
30	1,609.30	7.32	0.102	0.57	1,611.43	2.65	0.99
50	2,185.75	9.20	0.106	0.55	2,188.65	2.65	0.99
70	2,499.70	74.13	0.072	0.52	2,503.02	2.65	0.99
80	2,317.35	113.11	0.066	0.37	2,320.42	2.65	0.99
90	2,107.70	132.01	0.066	0.37	2,110.50	2.65	0.99

As shown in **Table 4.5**, this study has formulated pseudo-first order kinetic in both linear and non-linear forms. This study has also observed that the experimental adsorption capacity is well fitted to non-linear pseudo first order rather than in linear form. This is due to the regression value of the non-linear model ($R^2 = 0.99$) being higher than linear model ($R^2 < 0.75$). According to Mehri et al. (2021), the value of R^2 that is less than 0.75 signifies inaccuracy of formulated model. In comparison to adsorption capacity, the model values of non-linear form show similar observations to experimental values as compared to linear form. In addition, this study has found that the plot between log ($q_e - q_t$) and t does not show any correlation to each other as shown in **Figure 4.12**. This study has noticed that the plot of log ($q_e - q_t$) against time generates scattering patterns of lines. This signifies that linear model could not be utilized to predict the adsorption rate constant for salinity reduction in brackish peat water due to the linearized pseudo-first-order model requires an estimated q_e in order

to attain straightforward parameter estimation (Sahoo & Prelot, 2020). Although estimation of q_e could attain instant parameter values, this method is not suitable for some direct parameter estimation owing to unreachable equilibrium to the unknown q_e (Shen et al., 2022).

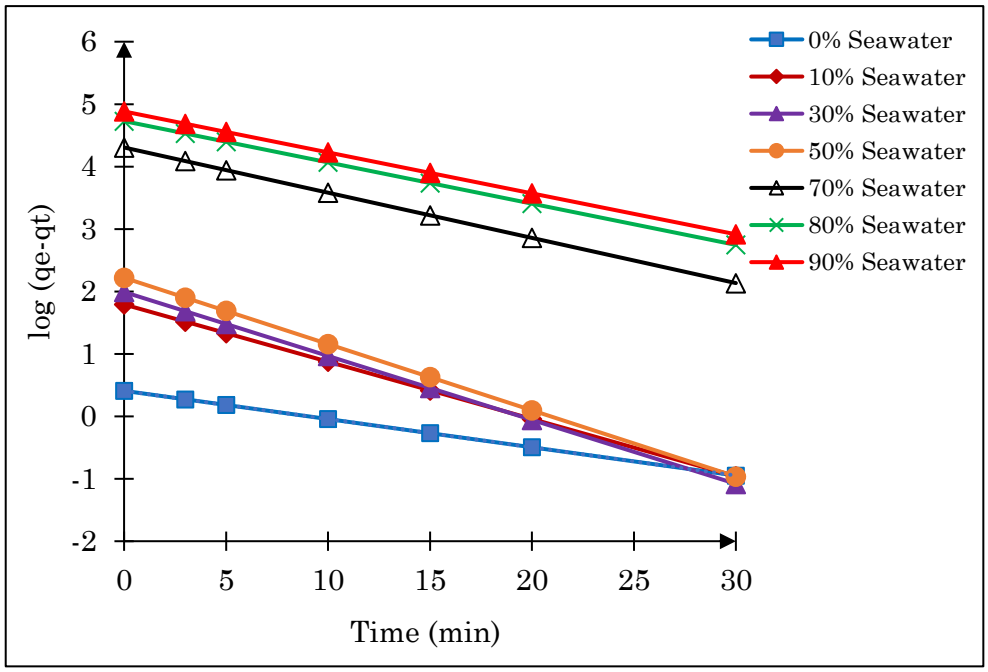

Figure 4.12: Linear Pseudo-first Order Kinetic for Salinity Reduction in Brackish Peat Water with Electrocoagulation Treatment

Realizing this problem, this study formulates salinity adsorption with the non-linear pseudo-first-order kinetic model as shown in **Figure 4.13**. This study has noticed the salinity adsorption in brackish peat water correlates well with the non-linear pseudo-first-order model. The highest adsorption capacity is attained at 2,503.02 mg/g in brackish peat water with a 70% of seawater percentage. The adsorption capacity increased from 79.10 mg/g to 2,503.02 mg/g when the seawater percentage being raised from 0% to 70%, thus, indicating an effective salinity reduction efficiency within this range of seawater percentage. The non-linear pseudo first order model provides an accurate estimation of kinetic model parameters to describe the whole adsorption process instead of modelling the initial stage only (Jasper et al., 2020).

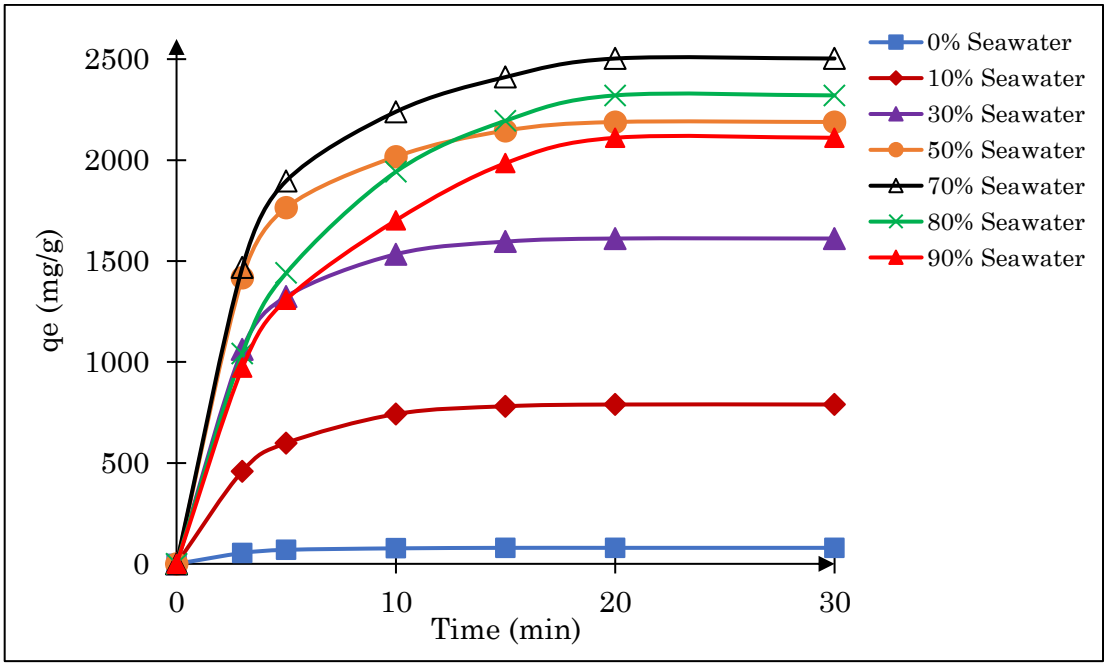

Figure 4.13: Non-Linear Pseudo-First Order Kinetic Models for Salinity Reduction in Brackish Peat Water with Electrocoagulation Treatment

From the formulated non-linear pseudo first order model, this study has evaluated adsorption rate constant for salinity reduction in brackish peat water as tabulated in **Table 4.6**.

Table 4.6: Kinetic Parameters for Salinity Reduction in Brackish Peat Water with Non-Linear Pseudo-First-Order Model

Seawater Percentage (%)	Experimental Adsorption Capacity, q_e (mg/g)	Modelled Adsorption Capacity, q_e (mg/g)	Adsorption Rate Constant, K_1 (min^{-1})	R^2	Deviation (%)	Salinity Reduction Efficiency (%)
0	79.10	79.20	2.65	0.99	0.13	71.52
10	788.20	789.25	2.65	0.99	0.13	89.01
30	1,609.30	1,611.43	2.65	0.99	0.13	91.78
50	2,185.75	2,188.65	2.65	0.99	0.13	83.38
70	2,499.70	2,503.02	2.65	0.99	0.13	71.59
80	2,317.35	2,320.42	2.65	0.99	0.13	52.98
90	2,107.70	2,110.50	2.65	0.99	0.13	40.18

The adsorption rate constant in brackish peat water with seawater percentage that ranged from 0% to 90% equals to 2.65 min^{-1}. This study has also noticed the percentage deviation between experimental and modelled adsorption capacity is approximately 0.13%. This indicates the formulated pseudo-first-order kinetic model is

valid for kinetic parameter estimation during to deviation is less than 10% (Acharya et al., 2018).

4.3.3 Energy Dispersive X-Ray Analysis of Electrocoagulation Flocs

The electrocoagulation treatment system produces in-situ aluminium hydroxide coagulants that bind to salinity elements in brackish peat water and then form electrocoagulation flocs and the compositions is depicted by **Figure 4.14**. From conducted EDX analysis, the study has observed the presence of oxygen, aluminium, carbon, ytterbium, silica, sodium, sulphate, magnesium, chloride, and calcium on the electrocoagulation flocs. The EDX analysis also examined the levels of intensity and dispersive energy of atomic molecules in order to examine the composition of electrocoagulation flocs. The incidence beam in EDX could excite the inner shell electron which caused this electron to be ejected from the shell, thus, generating an electron-hole filled by an electron from a higher energy shell (Titus et al., 2019).

The energy differential between higher and lower energy shells that are emitted in the form of X-rays have under signal processing to generate elemental mass percentage as tabulated in **Table 4.7**. In this study, the highest mass composition of aluminium (18.57%) and oxygen (45.58%) are found in electrocoagulation flocs that are being produced in brackish peat water with a 30% of seawater percentage. The EDX analysis which is conducted in this study has also confirmed that electrocoagulation treatment produced in-situ aluminium hydroxide coagulants owing to redox reactions (Hu et al., 2017; Sakthisharmila et al., 2018). This also signifies that electrocoagulation flocs are mainly constituted with aluminium hydroxide coagulants.

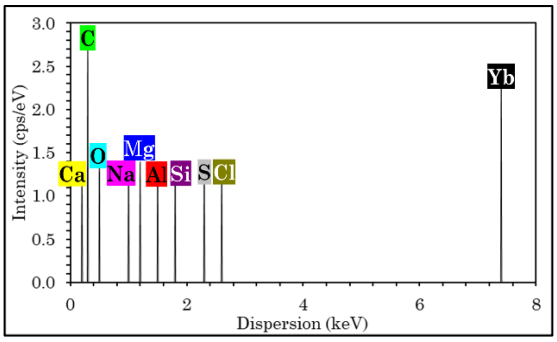

(A) Electrocoagulation Flocs from Brackish Peat Water with 0% of Seawater Percentage

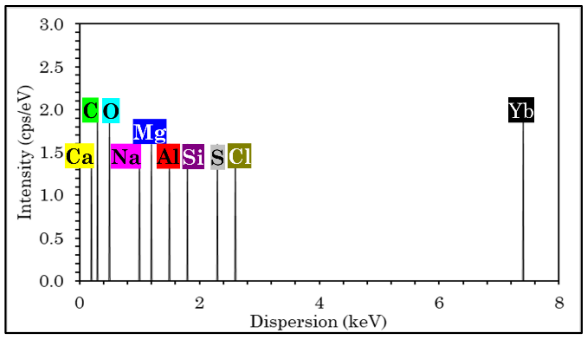

(B) Electrocoagulation Flocs from Brackish Peat Water with 10% of Seawater Percentage

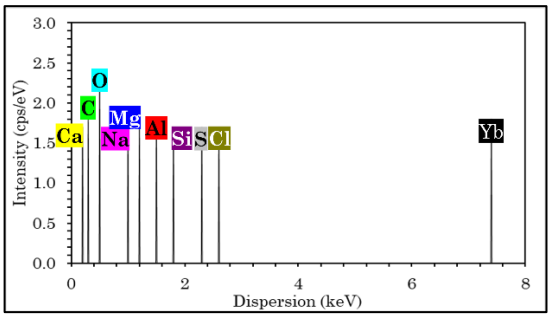

(C) Electrocoagulation Flocs from Brackish Peat Water with 30% of Seawater Percentage

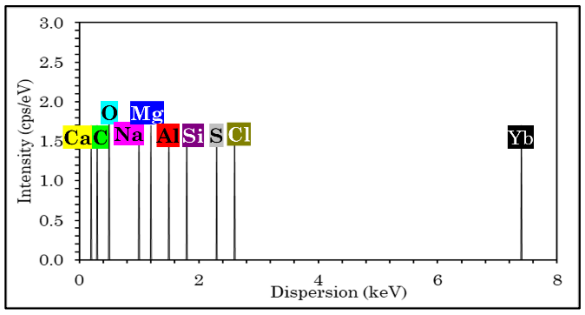

(D) Electrocoagulation Flocs from Brackish Peat Water with 50% of Seawater Percentage

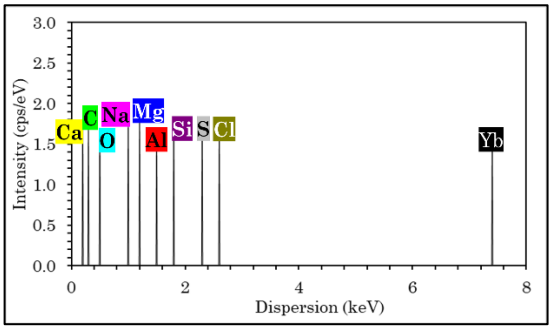

(E) Electrocoagulation Flocs from Brackish Peat Water with 70% of Seawater Percentage

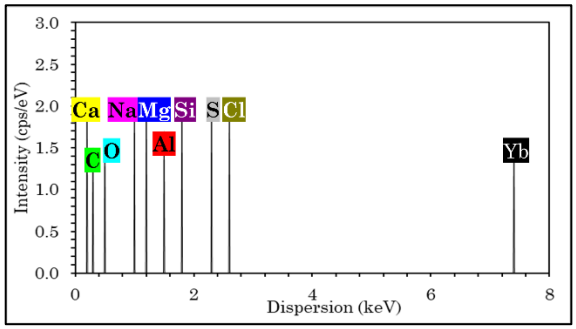

(F) Electrocoagulation Flocs from Brackish Peat Water with 80% of Seawater Percentage

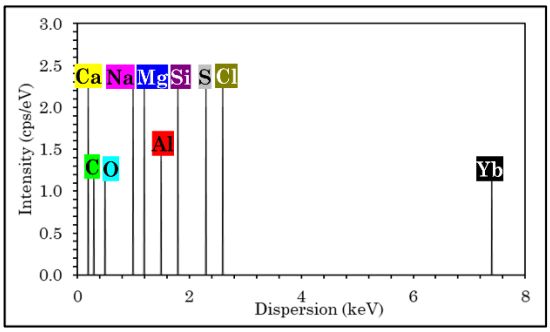

(G) Electrocoagulation Flocs from Brackish Peat Water with 90% of Seawater Percentage

Legend

Ca	:	Calcium
C	:	Carbon
O	:	Oxygen
Na	:	Sodium
Mg	:	Magnesium
Al	:	Aluminium
Si	:	Silicon
S	:	Sulphur
Cl	:	Chloride
Yb	:	Ytterbium

Figure 4.14: Analysis of Electrocoagulation Flocs from Brackish Peat Water with Energy Dispersive X-Ray

Table 4.7: Elemental Mass Percentage on Electrocoagulation Flocs from Brackish Peat Water with Seawater Percentage That Ranged from 0% to 90%

Seawater Percentage (%)	**0**	**10**	**30**	**50**	**70**	**80**	**90**
Elemental Composition (%)							
Oxygen	45.80	45.49	45.58	44.44	43.85	42.29	36.87
Aluminium	17.00	18.31	18.57	18.50	18.00	17.11	16.00
Carbon	30.05	19.48	13.92	9.98	3.62	2.42	2.05
Ytterbium	4.20	3.93	3.84	3.65	3.59	3.52	2.79
Silica	1.22	2.13	2.88	3.75	4.06	5.29	6.88
Sodium	1.02	1.48	2.92	5.09	7.78	8.12	9.28
Sulphate	0.84	1.16	1.27	1.33	2.81	2.17	2.12
Magnesium	0.46	3.30	3.26	3.33	3.39	3.94	4.02
Chloride	0.42	3.78	7.37	8.91	12.62	13.41	15.99
Calcium	0.37	0.58	0.73	1.02	1.32	1.72	1.63

Electrocoagulation flocs also contain several salts element particularly silica, sodium, sulphate, magnesium, chloride, and calcium. It is found that the presence of sodium and chloride on electrocoagulation flocs has possibly led to salinity reduction in brackish peat water as shown by **Figure 4.15**. This indicates that aluminium hydroxide coagulants in electrocoagulation treatment could separate salt elements in brackish peat water in the form of flocs. The salinity reduction efficiency has increased from 71.52% to 91.78% when the seawater percentage in brackish peat water is raised from 0% to 30%. The treatment of brackish peat water with electrocoagulation treatment has achieved high salinity reduction efficiency due to the effective production of aluminium hydroxide coagulants. A study conducted by Al-Raad et al. (2019) informed that electrocoagulation treatment could remove chlorides ion from saline water sources with the aid of aluminium hydroxide coagulants. Additionally, the salinity reduction efficiency has reduced from 91.78% to 40.18% when the seawater percentage in brackish peat water is raised from 30% to 90% as depicted by **Figure 4.15**.

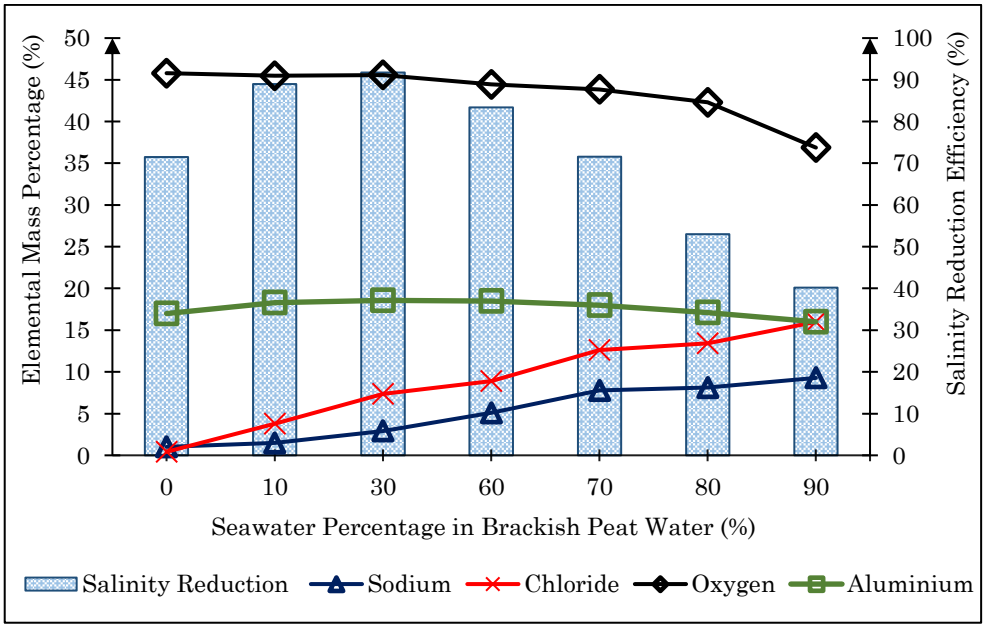

Figure 4.15: Relationship Between Salinity Reduction Efficiency, Sodium Chloride, and Aluminium Hydroxides in Electrocoagulation Treatment

4.4 Stage 3: Statistical Analysis of Salinity Reduction with Electrocoagulation Treatment

A statistical model has been developed in this study to achieve maximum salinity reduction efficiency and minimum energy operating cost in electrocoagulation. The study has also utilized Design Expert (State Ease Inc.) software to develop statistical analysis model with response surface methodology.

4.4.1 Experimental Statistical Design

In this study, the experimental design has been employed with three level factors of central composite design (CCD) particularly to optimize the operating parameters as shown in **Table 4.8**. This study has investigated the effects of seawater percentage (0% to 90%), electric current (1 A to 5 A), and flow rate (0.4 L/min to 2.0 L/min) on salinity reduction efficiency and energy operating cost with continuous electrocoagulation treatment.

Table 4.8: Central Composite Design (CCD) Experimental Statistical Design

No	Seawater Percentage (%)	Electric Current (A)	Flow Rate (L/min)	Salinity Reduction Efficiency (%)			Energy Operating Cost (RM/m³)		
				Exp	*RSM*	*Error (%)*	*Exp.*	*RSM*	*Error (%)*
1	0	1	0.4	12.04	12.37	2.63	0.22	0.23	2.64
2	0	2	0.8	33.85	35.95	5.82	0.22	0.22	0.01
3	0	3	1.2	50.93	50.24	1.38	0.17	0.18	5.53
4	0	4	1.6	47.12	45.24	4.16	0.18	0.18	3.57
5	0	5	2.0	49.37	50.95	3.11	0.17	0.16	6.66
6	10	1	0.4	24.00	25.41	5.55	0.22	0.23	2.64
7	10	2	0.8	49.29	48.08	2.50	0.22	0.22	0.01
8	10	3	1.2	62.04	61.47	0.93	0.17	0.18	5.53
9	10	4	1.6	70.25	65.57	7.14	0.18	0.18	3.57
10	10	5	2	62.26	60.37	3.13	0.17	0.16	6.66
11	30	1	0.4	41.42	40.64	1.92	0.22	0.23	2.64
12	30	2	0.8	60.29	61.50	1.97	0.22	0.22	0.01
13	30	3	1.2	80.36	73.08	9.96	0.17	0.18	5.53
14	30	4	1.6	77.59	75.36	2.95	0.18	0.18	3.57
15	30	5	2	74.97	68.36	9.68	0.17	0.16	6.66
16	50	1	0.4	42.76	41.39	3.30	0.22	0.23	2.64
17	50	2	0.8	58.32	60.44	3.51	0.22	0.22	0.01
18	50	3	1.2	69.61	70.20	0.84	0.17	0.18	5.53
19	50	4	1.6	73.71	70.68	4.29	0.18	0.18	3.57
20	50	5	2	53.86	61.86	12.94	0.17	0.16	6.66
21	70	1	0.4	25.39	27.66	8.22	0.22	0.23	2.64
22	70	2	0.8	42.64	44.90	5.03	0.22	0.22	0.01
23	70	3	1.2	55.82	52.85	5.62	0.17	0.18	5.53
24	70	4	1.6	47.50	51.51	7.78	0.18	0.18	3.57
25	70	5	2	34.86	37.88	7.96	0.17	0.16	6.66
26	80	1	0.4	14.72	15.37	4.19	0.22	0.23	2.64
27	80	2	0.8	33.85	31.70	6.77	0.22	0.22	0.01
28	80	3	1.2	37.07	38.75	4.32	0.17	0.18	5.53
29	80	4	1.6	35.83	36.50	1.83	0.18	0.18	3.57
30	80	5	2	26.92	24.97	7.84	0.17	0.16	6.66
31	90	1	0.4	7.19	8.39	14.27	0.22	0.23	2.64
32	90	2	0.8	15.10	14.88	1.45	0.22	0.22	0.01
33	90	3	1.2	21.98	21.02	4.57	0.17	0.18	5.53
34	90	4	1.6	19.38	17.87	8.43	0.18	0.18	3.57
35	90	5	2	8.82	8.43	4.65	0.17	0.16	6.66

Note: Exp - Experimental Data; RSM – Response Surface Methodology; Error – Deviation

Three independent variables which have been identified in designing the continuous electrocoagulation treatment of brackish peat water are utilized for optimization study. From the developed experimental design, the developed statistical design experiment has high accuracy and adequacy due to the percentage deviation between experimental and modelled values being less than 10% (Acharya et al., 2018).

4.4.2 Mathematical Quadratic Equations

From the developed statistical experimental model with central composite design (CCD), this study has noticed that salinity reduction in brackish peat water with electrocoagulation treatment follows polynomial quadratic equations. The empirical relationship between responses and investigated variables has been formulated with second-order polynomial equations in which the interaction terms of mathematical models are fitted to experimental values. The formulated quadratic models for salinity reduction efficiency and energy operating cost are equated as in **Equation 4.1** and **Equation 4.2** respectively.

$$SRE\ (\%) : -20.50 + 1.58X_1 + 12.46X_2 + 62.64X_3 - 0.09137X_1X_2 + 1.59X_2X_3 - 0.02X_1^2 + 0.01X_2^2 - 25.10X_3^2 \quad \textbf{(4.1)}$$

$$EOC\ (RM/m^3) : 0.36 + 0.000095X_1 + 0.23X_2 - 0.79X_3 - 0.000011X_1X_2 - 0.000027X_1X_3 - 0.12X_2X_3 + 0.00064X_2^2 + 0.33X_3^2 \quad \textbf{(4.2)}$$

Where *SRE (%)* refers to salinity reduction efficiency, *EOC (RM/m³)* refers to energy operating cost, X_1 refers to seawater percentage in brackish peat water, X_2 refers to electric current, and X_3 refers to flow rate. In order to assess the adequacy of mathematical models, this study has conducted a coefficient of determination (R^2) test as depicted in **Figure 4.16** and **Figure 4.17** respectively.

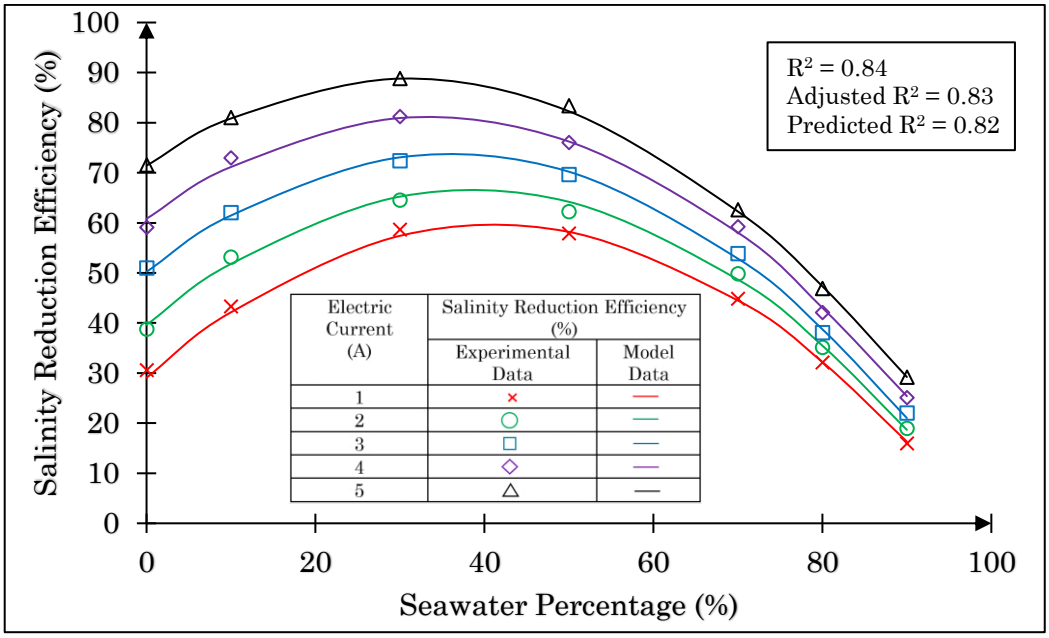

Figure 4.16: Regression Coefficient of Mathematical Equation for Salinity Reduction Efficiency

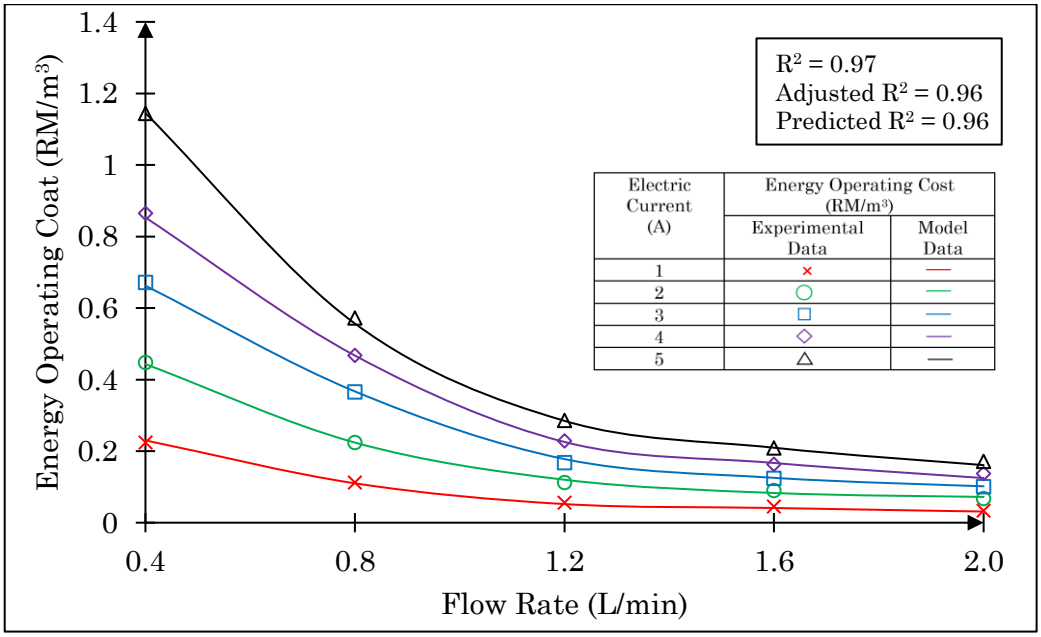

Figure 4.17: Regression Coefficient of Mathematical Model for Energy Operating Cost

This study has observed the data points between experimental and model values lie close to each other and this led to low residual errors as observed in **Figure 4.16** and **Figure 4.17. T**he R^2 values of mathematical models are higher than 0.75 which signifies the formulated models are valid for optimization purposes (Haas, 2020;

Rahman et al., 2020d). The adjusted and predicted R^2 values are also less than actual R^2 values due to the comparative explanatory power of mathematical models that require several variable reductions to correlate with experimental values (Piepho, 2020).

4.4.3 Model Validation with Analysis of Variance

This study employs analysis of variance (ANOVA) to correlate the interactions between process variables and responses as shown in **Table 4.9**. ANOVA reports the significant interaction between variables in terms of mean square, F- value, p-value.

Table 4.9: ANOVA and Statistical Parameters of Salinity Reduction Efficiency and Energy Operating Cost

Source	Salinity Reduction Efficiency (%)			Energy Operating Cost (RM/m^3)		
	Mean Square	**F-value**	**p-value**	**Mean Square**	**F-value**	**p-value**
Model	8,208.63	96.45	< 0.0001	1.4	510.23	< 0.0001
X_1-Seawater Percentage (%)	19,104.38	224.48	< 0.0001	0	0.0078	0.9298
X_2-Electric Current (A)	14,465.77	169.97	< 0.0001	3.22	1170.16	< 0.0001
X_3-Flow Rate (L/min)	284.27	3.34	0.0394	6.4	2323.59	< 0.0001
X_1X_2	2,996.41	35.21	< 0.0001	0	0.0148	0.9034
X_1X_3	0.2254	0.0026	0.959	0	0.0148	0.9034
X_2X_3	274.71	3.23	0.0742	1.47	533.6	< 0.0001
X_1^2	31,350.39	368.37	< 0.0001	0	0.0076	0.9307
X_2^2	0.0192	0.0002	0.988	0.0002	0.0726	0.7879
X_3^2	7,829.77	92	< 0.0001	1.38	501.56	< 0.0001
Residual	85.11			0.0028		
Coefficient of Variation	20.56%			18.11%		
Adequate Precision	40.54			84.60		

The developed statistical models for salinity reduction efficiency and energy operating cost are significant in this study due to the p-values of these models being less than 0.05 (Thakur, 2020). The model F-value of 96.45 which represents salinity

reduction efficiency and 510.23 refers to energy operating cost indicating there is only 0.01% chance that an F-value this large could occur due to noise. This study has also found that the interactions between seawater percentage, electric current, and flow rate are highly significant to salinity reduction efficiency owing to p-value is less than 0.05. The developed statistical model is highly significant due to acceptable residuals and coefficient of variation. This is due to the ratio of adequacy precision of the statistical model being more than four and suggesting that the developed model could be utilized for model optimization (Design Expert, 2022).

4.4.4 Three-Dimensional (3D) Response Surface Plots

The statistical model analysis determines the critical point on surface plots in terms of maximum, minimum, or saddle points. From the formulated mathematical models, this study has generated three-dimensional (3D) response surface plots to study the relationship between seawater percentage, electric current, and flow rate on salinity reduction efficiency and energy operating cost with electrocoagulation treatment.

i. Relationship between Seawater Percentage, Electric Current, and Flow Rate on Salinity Reduction Efficiency.

The effects of investigated variables particularly seawater percentage, electric current, and flow rate on salinity reduction have been identified in this study. RSM is employed to illustrate the effects of these varied variables as depicted in **Figure 4.18**, **Figure 4.19**, and **Figure 4.20** respectively. This study has found that the highest salinity reduction efficiency of 89% could be achieved at 5 A of electric current with a 30% of seawater percentage as shown by **Figure 4.18**. These conditions also favours

high generation of in-situ aluminium hydroxide coagulants that aid in the separation of salinity from brackish peat water sources with adsorption process.

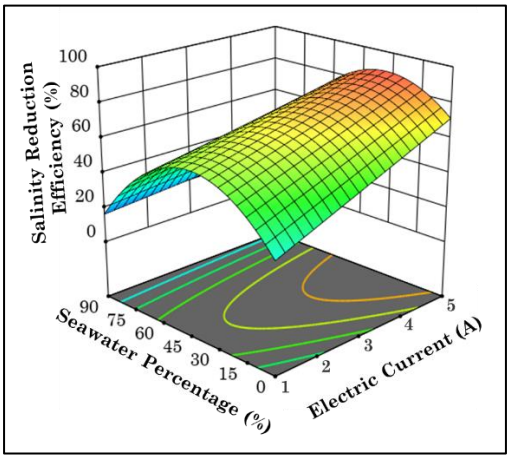

Figure 4.18: Relationship between Seawater Percentage and Electric Current on Salinity Reduction Efficiency at 1.2 L/min of Flow Rate

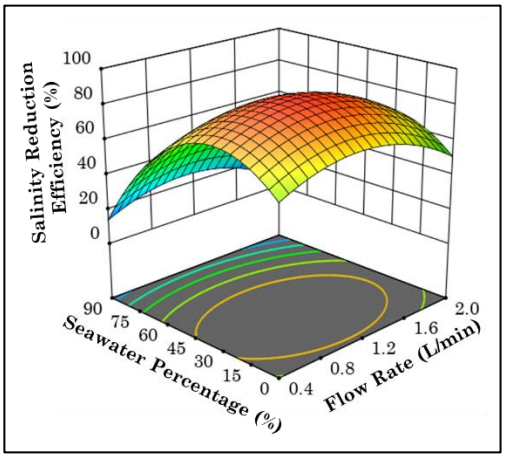

Figure 4.19: Relationship between Seawater Percentage and Flow Rate on Salinity Reduction Efficiency at 5 A of Electric Current

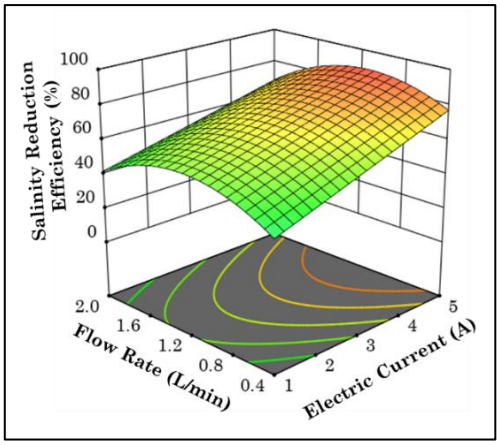

Figure 4.20: Relationship between Flow Rate and Electric Current on Salinity Reduction Efficiency at 30% of Seawater Percentage

This study has also noticed that the highest salinity reduction efficiency at 89% could also be achieved at 1.2 L/min of flow rate as shown in **Figure 4.19**. This is possibly due to such conditions also favour an effective mixing between in-situ aluminium hydroxides coagulants and salinity in brackish peat water as well as prevent further oxidation of these coagulants to form transitory compounds (Bendaia et al., 2021). As illustrated in **Figure 4.20**, this study has noticed that electrocoagulation could

effectively reduce 89% of salinity levels in brackish peat water sources at 5 A of electric current and 1.2 L/min of flow rate with a 30% of seawater percentage.

ii. Relationship between Seawater Percentage, Electric Current, and Flow Rate on Energy Operating Cost.

The relationship between seawater percentage, electric current, and flow rate on energy operating cost are depicted in **Figure 4.21** to **Figure 4.23**.

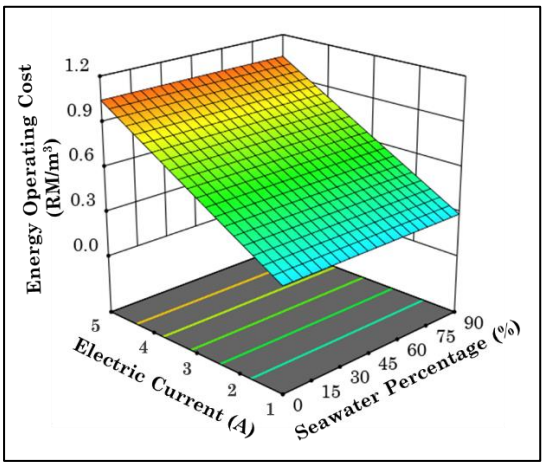

Figure 4.21: Relationship between Electric Current and Seawater Percentage on Energy Operating Cost at 1.2 L/min of Flow Rate

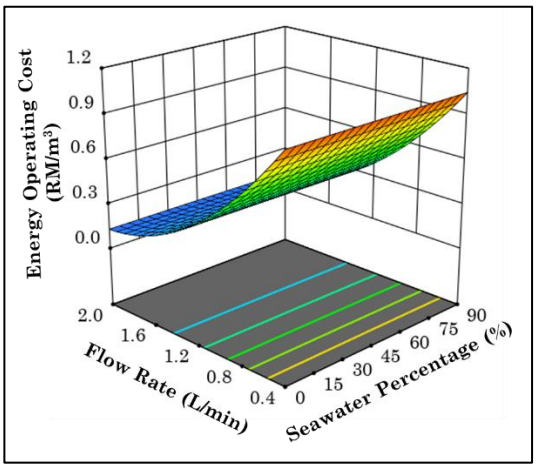

Figure 4.22: Relationship between Flow Rate and Seawater Percentage on Energy Operating Cost at 5 A of Electric Current

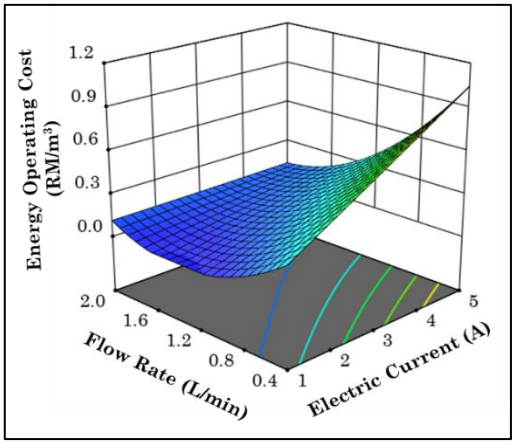

Figure 4.23: Relationship between Electric Current and Flow Rate on Energy Operating Cost at 30% of Seawater Percentage

As depicted in **Figure 4.21**, this study has noticed the seawater percentage has no significant interaction with energy operating cost due to the surface plot exhibiting a plateau shape. This observation is also similar to a study conducted by Khedher et al. (2023) which reported plateau plot surface indicates one of the investigated variables has no significant effect on the model response. In addition, this study has noticed that energy operating cost is directly proportional to the electric current as shown in **Figure 4.22**. Although high electric current could generate many in-situ aluminium hydroxides, such conditions could make electrocoagulation an energy-intensive treatment system. This is due to high electric current in electrocoagulation consuming high energy consumption as stated in Faraday's law (Papadopoulus et al., 2019). In order to mitigate this issue, this study has found that energy operating costs in electrocoagulation treatment could be conducted at a low flow rate of 1.2 L/min as shown in **Figure 4.23**.

iii. Numerical Optimization

Numerical optimization is conducted in this study to determine the optimum process parameters for maximum salinity reduction efficiency and minimum energy operating cost. From conducted numerical optimization, this study has found that the optimum operating parameters to attain maximum salinity reduction efficiency and minimum energy operating cost are compatible at 5 A of electric current and 1.2 L/min of flow rate with suitable seawater percentage at 30% as shown in **Table 4.10**.

Table 4.10: Electrocoagulation Treatment of Brackish Peat Water at Optimum 5 A of Electric Current, 1.2 L/min of Flow Rate, and 30% of Seawater Percentage

Responses	Model	Experiment	Deviation (%)
Salinity Reduction Efficiency (%)	89.00	91.78	2.72
Energy Operating Cost (RM/m^3)	0.28	0.29	3.45

CHAPTER 5

CONCLUSIONS

An experimental study has been conducted to reduce the salinity levels in brackish peat water by utilizing continuous electrocoagulation with aluminium electrodes. Correspondingly, this study has found that electrocoagulation treatment could be utilized to reduce the salinity levels in brackish peat water sources in Sarawak. The water quality analysis done in this study has found that the treated salinity levels of brackish peat water are considered suitable for domestic consumption when the seawater percentage being less than 30%. This is due to the fact that the treated salinity levels meet Class I standard in National Water Quality Standard because the salinity level is less than 500 mg/L as recommended by the Department of Environment in Malaysia.

The adsorption mechanism that leads to salinity reduction in brackish peat water follows both Langmuir (R^2=0.91) and Freundlich (R^2=0.90) adsorption isotherm models when the seawater percentage being less than 70%. This suggests the adsorption of salts on aluminium hydroxide coagulants is due to the microscopic heterogeneous structures with multiple active sites that are not limited only to monolayer adsorption. Correspondingly, the salinity reduction in brackish peat water is also well fitted to the non-linear pseudo-first-order model (R^2=0.99) as compared to pseudo-first-order model in linear form (R^2<0.75). Based on the non-linear pseudo-first-order model, the in-situ aluminium hydroxide coagulants could effectively reduce salinity levels in brackish peat water at 2.65 min^{-1} of adsorption rate and 2,503 mg/g of maximum adsorption capacity especially when the seawater percentage in brackish peat water is lower than 70%. An analysis with Energy Dispersive X-Ray (EDX) has

also detected the presence of aluminium hydroxides and sodium chlorides on the electrocoagulation flocs.

This study has developed a statistical model analysis with three level factors of central composite design (CCD) to study the significant effects of seawater percentage, electric current, and flow rate for optimizing the salinity reduction efficiency and energy operating cost. The developed statistical model has been utilized to formulate polynomial mathematical quadratic equations for salinity reduction efficiency (R^2=0.84) and energy operating cost (R^2=0.97). From the conducted analysis of variance (ANOVA), this study has also observed that seawater percentage, electric current, and flow rate have significant effects on salinity reduction efficiency and energy operating cost due to the p-value being less than 0.05. The process optimization done in this study obtained an optimum 5 A of electric current and 1.2 L/min of flow rate in order to achieve 91.78% of salinity reduction efficiency in brackish peat water with 30% of seawater percentage with a cost of RM 0.29 per meter cubic of treated water. A detailed investigation on Faradaic efficiency analysis of salinity reduction with electrocoagulation treatment is proposed for further study. Overall, this study demonstrates that continuous electrocoagulation treatment could reduce the salinity levels in brackish peat water with a 30% of seawater percentage which is deemed suitable for domestic consumption in Sarawak coastal rural areas at reasonable cost.

REFERENCES

Abakedi, O., Mkpenie, V., & Okafor, J. (2019). Parameterization, kinetics, and adsorption isotherm of electrocoagulation process of bromothymol blue in aqueous medium using aluminum electrodes. *Turkish Journal of Chemistry, 43*, 926-935. doi:10.3906/kim-1807-132

Abdul Jalal, N.S. (2022). Comparison of kinetic and statistical modeling approaches for continuous electrocoagulation for peat water treatment design simulation. (*Bachelor's Thesis*). Universiti Malaysia Sarawak, Kota Samarahan, Sarawak. doi:http://ir.unimas.my/id/eprint/39352/

Abdulkarem, E., Ahmed, I., Abu-Zahra, M. R. M., & Hasan, S. W. (2017). Electrokinetic pretreatment of seawater to decrease the Ca^{2+}, Mg^{2+}, SO_4^{2-} and bacteria contents in membrane desalination applications. *Desalination, 403*, 107-116. doi:https://doi.org/10.1016/j.desal.2016.06.004

Abujazar, M. S. S., Fatihah, S., & Kabeel, A. E. (2017). Seawater desalination using inclined stepped solar still with copper trays in a wet tropical climate. *Desalination, 423*, 141-148. doi:https://doi.org/10.1016/j.desal.2017.09.020

Acharya, S., Sharma, S. K., Chauhan, G., & Shree, D. (2018). Statistical optimization of electrocoagulation process for removal of nitrates using response surface methodology. *Indian Chemical Engineer, 60*(3), 269-284. doi:10.1080/00194506.2017.1365630

Adeogun, A. I., & Balakrishnan, R. B. (2017). Kinetics, isothermal and thermodynamics studies of electrocoagulation removal of basic dye rhodamine B from aqueous solution using steel electrodes. *Applied Water Science, 7*(4), 1711-1723. doi:10.1007/s13201-015-0337-4

Agha, M., Ennen, J. R., Bower, D. S., Nowakowski, A. J., Sweat, S. C., & Todd, B. D. (2018). Salinity tolerances and use of saline environments by freshwater turtles: implications of sea level rise. *Biological Reviews, 93*(3), 1634-1648. doi: https://doi.org/10.1111/brv.12410

Akhtar, A., Aslam, Z., Asghar, A., Bello, M. M., & Raman, A. A. A. (2020). Electrocoagulation of congo red dye-containing wastewater: Optimization of

operational parameters and process mechanism. *Journal of Environmental Chemical Engineering, 8*(5), 104055. doi:https://doi.org/10.1016/j.jece.2020.104055

Akrawi, H., Al-Obaidi, M., & Abdulrahman, C. (2021). Evaluation of Langmuir and Frendlich isotherm equation for zinc adsorption in some calcareous soil of Erbil province north of Iraq. *IOP Conference Series: Earth and Environmental Science, 761*, 012017. doi:10.1088/1755-1315/761/1/012017

Al Umairi, A. R., How, Z. T., & Gamal El-Din, M. (2021). Enhanced primary treatment during wet weather flow using ferrate as a coagulant, coagulant aid and disinfectant. *Journal of Environmental Management, 290*, 112603. doi: https://doi.org/10.1016/j.jenvman.2021.112603

Al-Abri, M., Al-Ghafri, B., Bora, T., Dobretsov, S., Dutta, J., Castelletto, S., & Boretti, A. (2019). Chlorination disadvantages and alternative routes for biofouling control in reverse osmosis desalination. *Clean Water, 2*(1), 2. doi:10.1038/s41545-018-0024-8

Alam, R., Khan, S. U., Usman, M., Asif, M., & Farooqi, I. H. (2022). A critical review on treatment of saline wastewater with emphasis on electrochemical based approaches. *Process Safety and Environmental Protection*, *158*, 625-643. doi: https://doi.org/10.1016/j.psep.2021.11.054

Albania Linus, A. (2022). Electrocoagulation treatment of peat water in Sarawak with aluminium electrodes. (*Master's Thesis*). Universiti Malaysia Sarawak, Kota Samarahan, Sarawak. doi:https://ir.unimas.my/id/eprint/39293/1/Allene%20Albania%20Linus%20ft.pdf

Alenyorege, E. A., Ma, H., Aheto, J. H., Ayim, I., Chikari, F., Osae, R., & Zhou, C. (2020). Response surface methodology centred optimization of mono-frequency ultrasound reduction of bacteria in fresh-cut Chinese cabbage and its effect on quality. *Food Science and Technology, 122*, 108991. doi:https://doi.org/10.1016/j.lwt.2019.108991

Al-Ghouti, M. A., & Da'ana, D. A. (2020). Guidelines for the use and interpretation of adsorption isotherm models: A review. *Journal of Hazardous Materials, 393*, 122383. doi:https://doi.org/10.1016/j.jhazmat.2020.122383

Ali, F., Lestari, D., & Putri, M. (2021). Peat water treatment as an alternative for raw water in peatlands area. *IOP Conference Series: Materials Science and Engineering, 1144*, 012052. doi:10.1088/1757-899X/1144/1/012052

Alif, M. F., Aprillia, W., & Arief, S. (2018). Peat water purification by hydroxyapatite (HAp) synthesized from waste pensi (Corbicula moltkiana) shells. *IOP Conference Series: Materials Science and Engineering, 299*, 012002. doi:10.1088/1757-899x/299/1/012002

AlJaberi, F. Y. (2019). Operating cost analysis of a concentric aluminum tubes electrodes electrocoagulation reactor. *Heliyon, 5*(8), e02307. doi:https://doi.org/10.1016/j.heliyon.2019.e02307

AlJaberi, F. Y., Alardhi, S. M., Ahmed, S. A., Salman, A. D., Juzsakova, T., Cretescu, I., & Nguyen, D. D. (2022). Can electrocoagulation technology be integrated with wastewater treatment systems to improve treatment efficiency?. *Environmental Research, 214*, 113890. doi:https://doi.org/10.1016/j.envres.2022.113890

AlJaberi, F., & Mohammed, W. (2018). Adsorption of lead from simulated wastewater via electrocoagulation process: kinetics and isotherm studies. *Mesopotamia Environmental Journal, 4* (2). 45-65. doi:https://www.iasj.net/iasj/article/171999

Almukdad, A., Hafiz, M., Yasir, A., Alfahel, R., & Al Hawari, A. (2021). Unlocking the application potential of electrocoagulation process through hybrid processes. *Journal of Water Process Engineering, 40*, 101956. doi:10.1016/j.jwpe.2021.101956

Al-Raad, & Hanafiah, M. M. (2021). Removal of inorganic pollutants using electrocoagulation technology: A review of emerging applications and mechanisms. *Journal of Environmental Management, 300*, 113696. doi: https://doi.org/10.1016/j.jenvman.2021.113696

Al-Raad, Hanafiah, M., Samir, A., Ajeel, M., Basheer, A., Aljayashi, T., & Toriman, M. (2019). Treatment of saline water using electrocoagulation with combined electrical connection of electrodes. *Processes, 7*, 242. doi:10.3390/pr7050242

Amri, I., Herman, S., Fadhlah Ramadan, A., & Hamzah, N. (2022). Effect of electrode and electric current on peat water treatment with continuous electrocoagulation

process. *Materials Today: Proceedings, 63*, S520-S525. doi:https://doi.org/10.1016/j.matpr.2022.04.873

Amri, N., Abdullah, A. Z., & Ismail, S. (2020). Removal efficiency of acid red 18 dye from aqueous solution using different aluminium-based electrode materials by electrocoagulation process. *Indonesian Journal of Chemistry, 20*, 536. doi:10.22146/ijc.43206

An, B. (2020). Cu(II) and As(V) adsorption kinetic characteristic of the multifunctional amino groups in chitosan. *Processes, 8*(9), 1194. doi:10.3390/pr8091194

Anders, K. (2017). Resolution of students t-tests, ANOVA and analysis of variance components from intermediary data. *Biochemia Medica, 27*(2), 253-258. doi:10.11613/bm.2017.026

Anfar, Z., Ait Ahsaine, H., Zbair, M., Amedlous, A., Ait El Fakir, A., Jada, A., & El Alem, N. (2020). Recent trends on numerical investigations of response surface methodology for pollutants adsorption onto activated carbon materials: A review. *Critical Reviews in Environmental Science and Technology, 50*(10), 1043-1084. doi:10.1080/10643389.2019.1642835

Apshankar, K. R., & Goel, S. (2020). Nitrate removal from drinking water using direct current or solar powered electrocoagulation. *SN Applied Sciences, 2*(2), 304. doi:10.1007/s42452-020-2069-9

Aryanti, P. T. P., Noviyani, A. M., Kurnia, M. F., Rahayu, D. A., & Nisa, A. Z. (2018). Modified polysulfone ultrafiltration membrane for humic acid removal during peat water treatment. *IOP Conference Series: Materials Science and Engineering, 288*, 012118. doi:10.1088/1757-899x/288/1/012118

Ashoor, B. B., Giwa, A., & Hasan, S. W. (2019). Full-scale membrane distillation systems and performance improvement through modeling: A Review. *Current Trends and Future Developments on (Bio-) Membranes*, *2019* 105-140. doi: https://doi.org/10.1016/B978-0-12-813551-8.00005-X

Ashraf, S. N., Rajapakse, J., Dawes, L. A., & Millar, G. J. (2021). Impact of turbidity, hydraulic retention time, and polarity reversal upon iron electrode-based electrocoagulation pre-treatment of coal seam gas associated water.

Environmental Technology & Innovation, *23*, 101622. doi:https://doi.org/10.1016/j.eti.2021.101622

Ayawei, N., Ebelegi, A. N., & Wankasi, D. (2017). Modelling and interpretation of adsorption isotherms. *Journal of Chemistry, 2017*, 3039817. doi:10.1155/2017/3039817

Ayoub, G. M., Korban, L., Al-Hindi, M., & Zayyat, R. (2019). Brackish water desalination: An effective pretreatment process for reverse osmosis systems. *Water, Air, & Soil Pollution, 230*(10), 238. doi:10.1007/s11270-019-4299-2

Ayub, A., Raza, Z. A., Majeed, M. I., Tariq, M. R., & Irfan, A. (2020). Development of sustainable magnetic chitosan biosorbent beads for kinetic remediation of arsenic contaminated water. *International Journal of Biological Macromolecules, 163*, 603-617. doi:https://doi.org/10.1016/j.ijbiomac.2020.06.287

Ayyappan, U., Adithya, I., Murickan, G., Balagopal, J., Kumar, A. S., & Priya, K. L. (2021). Continuous flow electrocoagulation system for the treatment of coir industry wastewater. *Proceedings of International Web Conference in Civil Engineering for a Sustainable Planet, 2021.* doi:https://doi.org/10./proceedings.112.29

Azizi, A., Dargahi, A., & Almasi, A. (2021). Biological removal of diazinon in a moving bed biofilm reactor – process optimization with central composite design. *Toxin Reviews, 40*(4), 1242-1252. doi:10.1080/15569543.2019.1675708

Azizian, S., & Eris, S. (2021). Chapter 6 - Adsorption isotherms and kinetics. *Interface Science and Technology, 33,* 445-509. doi:https://doi.org/10.1016/B978-0-12-818805-7.00011-4

Bahrodin, M., Zaidi, N. S., Hussein, N., Sillanpää, M., Prasetyo, D., & Syafiuddin, A. (2021). Recent advances on coagulation-based treatment of wastewater: transition from chemical to natural coagulant. *Current Pollution Reports, 7.* doi:10.1007/s40726-021-00191-7

Bajpai, M., Singh Katoch, S., & Singh, M. (2020). Optimization and economical study of electro-coagulation unit using CCD to treat real greywater and its reuse

potential. *Environmental Science and Pollution Research, 27*(33), 42040-42050. doi:10.1007/s11356-020-10171-x

Bakewell, D., Wong, A., Kong, D., & Au, R. (2017). Waterbird surveys of the Sarawak coast (2010–2012). *Malaysian Nature Society-Bird Conservation Council (MNS-BCC) and Sarawak Forestry Corporation, Malaysia*. doi:https://www.researchgate.net/publication/314154132_Waterbird_Surveys_of_the_Sarawak_Coast_2010-2012

Baradey, Y., Hawlader, M.N.A., Hrairi, M. & Ismail, A.F. (2018). Desalination technologies: A critical review. *International Journal of Engineering Technology and Scientific Innovation, 4*(4). doi:http://ijetsi.org/2018files/ijetsi_03__13.pdf

Barrera-Díaz, C. E., Balderas-Hernández, P., & Bilyeu, B. (2018). *Chapter 3 - Electrocoagulation: Fundamentals and prospectives*. (pp. 61-76): Butterworth-Heinemann. doi: https://doi. org/10.1016/B978-0-12-813160-2.00003-1

Bassyouni, D. G., Hamad, H. A., El-Ashtoukhy, E. S. Z., Amin, N. K., & El-Latif, M. M. A. (2017). Comparative performance of anodic oxidation and electrocoagulation as clean processes for electrocatalytic degradation of diazo dye Acid Brown 14 in aqueous medium. *Journal of Hazardous Materials, 335*, 178-187. doi:https://doi.org/10.1016/j.jhazmat.2017.04.045

Bendaia, M., Hazourli, S., Aitbara, A., & Nait Merzoug, N. (2021). Performance of electrocoagulation for food azo dyes treatment in aqueous solution: Optimization, kinetics, isotherms, thermodynamic study and mechanisms. *Separation Science and Technology, 56*(12), 2087-2103. doi:10.1080/01496395.2020.1806883

Betancor-Abreu, A., Mena, V. F., González, S., Delgado, S., Souto, R. M., & Santana, J. J. (2019). Design and optimization of an electrocoagulation reactor for fluoride remediation in underground water sources for human consumption. *Journal of Water Process Engineering*, *31*, 100865. doi:https://doi.org/10.1016/j.jwpe.2019.100865

Bhatti, M.S., Thukral, A.K., Reddy, A.S., & Kalia, R.K. (2017). RSM and ANN-GA experimental design optimization for electrocoagulation removal of chromium. In: Kurisu, F., Ramanathan, A., Kazmi, A., Kumar, M. (eds) *Trends in Asian*

Water Environmental Science and Technology. Springer, Cham. https://doi.org/10.1007/978-3-319-39259-2_1

Budhiary, K., & Sumantri, I. (2021). Langmuir and Freundlich isotherm adsorption using activated charcoal from banana peel to reduce total suspended solid (TSS) levels in tofu industry liquid waste. *IOP Conference Series: Materials Science and Engineering, 1053*, 012113. doi:10.1088/1757-899X/1053/1/012113

Bujang, A. H. (2018). *RM5 million to repair desalination plants*. Borneo Post Online Accessed on 10th October 2021 and retrieved from https://www.theborneopost.com/2018/03/07/rm5-million-to-repair-desalination-plants/

Bun, S., Hong, P., Chawaloesphosiya, N., Pang, S., Vet, S., Ham, P., & Paimanakul, P. (2022). Development of integrated electrocoagulation-sedimentation (IECS) in continuous mode for turbidity and color removal. *ChemEngineering, 6*, 2-16. doi:10.3390/chemengineering6010003

Chan, K. S., Greaves, S. J., & Rahardja, S. (2019). Techniques for addressing saddle points in the response surface methodology (RSM). *IEEE Access, 7*, 85613-85621. doi:10.1109/ACCESS.2019.2922975

Chen, X., Ren, P., Li, T., Trembly, J. P., & Liu, X. (2018). Zinc removal from model wastewater by electrocoagulation: Processing, kinetics and mechanism. *Chemical Engineering Journal, 349*, 358-367. doi:https://doi.org/10.1016/j.cej.2018.05.099

Chibani, A., Barhoumi, A., Ncib, S., Bouguerra, W., & Elaloui, E. (2019). Fluoride removal from synthetic groundwater by electrocoagulation process: Parametric and energy evaluation. *Desalination and Water Treatment, 157*, 100-109. doi:10.5004/dwt.2019.24087

Cole, L. E. S., Willis, K. J., & Bhagwat, S. A. (2021). The future of Southeast Asia's tropical peatlands: Local and global perspectives. *Anthropocene, 34*, 100292. doi:https://doi.org/10.1016/j.ancene.2021.100292

Colpan, C. O., Nalbant, Y., & Ercelik, M. (2018). 4.28 Fundamentals of fuel cell technologies. In Dincer, I. (Ed.), *Comprehensive Energy Systems* (pp. 1107-1130). Oxford: Elsevier. doi:10.1016/B978-0-12-809597-3.00446-6

Davoodi, S. M., Taheran, M., Brar, S. K., Galvez-Cloutier, R., & Martel, R. (2019). Hydrophobic dolomite sorbent for oil spill clean-ups: Kinetic modeling and isotherm study. *Fuel*, *251*, 57-72. doi:https://doi.org/10.1016/j.fuel.2019.04.033

Dayarathne, H. N. P., Angove, M., Aryal, R., Abuel-Naga, H., & Mainali, B. (2020). Removal of natural organic matter from source water: Review on coagulants, dual coagulation, alternative coagulants, and mechanisms. *Journal of Water Process Engineering, 40*. doi:10.1016/j.jwpe.2020.101820

Delgado, N., Capparelli, A., Navarro, A., & Marino, D. (2019). Pharmaceutical emerging pollutants removal from water using powdered activated carbon: Study of kinetics and adsorption equilibrium. *Journal of Environmental Management, 236*, 301-308. doi:https://doi.org/10.1016/j.jenvman.2019.01.116

Department of Environment. (2020). *Malaysia water quality standards and index*. Accessed on 14th December 2020 and retrieved from https://www.doe.gov.my/portalv1/en/standard-dan-indeks-kualiti-jabatan-alam-sekitar

Department of Irrigation and Drainage Sarawak. (2020). *Peat swamp development*. Accessed on 11 November 2020 and retrieved from https://did.sarawak.gov.my/page-0-314-315-Resource-Centre-IRBM-22-Basins.html

Department of Irrigation and Drainage Sarawak. (2022). *Introduction to integrated coastal zone management*. Accessed on 7 March 2022 and retrieved from https://did.sarawak.gov.my/page-0-123-476-integrated-coastal-zone-management.html

Design Expert. (2022). *Numerical optimization*. Accessed on 7th August 2022 and retrieved from https://www.statease.com/docs/v11/navigation/numerical-optimization/#:~:text=Choose%20the%20desired%20goal%20for,provided%20for%20each%20parameter%20included.

Dessu, S. B., Price, R. M., Troxler, T. G., & Kominoski, J. S. (2018). Effects of sea-level rise and freshwater management on long-term water levels and water quality in the Florida coastal everglades. *Journal of Environmental Management*, *211*, 164-176. doi:https://doi.org/10.1016/j.jenvman.2018.01.025

Dey, M. (2017). Study in copper price linkage between international and Indian commodity market. *International Journal of Recent, Trends, in Business and Tourism, 1*(3). doi:https://ejournal.lucp.net/index.php/ijrtbt/article/view/275

Dijk, V.G., Nijp, J. J., Metselaar, K., Lamers, L. P., & Smolders, A. J. (2017). Salinity-induced increase of the hydraulic conductivity in the hyporheic zone of coastal wetlands. *Hydrological Processes*, *31*(4), 880-890. doi:https://doi.org/10.1002/hyp.11068

Ding, N., Ying, D., Cheng, J., Jiang, X., Li, K., Wang, Y., & Jia, J. (2019). Green recycle of copper ions in saccharin sodium wastewater by direct electrodeposition using rotating thin copper disc electrode. *ACS Sustainable Chemistry & Engineering, 7*(21), 17888-17895. doi:10.1021/acssuschemeng.9b04465

Du, X., Shi, Y., Jegatheesan, V., & Haq, I. U. (2020). A review on the mechanism, impacts and control methods of membrane fouling in MBR system. *Membranes (Basel), 10*(2). doi:10.3390/membranes10020024

Ebba, M., Asaithambi, P., & Alemayehu, E. (2021). Investigation on operating parameters and cost using an electrocoagulation process for wastewater treatment. *Applied Water Science, 11*(11), 175. doi:10.1007/s13201-021-01517-y

Economic Planning Unit. (2018). *Strengthening infrastructure to support economic expansion in eleventh Malaysia plan 2016-2020*. Kuala Lumpur, Malaysia: Percetakan Nasional Malaysia Berhad. doi:https://www.epu.gov.my/sites/default/files/202008/9.%20Chapter%206%20Strengthening%20Infrastructure%20to%20Support%20Economic%20Expansion.pdf

Edward, C. (2020). *Plan to resettle villagers in low-lying areas in Lundu approved*. Accessed on 18th July 2022 and retrieved from https://www.theborneopost.com/2020/09/15/plan-to-resettle-villagers-in-low-lying-areas-in-lundu-approved/

Ehiomogue, P., Ahuchaogu, I., & Ahaneku, I. (2022). Review of adsorption isotherms models. *Acta Technica Corviniensis, 24*(4). doi:https://www.researchgate.net/publication/358271705_review_of_adsorption_isotherms_models

El-Ashtoukhy, E. S. Z., Amin, N. K., Fouad, Y. O., & Hamad, H. A. (2020). Intensification of a new electrocoagulation system characterized by minimum

energy consumption and maximum removal efficiency of heavy metals from simulated wastewater. *Chemical Engineering and Processing - Process Intensification, 154*, 108026. doi:https://doi.org/10.1016/j.cep.2020.108026

El-Hosiny, F. I., Selim, K. A., Abdel-Khalek, M. A., & Osama, I. A. (2017). Physicochemical study of dye removal using electro-coagulation-flotation process. *Physicochemical Problems of Mineral Processing, 54*, 321-333. doi: https://doi.org/10.5277/ppmp1825

Elma, M., Pratiwi, A. E., Rahma, A., Rampun, E. L. A., Mahmud, M., Abdi, C., & Bilad, M. R. (2022). Combination of coagulation, adsorption, and ultrafiltration processes for organic matter removal from peat water. *Sustainability, 14*(1), 370. doi:https://www.mdpi.com/2071-1050/14/1/370

Elma, M., Rahma, A., Pratiwi, A. E., & Rampun, E. L. A. (2020). Coagulation as pretreatment for membrane-based wetland saline water desalination. *Asia-Pacific Journal of Chemical Engineering, 15*. doi:https://doi.org/10.1002/apj.2461

Ersan, G., Kaya, Y., Ersan, M. S., Apul, O. G., & Karanfil, T. (2019). Adsorption kinetics and aggregation for three classes of carbonaceous adsorbents in the presence of natural organic matter. *Chemosphere, 229*, 515-524. doi:https://doi.org /10.1016/j.chemosphere.2019.05.014

Ezzati, R. (2020). Derivation of Pseudo-First-Order, Pseudo-Second-Order and modified Pseudo-First-Order rate equations from Langmuir and Freundlich isotherms for adsorption. *Chemical Engineering Journal, 392*, 123705. doi:https://doi.org/10. 1016/j.cej.2019.123705

Feng, Q., Zhang, K., Liu, X., Guan, W., Chen, X., Song, L., & Jiashun, C. (2021). An improved kinetic model for dephosphorization of laundry wastewater by electrocoagulation. *Journal of Water Process Engineering, 39*, 101750. doi:https: //doi.org/10.1016/j.jwpe.2020.101750

Ferreira, S. L. C., Lemos, V. A., de Carvalho, V. S., da Silva, E. G. P., Queiroz, A. F. S., Felix, C. S. A., & Oliveira, R. V. (2018). Multivariate optimization techniques in analytical chemistry - An overview. *Microchemical Journal, 140*, 176-182. doi:https://doi.org/10.1016/j.microc.2018.04.002

Follmann, H. V. D. M., Souza, E., Aguiar Battistelli, A., Rubens Lapolli, F., & Lobo-Recio, M. Á. (2020). Determination of the optimal electrocoagulation operational conditions for pollutant removal and filterability improvement during the treatment of municipal wastewater. *Journal of Water Process Engineering, 36*, 101295. doi:https://doi.org/10.1016/j.jwpe.2020.101295

Garcia-Segura, S., Eiband, M. M. S. G., de Melo, J. V., & Martínez-Huitle, C. A. (2017). Electrocoagulation and advanced electrocoagulation processes: A general review about the fundamentals, emerging applications and its association with other technologies. *Journal of Electroanalytical Chemistry, 801*, 267-299. doi:https://doi.org/10.1016/j.jelechem.2017.07.047

Gasmi, A., Ibrahimi, S., Elboughdiri, N., Tekaya, M. A., Ghernaout, D., Hannachi, A., & Kolsi, L. (2022). Comparative study of chemical coagulation and electrocoagulation for the treatment of real textile wastewater: Optimization and operating cost estimation. *ACS Omega, 7*(26), 22456-22476. doi:10.1021/acsomega.2c01652

Ghernaout, D. (2019). Disinfection via electrocoagulation process: Implied mechanisms and future tendencies. *EC Microbiology, 15*, 79-90. doi:https://doi.org/10.4236/oalib.1106083

Gilpavas, E., & Correa-Sanchez, S. (2020). Assessment of the optimized treatment of indigo-polluted industrial textile wastewater by a sequential electrocoagulation-activated carbon adsorption process. *Journal of Water Process Engineering, 36*, 101306. doi:https://doi.org/10.1016/j.jwpe.2020.101306

Gniadek, M., & Dąbrowska, A. (2019). The marine nano- and microplastics characterisation by SEM-EDX: The potential of the method in comparison with various physical and chemical approaches. *Marine Pollution Bulletin, 148*, 210-216. doi:https://doi.org/10.1016/j.marpolbul.2019.07.067

Gohil, J. M., & Suresh, A. K. (2017). Chlorine attack on reverse osmosis membranes: Mechanisms and mitigation strategies. *Journal of Membrane Science, 541*, 108-126. doi:https://doi.org/10.1016/j.memsci.2017.06.092

Gonzalez, B., Carreño Aguilera, G., Alquiza, P., Avilés, R., Jacobo-Azuara, A., & Guanajuato, M. (2019). Sulphate ions removal from an abandoned mine water

using electrocoagulation. Characterization of the flocs originated through chemical and morphological analysis. *International Journal of Electrochemical Science*, 6500-6512. doi:10.20964/2019.07.60

Google Maps. (2022). *Kampung Metang Terap, Lundu, Kuching, Sarawak, Malaysia*. Accessed on 10th July 2022 and retrieved from https://www.google.com/maps/place/Surau+Nur+Ikhlas+Kg.Melayu+Metang+Terap/@1.6966116,109.8875322,6268m/data=!3m1!1e3!4m5!3m4!1s0x31fb211967b63f97:0x274ef69ed87c1d1c!8m2!3d1.6876502!4d109.8811587

Gosch, L., Janssen, M., & Lennartz, B. (2018). Impact of the water salinity on the hydraulic conductivity of fen peat. *Hydrological Processes, 32*(9), 1214-1222. doi:https://doi.org/10.1002/hyp.11478

Graça, N., Ribeiro, A., & Rodrigues, A. (2019). Modeling the electrocoagulation process for the treatment of contaminated water. *Chemical Engineering Science, 197*. doi:10.1016/j.ces.2018.12.038

Grzegorzek, M., & Majewska-Nowak, K. (2017). The influence of humic acids on desalination process with the use of electrodialysis. *E3S Web of Conferences, 17*, 00027. doi:10.1051/e3sconf/20171700027

Guisela, Z., Ohana N, D. A., Dalvani S, D., Fermin G, V., Francisco Hm, L., & Luis, N.G. (2022). Adsorption of arsenic anions in water using modified lignocellulosic adsorbents. *Results in Engineering, 13*, 100340. doi:https://doi.org/10.1016/j.rineng.2022.100340

Gunten, V. U. (2018). Oxidation processes in water treatment: are we on track?. *Environmental Science & Technology, 52*(9), 5062-5075. doi:https://doi.org/10.1021/acs.est.8b00586

Guo, X., & Wang, J. (2019). Comparison of linearization methods for modeling the Langmuir adsorption isotherm. *Journal of Molecular Liquids, 296*, 111850. doi:https://doi.org/10.1016/j.molliq.2019.111850

Gürses, A., Güneş, K., & Şahin, E. (2021). Chapter 5 - Removal of dyes and pigments from industrial effluents. In Sharma, S. K. (Ed.), *Green Chemistry and Water*

Remediation: Research and Applications (pp. 135-187): Elsevier. doi:https://doi.org/10.1016/B978-0-12-817742-6.00005-0

Gutekunst, C. N., Liebner, S., Jenner, A. K., Knorr, K. H., Unger, V., Koebsch, F., & Jurasinski, G. (2022). Effects of brackish water inflow on methane cycling microbial communities in a freshwater rewetted coastal fen. *EGUsphere, 2022*, 1-42. doi:10.5194/egusphere-2022-65

Haas, K. (2020). Limiting Machine Learning Overfitting Uncertainties Through Persistent Homology. *Verification and Validation, 83594*, V001T08A001. doi: https://doi.org/10.1115/VVS2020-8833

Hailemariam, R. H., Woo, Y. C., Damtie, M. M., Kim, B. C., Park, K.-D., & Choi, J. S. (2020). Reverse osmosis membrane fabrication and modification technologies and future trends: A review. *Advances in Colloid and Interface Science, 276*, 102100. doi:https://doi.org/10.1016/j.cis.2019.102100

Hakizimana, Najid, N., Gourich, B., Vial, C., Stiriba, Y., & Naja, J. (2017). Hybrid electrocoagulation/electroflotation/electrodisinfection process as a pretreatment for seawater desalination. *Chemical Engineering Science, 170*, 530-541. doi:https://doi.org/10.1016/j.ces.2017.04.029

Hamid, M. A. A., Aziz, H. A., Yusoff, M. S., & Rezan, S. A. (2020). Optimization and analysis of zeolite augmented electrocoagulation process in the reduction of high-strength ammonia in saline landfill leachate. *Water, 12*(1), 247. doi: https://www.mdpi.com/2073-4441/12/1/247

Hashim, K. S., Kot, P., Zubaidi, S. L., Alwash, R., Al Khaddar, R., Shaw, A., & Aljefery, M. H. (2020). Energy efficient electrocoagulation using baffle-plates electrodes for efficient Escherichia coli removal from wastewater. *Journal of Water Process Engineering, 33*, 101079. doi:https://doi.org/10.1016/j.jwpe.2019.101079

Hendaoui, K., Ayari, F., Rayana, I. B., Amar, R. B., Darragi, F., & Trabelsi-Ayadi, M. (2018). Real indigo dyeing effluent decontamination using continuous electrocoagulation cell: Study and optimization using Response Surface Methodology. *Process Safety and Environmental Protection, 116*, 578-589. doi:https://doi.org/10.1016/j.psep.2018.03.007

Honarparvar, S., Zhang, X., Chen, T., Na, C., & Reible, D. (2019). Modeling technologies for desalination of brackish water—toward a sustainable water supply. *Current Opinion in Chemical Engineering*, 26, 104-111. doi:https://doi.org/10.1016/j.coche.2019.09.005

Houssini, N.S., Essadki, A., & El-Qars, E. (2020). The simultaneous removal of reactive and disperse dyes by electrocoagulation process with a bipolar connection of combined iron and aluminum electrodes: Experimental design and kinetic studies. *Mediterranean Journal of Chemistry, 10*(2). 171-184. doi:http://dx.doi.org/10.13171/mjc10202002191222ae

Hu, C., Sun, J., Wang, S., Liu, R., Liu, H., & Qu, J. (2017). Enhanced efficiency in HA removal by electrocoagulation through optimizing flocs properties: Role of current density and pH. *Separation and Purification Technology, 175*, 248-254. doi:https://doi.org/10.1016/j.seppur.2016.11.036

Hu, Q., He, L., Lan, R., Feng, C., & Pei, X. (2022). Recent advances in phosphate removal from municipal wastewater by electrocoagulation process: A review. *Separation and Purification Technology*, 122944. doi:https://doi.org/10.1016/j.seppur.2022.122944

Hu, Q., Liu, Y., Feng, C., Zhang, Z., Lei, Z., & Shimizu, K. (2018). Predicting equilibrium time by adsorption kinetic equations and modifying Langmuir isotherm by fractal-like approach. *Journal of Molecular Liquids, 268*, 728-733. doi:https://doi.org/10.1016/j.molliq.2018.07.113

Huang, C. H., Shen, S. Y., Dong, C. D., Kumar, M., & Chang, J. H. (2020). Removal mechanism and effective current of electrocoagulation for treating wastewater containing Ni(II), Cu(II), and Cr(VI). *Water, 12*(9), 2614. doi: https://www.mdpi.com/2073-4441/12/9/2614

Igwegbe, C., Onukwuli, O., & Onyechi, P. (2019). Optimal route for turbidity removal from aquaculture wastewater by electrocoagulation-flocculation process. *Journal of Engineering and Applied Sciences, 15*, 99-108. doi: http://www.facultyofengineeringnau.org/read_journal.php?id=182

Igwegbe, C., Onukwuli, O., O. Ighalo, J., Umembamalu, C. J., & Adeniyi, A. (2021). Comparative analysis on the electrochemical reduction of colour, COD and

turbidity from municipal solid waste leachate using aluminium, iron and hybrid electrodes. *Sustainable Water Resources Management, 7*. doi:10.1007/s40899-021-00524-w

Ingelsson, M., Yasri, N., & Roberts, E. P. (2020). Electrode passivation, faradaic efficiency, and performance enhancement strategies in electrocoagulation—A review. *Water Research*, *187*, 116433. doi:https://doi.org/10.1016/j.watres.2020.116433

Ishika, T., Bahri, P. A., Laird, D. W., & Moheimani, N. R. (2018). The effect of gradual increase in salinity on the biomass productivity and biochemical composition of several marine, halotolerant, and halophilic microalgae. *Journal of Applied Phycology*, *30*, 1453-1464. doi:10.1007/s10811-017-1377-y

Jabatan Bekalan Air Luar Bandar. (2022). *Jurisdiction areas*. Accessed on 24th July 2022 and retrieved from https://jbalb.sarawak.gov.my/page-0-188-148-Jurisdiction-Areas.html

Jasper, E. E., Ajibola, V. O., & Onwuka, J. C. (2020). Nonlinear regression analysis of the sorption of crystal violet and methylene blue from aqueous solutions onto an agro-waste derived activated carbon. *Applied Water Science, 10*(6), 132. doi:10.1007/s13201-020-01218-y

Jenis, A. (2021). *Kampung Sibu Laut folk's decades-long wait for clean water supply finally ends*. Accessed on 20th July 2022 and retrieved from https://www.theborneopost.com/2021/12/05/kampung-sibu-laut-folks-decades-long-wait-for-clean-water-supply-finally-ends/

Kajjumba, G. W., Emik, S., Öngen, A., & Aydın, H. K. Ö. S. (2018). Modelling of adsorption kinetic processes—Errors, theory and application. In (Ed.), *Advanced Sorption Process Applications*. IntechOpen. doi:https://doi.org/10.5772/intechopen.80495

Kalam, S., Abu-Khamsin, S. A., Kamal, M. S., & Patil, S. (2021). Surfactant adsorption isotherms: A Review. *ACS Omega, 6*(48), 32342-32348. doi:10.1021/acsomega.1c04661

Karimifard, S., & Alavi Moghaddam, M. R. (2018). Application of response surface methodology in physicochemical removal of dyes from wastewater: A critical review. *Science of The Total Environment, 640-641*, 772-797. doi:https://doi.org/10.1016/j.scitotenv.2018.05.355

Kasmuri, N., Adnan, N., Ahmad, R., Santiagoo, R., & Ramasamy, S. (2021). Heavy metals reduction using electrocoagulation in enhancing the water quality near unlined landfill: A case study. *IOP Conference Series: Earth and Environmental Science, 646*(1), 012003. doi:10.1088/1755-1315/646/1/012003

Kecili, R., & Hussain, C. M. (2018). Chapter 4 - Mechanism of adsorption on nanomaterials. In Hussain, C. M. (Ed.), *Nanomaterials in Chromatography* (pp. 89-115): Elsevier. doi: https://doi.org/10.1016/b978-0-12-812792-6.00004-2

Kessentini, I., Mousser, H., Zouari, S., & Bargui, M. (2019). Removal of copper from aqueous solution using electrocoagulation: Importance of stirring effect. *Surface Engineering and Applied Electrochemistry, 55*(2), 210-218. doi:10.3103/S106837551902011X

Khalid, R. M. (2018). Review of the water supply management and reforms needed to ensure water security in Malaysia. *International Journal of Business and Society, 19*(S3), 472-483. doi: http://www.ijbs.unimas.my/index.php/volume-11-20/volume-19-s3-2018/500-review-of-the-water-supply-management-and-reforms-needed-to-ensure-water-security-in-malaysia

Khan, S. U., Islam, D. T., Farooqi, I. H., Ayub, S., & Basheer, F. (2019). Hexavalent chromium removal in an electrocoagulation column reactor: Process optimization using CCD, adsorption kinetics and pH modulated sludge formation. *Process Safety and Environmental Protection, 122*, 118-130. doi:https://doi.org/10.1016/j.psep.2018.11.024

Khedher, M., Awad, J., Donner, E., Drigo, B., Fabris, R., Harris, M., & Chow, C. W. (2023). Using the flocculation index to optimise coagulant dosing during drinking water treatment. *Journal of Water Process Engineering, 51*, 103394. doi:https://doi.org/10.1016/j.jwpe.2022.103394

Khor, C. M., Wang, J., Li, M., Oettel, B. A., Kaner, R. B., Jassby, D., & Hoek, E. M. V. (2020). Performance, energy and cost of produced water treatment by chemical

and electrochemical coagulation. *Water, 12*(12), 3426. doi:https://www.mdpi.com/2073-4441/12/12/3426

Khorram, A. G., & Fallah, N. (2018). Treatment of textile dyeing factory wastewater by electrocoagulation with low sludge settling time: Optimization of operating parameters by RSM. *Journal of Environmental Chemical Engineering, 6*(1), 635-642. doi:https://doi.org/10.1016/j.jece.2017.12.054

Khui, P. L., Rahman, R., Ahmed, A. S., King Kuok, K., bin Bakri, M. K., Tazeddinova, D., & Torebek, B. B. (2021). Morphological and thermal properties of composites prepared with poly(lactic acid), poly(ethylene-alt-maleic anhydride), and biochar from microwave-pyrolyzed jatropha seeds. *Bioresources, 16*, 3171-3185. doi: https://dx.doi.org/10.15376/biores.16.3171-3185

Kim, T. K. (2017). Understanding one-way ANOVA using conceptual figures. *Korean Journal of Anestheology, 70*(1), 22-26. doi:10.4097/kjae.2017.70.1.22

Kobya, M., Soltani, R. D. C., Omwene, P. I., & Khataee, A. (2020). A review on decontamination of arsenic-contained water by electrocoagulation: Reactor configurations and operating cost along with removal mechanisms. *Environmental Technology & Innovation*, *17*, 100519. doi:https://doi.org/10.1016/j.eti.2019.100519

Koster, K., Stafleu, J., Cohen, K. M., Stouthamer, E., Busschers, F. S., & Middelkoop, H. (2018). Three-dimensional distribution of organic matter in coastal-deltaic peat: Implications for subsidence and carbon dioxide emissions by human-induced peat oxidation. *Anthropocene*, *22*, 1-9. doi:https://doi.org/10.1016/j.ancene.2018.03.001

Krstić, V. (2021). Chapter 14 - Role of zeolite adsorbent in water treatment. In Bhanvase, B., Sonawane S., Pawade, V., & Pandit, A. (Eds.), *Handbook of Nanomaterials for Wastewater Treatment* (pp. 417-481): Elsevier. doi: https://doi.org/10.1016/B978-0-12-821496-1.00024-6

Kuching Water Board (KWB). (2018). *Annual report 2016*. Accessed on 1st July 2022 and retrieved from https://www.kwb.gov.my/modules/web/pages.php?mod=publication&menu_id=0&sub_id=175

Kul, A., Gökırmak Söğüt, E., & Caliskan, N. (2021). Adsorption of neutral red dye from aqueous solutions by natural adsorbent: an equilibrium, kinetic and thermodynamic study. *Communications Faculty of Science University of Ankara Series B Chemistry and Chemical Engineering, 63*, 27-60. doi:https://dergipark.org.tr/en/pub/communb/issue/64811/948429

Kuok, Po Chan, C., Rahman, M., Bakri, M. K., & Chin, M. (2021a). Performance of rainwater harvesting systems in institutional buildings under different reliability and future economy benefits. *Hunan Daxue Xuebao/Journal of Hunan University Natural Sciences, 48*, 58-66. doi:http://jonuns.com/index.php/journal/article/view/698/695

Kuok, Tay, Y. Y. S., & Chiu, P. C. (2021b). Integrated coastal zone management to protect the Sarawak shoreline. *Journal of Coastal Conservation, 25*(5), 48. doi:10.1007/s11852-021-00835-2

Lani, N., Yusop, Z., & Syafiuddin, A. (2018). A review of rainwater harvesting in Malaysia: Prospects and challenges. *Water, 10*, 506. doi:10.3390/w10040506

Laskar, I., & Hashisho, Z. (2020). Insights into modeling adsorption equilibria of single and multicomponent systems of organic and water vapors. *Separation and Purification Technology, 241*, 116681. doi:10.1016/j.seppur.2020.116681

Lima, E. C., Sher, F., Guleria, A., Saeb, M. R., Anastopoulos, I., Tran, H. N., & Hosseini-Bandegharaei, A. (2021). Is one performing the treatment data of adsorption kinetics correctly? *Journal of Environmental Chemical Engineering, 9*(2), 104813. doi:https://doi.org/10.1016/j.jece.2020.104813

Linares Hernández, I., Barrera Díaz, C., Valdés Cerecero, M., Almazán Sánchez, P. T., Castañeda Juárez, M., & Lugo Lugo, V. (2017). Soft drink wastewater treatment by electrocoagulation–electrooxidation processes. *Environmental Technology, 38*(4), 433-442. doi:10.1080/09593330.2016.1196740

Liu, L., Luo, X. B., Ding, L., & Luo, S. L. (2019). 4 - Application of nanotechnology in the removal of heavy metal from water. In Luo, X. & Deng, F. (Eds.), *Nanomaterials for the Removal of Pollutants and Resource Reutilization* (pp. 83-147): Elsevier. doi:https://doi.org/10.1016/B978-0-12-814837-2.00004-4

Liu, Y., Hu, X. M., Zhao, Y., Wang, J., Lu, M. X., Peng, F. H., & Bao, J. (2018). Removal of perfluorooctanoic acid in simulated and natural waters with different electrode materials by electrocoagulation. *Chemosphere, 201*, 303-309. doi:https://doi.org/10.1016/j.chemosphere.2018.02.129

López-Guzmán, M., Flores-Hidalgo, M. A., & Reynoso-Cuevas, L. (2021). Electrocoagulation process: An Approach to continuous processes, reactors design, pharmaceuticals removal, and hybrid systems—A Review. *Processes, 9(*10), 1831. doi:https://www.mdpi.com/2227-9717/9/10/1831

López-Luna, J., Ramírez-Montes, L. E., Martinez-Vargas, S., Martínez, A. I., Mijangos-Ricardez, O. F., González-Chávez, M. D. C. A., & Vázquez-Hipólito, V. (2019). Linear and nonlinear kinetic and isotherm adsorption models for arsenic removal by manganese ferrite nanoparticles. *SN Applied Sciences, 1*(8), 950. doi:10.1007/s42452-019-0977-3

Manilal, A. M., & Soloman, P. A. (2020). Influence of Operating Parameters on the Fraction of oil oxidized during electrocoagulation of produced water. *Water Conservation Science and Engineering, 5*(1), 41-52. doi:10.1007/s41101-020-00083-9

Marasović, M., Marasović, T., & Miloš, M. (2017). Robust nonlinear regression in enzyme kinetic parameters estimation. *Journal of Chemistry, 2017*, 6560983. doi:10.1155/2017/6560983

Martin, P., Cherukuru, N., Tan, A. S. Y., Sanwlani, N., Mujahid, A., & Müller, M. (2018). Distribution and cycling of terrigenous dissolved organic carbon in peatland-draining rivers and coastal waters of Sarawak, Borneo. *Biogeosciences, 15*(22), 6847-6865. doi:10.5194/bg-15-6847-2018

Mboyi, A.V., Kamika, I., & Momba, M. N. B. (2021). Chapter 24 - Comparing the biosorption of ZnO and Ag nanomaterials by consortia of protozoan and bacterial species. In Abd-Elsalam, K. A. (Ed.), *Silver Nanomaterials for Agri-Food Applications* (pp. 579-598): Elsevier. doi:https://doi.org/10.1016/B978-0-12-823528-7.00013-5

Mehri, M., Fallah, N., & Nasernejad, B. (2021). Mechanisms of heavy metal and oil removal from synthetic saline oilfield produced water by electrocoagulation. *Clean Water, 4*(1), 45. doi:10.1038/s41545-021-00135-0

Mena, V. F., Betancor-Abreu, A., González, S., Delgado, S., Souto, R. M., & Santana, J. (2019). Fluoride removal from natural volcanic underground water by an electrocoagulation process: Parametric and cost evaluations. *Journal of Environmental Management, 246*, 472-483. doi:https://doi.org/10.1016/j.jenvman.2019.05.147

Mikšík, F., Miyazaki, T., & Thu, K. (2020). Adsorption isotherm modelling of water on nano-tailored mesoporous silica based on distribution function. *Energies, 13*(16), 4247. doi:https://www.mdpi.com/1996-1073/13/16/4247

Mishra, P., Pandey, C. M., Singh, U., Keshri, A., & Sabaretnam, M. (2019). Selection of appropriate statistical methods for data analysis. *Annals of Cardiac Anaesthesia, 22*(3), 297-301. doi:10.4103/aca.ACA_248_18

Mohammadi, A., Khadir, A., & Tehrani, M. A. R. (2019). Optimization of nitrogen removal from an anaerobic digester effluent by electrocoagulation process. *Journal of Environmental Chemical Engineering, 7*(3), 103195. doi:https://doi.org/10.1016/j.jece.2019.103195

Moomaw, W. R., Chmura, G. L., Davies, G. T., Finlayson, C. M., Middleton, B. A., Natali, S. M., & Sutton-Grier, A. E. (2018). Wetlands in a changing climate: Science, policy and management. *Wetlands, 38*(2), 183-205. doi:10.1007/s13157-018-1023-8

Moradi, M., Vasseghian, Y., Arabzade, H., & Mousavi Khaneghah, A. (2021). Various wastewaters treatment by sono-electrocoagulation process: A comprehensive review of operational parameters and future outlook. *Chemosphere, 263*, 128314. doi:https://doi.org/10.1016/j.chemosphere.2020.128314

Moussa, D.T., El-Naas, M. H., Nasser, M., & Al-Marri, M. J. (2017). A comprehensive review of electrocoagulation for water treatment: Potentials and challenges. *Journal of Environmental Management, 186*, 24-41. doi:https://doi.org/10.1016/j.jenvman.2016.10.032

Mu, T. H., & Sun, H. N. (2019). Chapter 22 - Sweet potato leaf polyphenols: preparation, individual phenolic compound composition and antioxidant activity. In R. R. Watson (Ed.), *Polyphenols in Plants* (Second Edition) (pp. 365-380): Academic Press. doi:http://dx.doi.org/10.1016/B978-0-12-813768-0.00022-0

Muhdarina, M., Linggawati, A., Putri, K., Muharani, D., Awaluddin, A., & Bahri, S. (2018). Peat water treatment by two stages coagulation processes using natural clay based liquid coagulant. *International Journal of Science and Research (IJSR), 7*. doi:10.21275/ART20181761

Muniasamy, S. K., Gameda, T. T., Mallaian, L. S., Rengaraju, I., Segaran, J., Periyasamy, Y., & Subramanian, S. (2022). Investigation on solar-powered electrocoagulation (SPEC) for the treatment of domestic wastewater (DWW). *Advances in Materials Science and Engineering, 2022*, 5389340. doi:10.1155/2022/5389340

Muttakin, M., Mitra, S., Thu, K., Ito, K., & Saha, B. B. (2018). Theoretical framework to evaluate minimum desorption temperature for IUPAC classified adsorption isotherms. *International Journal of Heat and Mass Transfer, 122*, 795-805. doi: https://doi.org/10.1016/j.ijheatmasstransfer.2018.01.107

Naje, A. S., Chelliapan, S., Zakaria, Z., Ajeel, M. A., & Alaba, P. A. (2017). A review of electrocoagulation technology for the treatment of textile wastewater. *Reviews in Chemical Engineering, 33*(3), 263-292. doi:10.1515/revce-2016-0019

Nakama, Y. (2017). Chapter 15 - Surfactants. In Sakamoto, K., Lochhead, R. Y., Maibach, H. I. & Yamashita, Y. (Eds.), *Cosmetic Science and Technology* (pp. 231-244). Amsterdam: Elsevier. doi: https://doi.org/10.1016/B978-0-12-802005-0.00015-X

National Audit Department (NAD). (2022). *Laporan ketua audit negara tahun 2017 pengurusan aktiviti kementerian/jabatan/agensi dan pengurusan syarikat kerajaan negeri sarawak siri 2*. Accessed on 1st July 2022 and retrieved from https://lkan.audit.gov.my/laporan/manage/443

Nawarkar, C. J., & Salkar, V. D. (2019). Solar powered electrocoagulation system for municipal wastewater treatment. *Fuel, 237*, 222-226. doi:https://doi.org/10.1016/j.fuel.2018.09.140

New Sarawak Tribune. (2019). *Challenges facing JBALB in resolving state's water woes*. Accessed on 1st July 2022 Retrieved from https://www.newsarawaktribune.com.my/challenges-facing-jbalb-in-resolving-states-water-woes/

Nguyen, D. D., Yoon, Y. S., Bui, X. T., Kim, S. S., Chang, S. W., Guo, W., & Ngo, H. H. (2017). Influences of operational parameters on phosphorus removal in batch and continuous electrocoagulation process performance. *Environmental Science and Pollution Research International, 24*(32), 25441-25451. doi:10.1007/s11356-017-0180-2

Ni, C., Wang, J., Guan, Y., Jiang, B., Meng, X., Luo, S., & Wang, L. (2020). Self-powered peroxi-coagulation for the efficient removal of p-arsanilic acid: pH-dependent shift in the contributions of peroxidation and electrocoagulation. *Chemical Engineering Journal, 391*, 123495. doi:https://doi.org/10.1016/j.cej.2019.123495

Nidheesh, P. V., Kumar, A., Syam Babu, D., Scaria, J., & Suresh Kumar, M. (2020). Treatment of mixed industrial wastewater by electrocoagulation and indirect electrochemical oxidation. *Chemosphere, 251*, 126437. doi:https://doi.org/10.1016/j.chemosphere.2020.126437

Nthunya, L. N., Maifadi, S., Mamba, B. B., Verliefde, A. R., & Mhlanga, S. D. (2018). Spectroscopic determination of water salinity in brackish surface water in Nandoni dam, at Vhembe District, Limpopo Province, South Africa. *Water, 10*(8), 990. doi:https://www.mdpi.com/2073-4441/10/8/990

Nugroho, F. A., Arif, A., Sabila, G., & Aryanti, P. T. P. (2021). Slaughterhouse wastewater treatment by electrocoagulation process. *IOP Conference Series: Materials Science and Engineering, 1115*, 012037. doi:10.1088/1757-899X/ 1115/1/012037

Nyangi, M. J., Chebude, Y., Kilulya, K. F., & Salim, C. J. (2021). Comparative study on adsorption isotherm and kinetics of defluoridation using aluminum and iron electrodes in electrocoagulation. *Chemistry Africa, 4*(2), 391-398. doi:10.1007/s42250-021-00228-w

Oden, M. K. (2020). Treatment of CNC industry wastewater by electrocoagulation technology: an application through response surface methodology. *International*

Journal of Environmental Analytical Chemistry, 100(1), 1-19. doi:10.1080/03067319.2019.1628955

Omar, M. S., Ifandi, E., Sukri, R. S., Kalaitzidis, S., Christanis, K., Lai, D. T. C., & Tsikouras, B. (2022). Peatlands in Southeast Asia: A comprehensive geological review. *Earth-Science Reviews, 232*, 104149. doi:https://doi.org/10.1016/j.earscirev.2022.104149

Padmaja, K., Cherukuri, J., & Anji Reddy, M. (2020). A comparative study of the efficiency of chemical coagulation and electrocoagulation methods in the treatment of pharmaceutical effluent. *Journal of Water Process Engineering, 34*, 101153. doi:https://doi.org/10.1016/j.jwpe.2020.101153

Palanisamy, S., Nachimuthu, P., Awasthi, M. K., Ravindran, B., Chang, S. W., Palanichamy, M., & Nguyen, D. D. (2020). Application of electrochemical treatment for the removal of triazine dye using aluminium electrodes. *Journal of Water Supply: Research and Technology-Aqua*, *69*(4), 345-354. doi:https://doi.org/10.2166/aqua.2020.109

Pandey, N., & Thakur, C. (2020). Statistical comparison of response surface methodology–based central composite design and hybrid central composite design for paper mill wastewater treatment by electrocoagulation. *Process Integration and Optimization for Sustainability, 4*(4), 343-359. doi:10.1007/s41660-020-00123-w

Papadopoulos, K. P., Argyriou, R., Economou, C. N., Charalampous, N., Dailianis, S., Tatoulis, T. I., & Vayenas, D. V. (2019). Treatment of printing ink wastewater using electrocoagulation. *Journal of Environmental Management, 237*, 442-448. doi:https://doi.org/10.1016/j.jenvman.2019.02.080

Perperoglou, A., Sauerbrei, W., Abrahamowicz, M., & Schmid, M. (2019). A review of spline function procedures in R. *BMC Medical Research Methodology, 19*(1), 46. doi:10.1186/s12874-019-0666-3

Petinggi, G. (2022). *RM150 mln spent yearly to subsidies treated water supply*. Accessed on 1st July 2022 and retrieved from https://www.pressreader.com/malaysia/the-borneo-post/20220208/281736977862420

Piepho, H. P. (2019). A coefficient of determination (R^2) for generalized linear mixed models. *Biometrical Journal, 61*(4), 860-872. doi:https://doi.org/10.1002/bimj.201800270

Politis, S., Colombo, P., Colombo, G., & M. Rekkas, D. (2017). Design of experiments (DoE) in pharmaceutical development. *Drug Development and Industrial Pharmacy, 43*(6), 889-901. doi:10.1080/03639045.2017.1291672

Pooi, C. K., & Ng, H. Y. (2018). Review of low-cost point-of-use water treatment systems for developing communities. *NPJ Clean Water*, *1*(1), 1-8. doi:10.1038/s41545-018-0011-0

Pooresmaeil, M., & Namazi, H. (2020). Chapter 14 - Application of polysaccharide-based hydrogels for water treatments. In Chen, Y. (Ed.), *Hydrogels Based on Natural Polymers* (pp. 411-455): Elsevier. doi:http://dx.doi.org/10.1016/B978-0-12-81642 1-1 .00014-8

Prasanna, M. V., Ramdzani, I. A. B. A., Nagarajan, R., Chidambaram, S., & Venkatramanan, S. (2019). Geoelectrical investigation along Miri coast, East Malaysia: Evaluate the vulnerability of coastal aquifer. *IOP Conference Series: Materials Science and Engineering, 495*, 012042. doi:10.1088/1757-899x/495/1/012042

Praveena, S. M., Shaifuddin, S. N. M., Sukiman, S., Nasir, F. A. M., Hanafi, Z., Kamarudin, N., & Aris, A. Z. (2018). Pharmaceuticals residues in selected tropical surface water bodies from Selangor (Malaysia): Occurrence and potential risk assessments. *Science of Total Environment, 642*, 230-240. doi:10.1016/j.scitotenv.2018.06.058

Qasim, M., Badrelzaman, M., Darwish, N. N., Darwish, N. A., & Hilal, N. (2019). Reverse osmosis desalination: A state-of-the-art review. *Desalination, 459*, 59-104. doi:https://doi.org/10.1016/j.desal.2019.02.008

Rafiee, P., Hosseini, M., & Ebrahimi, S. (2020). The evolution patterns of temperature, pH, and voltage during the removal of chemical oxygen demand from a landfill leachate using electrocoagulation under different conditions. *Reaction Kinetics, Mechanisms and Catalysis, 131*(1), 319-334. doi:10.1007/s11144-020-01846-0

Rahma, A., Elma, M., Rampun, E. L. A., Pratiwi, A., Rakhman, A., & Fitriani, F. (2020). Rapid thermal processing and long-term stability of interlayer-free silica-P123 membranes for wetland saline water desalination. *Journal of Advanced Research in Fluid Mechanics and Thermal Sciences, 71*, 1-9. doi:10.37934/arfmts.71.2.19

Rahman, N. A., Linus, A. A., Philip, A., Jihed, E. E., Gilan, U. J., Kumar, N. K. M. F., & Yassin, A. (2021). Development of solar power system for Sarawak peat water continuous electrocoagulation treatment process. *IOP Conference Series: Materials Science and Engineering, 1101*(1), 012039. doi:10.1088/1757-899x/1101/1/012039

Rahman, N.A., Albania Linus, A., Gilan, U. J., Jihed, E. E., Kumar, N. K. M. F., Yassin, A., & Philip, A. (2020a). Experimental study of batch electrocoagulation treatment of peat water in Sarawak with aluminium electrodes. *IOP Conference Series: Materials Science and Engineering, 778*, 012126. doi:10.1088/1757-899x/778/1/012126

Rahman, N.A., Allene Albania, L., Elisa Elizabeth, J., Umang Jata, G., Nurhidayah Kumar Muhammad Firdaus, K., Adarsh, P., & Arif, P. (2020b). Experimental studies on continuous electrocoagulation treatment of peat water in sarawak with copper electrodes. *International Journal of Integrated Engineering, 13*(2). doi:https://publisher.uthm.edu.my/ojs/index.php/ijie/article/view/7640

Rahman, N., Tomiran, N., & Hashim, A. (2020c). Batch electrocoagulation treatment of peat water in Sarawak with galvanized iron electrodes. *Materials Science Forum, 997*, 127-138. doi:10.4028/www.scientific.net/MSF.997.127Rahman

Rahman, N. A., Kumar, N. K. M. F., Gilan, U. J., Jihed, E. E., Phillip, A., Linus, A. A., & Ismail, V. (2020d). Kinetic study & statistical modelling of Sarawak peat water electrocoagulation system using copper and aluminium electrodes. *Journal of Applied Science & Process Engineering, 7*(1). doi:10.33736/jaspe.2195.2020

Rasmey, A. H., Aboseidah, A. A., & Youssef, A. K. (2018). Application of Langmuir and Freundlich Isotherm models on biosorption of Pb^{2+} by Freez-dried biomass of

Pseudomonas aeruginosa. *Egyptian Journal of Microbiology, 53*(1), 37-48. doi:10.21608/ejm.2018.2998.1050

Revellame, E. D., Fortela, D. L., Sharp, W., Hernandez, R., & Zappi, M. E. (2020). Adsorption kinetic modeling using pseudo-first order and pseudo-second order rate laws: A review. *Cleaner Engineering and Technology, 1*, 100032. doi: https://doi.org/10.1016/j.clet.2020.100032

Rodrigues, A. R., Seki, C. C., Ramalho, L. S., Argondizo, A., & Silva, A. P. (2020). Electrocoagulation in a fixed bed reactor – Color removal in batch and continuous mode. *Separation and Purification Technology, 253*, 117481. doi: https://doi.org/10.1016/j.seppur.2020.117481

Roy, R. (2019). An introduction to water quality analysis. *International Journal for Environmental Rehabilitation and Conservation, 6*, 201-205. doi:10.31786/0975 6272.18.9.2.214

Roy, U., Manna, S., Sengupta, S., Das, P., Datta, S., Mukhopadhyay, A., & Bhowal, A. (2018). Dye removal using microbial biosorbents. In Crini, G. & Lichtfouse, E. (Eds.), *Green Adsorbents for Pollutant Removal: Innovative materials* (pp. 253-280). Cham: Springer International Publishing. doi: http://dx.doi.org/10.1007/ 978-3-319-92162-4_8

Rusdianasari, Bow, Y., & Dewi, T. (2019). Peat water treatment by electrocoagulation using aluminium electrodes. *IOP Conference Series: Earth and Environmental Science, 258*, 012013. doi:10.1088/1755-1315/258/1/012013

Sabarinathan, C., Karuppasamy, P., Vijayakumar, C. T., & Arumuganathan, T. (2019). Development of methylene blue removal methodology by adsorption using molecular polyoxometalate: Kinetics, Thermodynamics and Mechanistic Study. *Microchemical Journal, 146*, 315-326. doi:https://doi.org/10.1016/j.microc.2019. 01.015

Sahoo, T. R., & Prelot, B. (2020). Chapter 7 - Adsorption processes for the removal of contaminants from wastewater: the perspective role of nanomaterials and nanotechnology. In Bonelli, B., Freyria, F. S., Rossetti, I., & Sethi, R. (Eds.), *Nanomaterials for the Detection and Removal of Wastewater Pollutants* (pp. 161-222): Elsevier. doi:http://dx.doi.org/10.1016/B978-0-12-818489-9.00007-4

Sahu, O., & Singh, N. (2019). 13 - Significance of bioadsorption process on textile industry wastewater. In Shahidul, I. & Butola, B. S. (Eds.), *The Impact and Prospects of Green Chemistry for Textile Technology* (pp. 367-416): Woodhead Publishing. doi: http://dx.doi.org/10.1016/B978-0-08-102491-1.00013-7

Sakthisharmila, P., Palanisamy, P. N., & Manikandan, P. (2018). Removal of benzidine based textile dye using different metal hydroxides generated in situ electrochemical treatment - A comparative study. *Journal of Cleaner Production, 172*, 2206-2215. doi: https://doi.org/10.1016/j.jclepro.2017.11.192

Samipour, S., Manshadi, M. D., & Setoodeh, P. (2020). Chapter 20 - CO_2 removal from biogas and syngas. In Rahimpour, M. R., Farsi, M. & Makarem, M. A. (Eds.), *Advances in Carbon Capture* (pp. 455-477): Woodhead Publishing. doi: http://dx.doi.org/10.1016/B978-0-12-819657-1.00020-7

Sangok, F. E., Sugiura, Y., Maie, N., Melling, L., Nakamura, T., Ikeya, K., & Watanabe, A. (2020). Variations in the rate of accumulation and chemical structure of soil organic matter in a coastal peatland in Sarawak, Malaysia. *CATENA, 184*, 104244. doi: https://doi.org/10.1016/j.catena.2019.104244

Sari, M. A., & Chellam, S. (2017). Electrocoagulation process considerations during advanced pretreatment for brackish inland surface water desalination: Nanofilter fouling control and permeate water quality. *Desalination, 410*, 66-76. doi: https://doi.org/10.1016/j.desal.2017.02.001

Scimeca, M., Bischetti, S., Lamsira, H. K., Bonfiglio, R., & Bonanno, E. (2018). Energy Dispersive X-ray (EDX) microanalysis: A powerful tool in biomedical research and diagnosis. *European Journal of Histochemistry: EJH*, *62*(1). doi:10.4081/ ejh.2018.2841

Sefatjoo, P., Moghaddam, M. R. A., & Mehrabadi, A. R. (2020). Evaluating electrocoagulation pretreatment prior to reverse osmosis system for simultaneous scaling and colloidal fouling mitigation: Application of RSM in performance and cost optimization. *Journal of Water Process Engineering, 35*, 101201. doi:https://doi.org/10.1016/j.jwpe.2020.101201

Selmane, B. H. H. E., Abderrazak, H., Ounissi, T., & Djebali, K. (2020). Experimental design and response surface methodologies use for the treatment of leachates by

electrocoagulation process. *Chemistry Africa, 3*(3), 821-829. doi:10.1007/ s42250-020-00149-0

Shahedi, A., Darban, A. K., Taghipour, F., & Jamshidi-Zanjani, A. (2020). A review on industrial wastewater treatment via electrocoagulation processses. *Current Opinion in Electrochemistry, 22*, 154-169. doi:https://doi.org/ 10.1016/j.coelec.2020.05.009

Shaker, A., Moneer, A., El-Saadawy, M., El-Mallah, N., & Ramadan, M. (2020). Comparative study for removal of acid green 20 dye by electrocoagulation technique using aluminum and iron electrodes. *Desalination and Water Treatment, 198*, 345–363. doi:10.5004/dwt.2020.26007

Shamaei, L., Khorshidi, B., Perdicakis, B., & Sadrzadeh, M. (2018). Treatment of oil sands produced water using combined electrocoagulation and chemical coagulation techniques. *Science of The Total Environment, 645*, 560-572. doi:https://doi.org/10.1016/j.scitotenv.2018.06.387

Sharip, Z., Yusoff, F. M., & Jamin, A. (2019). Seasonal water quality and trophic status of shallow lentic waters and their association with water levels. *International Journal of Environmental Science and Technology, 16*(8), 4851-4862. doi: 10.1007/s13762-018-2172-2

Sharma, L., Prabhakar, S., Tiwari, V., Dhar, A., & Halder, A. (2021). Optimization of EC parameters using Fe and Al electrodes for hydrogen production and wastewater treatment. *Environmental Advances, 3*, 100029. doi:https://doi.org/ 10.1016/j.envadv.2020.100029

Shen, Y., Yılmaz, M., Li, A., & Ji, B. (2022). Insights into the water depth for the non-aerated microalgal-bacterial granular sludge process via kinetic analysis. *Journal of Water Process Engineering, 48*, 102881. doi:10.1016/j.jwpe.2022. 102881

Sibiya, N. P., Rathilal, S., & Kweinor Tetteh, E. (2021). Coagulation treatment of wastewater: Kinetics and natural coagulant evaluation. *Molecules, 26*(3), 698. doi: https://www.mdpi.com/1420-3049/26/3/698

Sibu Water Board (SWB). (2018). *Annual report 2018*. Accessed on 1st July 2022 and retrieved from https://sarawak.gov.my/ebook/SWB/AnnualReport2018/mobile/index.html

Simonič, M., Čurlin, M., & Zemljič, L. (2020). Analysis of electrocoagulation process efficiency of compost leachate with the first order kinetic model. *The Holistic Approach to Environment, 10*, 35-40. doi:10.33765/thate.10.2.2

Sonda, M. T., Mihale, M. J., & Kileo, W. J. (2022). Geochemical parameters and seawater quality assessments around Dar es Salaam harbour, Tanzania. *International Journal of Energy and Water Resources, 6*(4), 495-507. doi: https://doi.org/10.1007/s42108-022-00194-0

Steyerberg, E. W. (2019). Overfitting and optimism in prediction models. In Steyerberg, E. W. (Ed.*), Clinical Prediction Models: A Practical Approach to Development, Validation, and Updating* (pp. 95-112). Cham: Springer International Publishing. doi: https://doi.org/10.1007/978-3-030-16399-0

Stromer, B. S., Woodbury, B., & Williams, C. F. (2018). Tylosin sorption to diatomaceous earth described by Langmuir isotherm and Freundlich isotherm models. *Chemosphere, 193*, 912-920. doi:https://doi.org/10.1016/j.chemosphere.2017.11.083

Sullivan, K., Thomas, S., & Rosano, M. (2018). Using industrial ecology and strategic management concepts to pursue the Sustainable Development Goals. *Journal of Cleaner Production*, *174*, 237-246. doi:https://doi.org/10.1016/j.jclepro.2017.10.201

Sultan, M., Miyazaki, T., & Koyama, S. (2018). Optimization of adsorption isotherm types for desiccant air-conditioning applications. *Renewable Energy, 121*, 441-450. doi:https://doi.org/10.1016/j.renene.2018.01.045

Sun, Y., Zhou, S., Chiang, P. C., & Shah, K. J. (2019). Evaluation and optimization of enhanced coagulation process: Water and energy nexus. *Water-Energy Nexus, 2*(1), 25-36. doi:https://doi.org/10.1016/j.wen.2020.01.001

Sundari, S. (2020). Dissolved organic carbon and physicochemical variables of peat water in tropical peat swamp forests. *IOP Conference Series: Earth and Environmental Science, 591*(1), 012045. doi:10.1088/1755-1315/591/1/012045

Sutapa, I. D. A., Prihatinningtyas, E., & Daryanta. (2020). IPAG60 as alternative solution to provide clean water in peatland areas. *IOP Conference Series: Earth and Environmental Science, 477*(1), 012030. doi:10.1088/1755-1315/477/1/012030

Swain, K., Abbassi, B., & Kinsley, C. (2020). Combined electrocoagulation and chemical coagulation in treating brewery wastewater. *Water, 12*(3). doi:10.3390/w12030726

Swenson, H., & Stadie, N. P. (2019). Langmuir's theory of adsorption: A centennial review. *Langmuir, 35*(16), 5409-5426. doi:10.1021/acs.langmuir.9b00154

Taheri, M. (2022). Techno-economical aspects of electrocoagulation optimization in three acid azo dyes' removal comparison. *Cleaner Chemical Engineering, 2*, 100007. doi:https://doi.org/10.1016/j.clce.2022.100007

Tahreen, A., Jami, M. S., & Ali, F. (2020). Role of electrocoagulation in wastewater treatment: A developmental review. *Journal of Water Process Engineering, 37*, 101440. doi:https://doi.org/10.1016/j.jwpe.2020.101440

Takahashi, H., Yamamoto, K., & Inoue, T. (2021). Principles of hydrological management of tropical peatland. In Osaki, M., Tsuji, N., Foead, N., & Rieley, J. (Eds.), *Tropical Peatland Eco-management* (pp. 537-566). Singapore: Springer Singapore. doi: http://dx.doi.org/10.1007/978-981-33-4654-3_19

Tan, K. L., & Hameed, B. H. (2017). Insight into the adsorption kinetics models for the removal of contaminants from aqueous solutions. *Journal of the Taiwan Institute of Chemical Engineers, 74*, 25-48. doi:https://doi.org/10.1016/j.jtice.2017.01.024

Tang, W., Wang, X., Zeng, G., Liang, J., Li, X., Xing, W., & Liu, Z. (2019). Electro-assisted adsorption of Zn(II) on activated carbon cloth in batch-flow mode: Experimental and theoretical investigations. *Environmental Science & Technology, 53*(5), 2670-2678. doi:10.1021/acs.est.8b05909

Teepol, B., Ng, J. J., Kong, D., Yong, D. L., Teo, J. J. H., & Au, N. J. (2021). Long-term count data demonstrate the regional significance of Bako-Buntal Bay, Malaysian Borneo, for wintering shorebird conservation. *Wader Study Group Bulletin, 128*, 174-182. doi:10.18194/ws.00239

Tetteh, E. K., & Sudesh, R. (2019). Application of organic coagulants in water and wastewater treatment. In Arpit, S. & Elsayed, Z. (Eds.), *Organic Polymers* (pp. Ch. 4). IntechOpen. doi:https://doi.org/10.5772/intechopen.84556

Thakur, C. (2020). Electrocoagulation treatment of automobile wastewater: Optimization by RSM. *IOP Conference Series: Earth and Environmental Science, 597*, 012017. doi:10.1088/1755-1315/597/1/012017

Titchou, F. E., Zazou, H., Afanga, H., El Gaayda, J., Akbour, R. A., & Hamdani, M. (2021). Removal of persistent organic pollutants (POPS) from water and wastewater by adsorption and electrocoagulation process. *Groundwater for Sustainable Development, 13*, 100575. doi:https://doi.org/10.1016/j.gsd.2021.100575

Titus, D., James Jebaseelan Samuel, E., & Roopan, S. M. (2019). Chapter 12 - Nanoparticle characterization techniques. In Shukla, A. K. & Iravani, S. (Eds.), *Green Synthesis, Characterization and Applications of Nanoparticles* (pp. 303-319): Elsevier. doi:http://dx.doi.org/10.1016/B978-0-08-102579-6.00012-5

Tones, A. R. M., Eyng, E., Zeferino, C. L., de Oliveira Ferreira, S., de Almeida Alves, A. A., Fagundes-Klen, M. R., & Sehn, E. (2020). Spectral deconvolution associated to the Gaussian fit as a tool for the optimization of photovoltaic electrocoagulation applied in the treatment of textile dyes. *Science of The Total Environment*, *713*, 136301. doi: https://doi.org/10.1016/j.scitotenv.2019.136301

Torres-Rivero, K., Bastos-Arrieta, J., Fiol, N., & Florido, A. (2021). Chapter Ten - Metal and metal oxide nanoparticles: An integrated perspective of the green synthesis methods by natural products and waste valorization: Applications and challenges. In Verma, S. K. & Das, A. K. (Eds.), *Comprehensive Analytical Chemistry* (Vol. 94, pp. 433-469): Elsevier. doi: http://dx.doi.org/10.1016/bs.coac.2020.12.001

Trompette, J. L., & Lahitte, J. F. (2021). Effects of some ion-specific properties in the electrocoagulation process with aluminum electrodes. *Colloids and Surfaces A: Physicochemical and Engineering Aspects, 629*, 127507. doi:10.1016/j.colsurfa. 2021.127507

Upadhyay, U., Sreedhar, I., Singh, S. A., Patel, C. M., & Anitha, K. L. (2021). Recent advances in heavy metal removal by chitosan-based adsorbents. *Carbohydrate Polymers, 251*, 117000. doi:https://doi.org/10.1016/j.carbpol.2020.117000

Verbeke, R., Eyley, S., Szymczyk, A., Thielemans, W., & Vankelecom, I. F. J. (2020). Controlled chlorination of polyamide reverse osmosis membranes at real scale for enhanced desalination performance. *Journal of Membrane Science, 611*, 118400. doi:https://doi.org/10.1016/j.memsci.2020.118400

Villalobos-Lara, A. D., Álvarez, F., Gamiño-Arroyo, Z., Navarro, R., Peralta-Hernández, J. M., Fuentes, R., & Pérez, T. (2021). Electrocoagulation treatment of industrial tannery wastewater employing a modified rotating cylinder electrode reactor. *Chemosphere, 264*, 128491. doi:https://doi.org/10.1016/j.chemosphere.2020.128491

Vogelgesang, F., Kumar, U., & Sundram, K. (2018). Building a sustainable future together: Malaysian palm oil and European consumption. *Journal of Oil Palm, Environment and Health (JOPEH)*, *9*, 1 – 49. doi:10.5366/jope.2018.01

Waller, M., & Kirby, J. (2021). Coastal peat-beds and peatlands of the southern North Sea: Their past, present and future. *Biological Reviews, 96*(2), 408-432. doi:https://doi.org/10.1111/brv.12662

Wang, J., & Guo, X. (2020). Adsorption isotherm models: Classification, physical meaning, application and solving method. *Chemosphere, 258*, 127279. doi:https://doi.org/10.1016/j.chemosphere.2020.127279

Wellner, D. B., Couperthwaite, S. J., & Millar, G. J. (2018). Influence of operating parameters during electrocoagulation of sodium chloride and sodium bicarbonate solutions using aluminium electrodes. *Journal of Water Process Engineering, 22*, 13-26. doi:https://doi.org/10.1016/j.jwpe.2017.12.014

Wenten, I. G., Khoiruddin, K., Wardani, A. K., Aryanti, P. T. P., Astuti, D. I., & Komaladewi, A. A. I. A. S. (2020). Preparation of antifouling polypropylene/ZnO composite hollow fiber membrane by dip-coating method for peat water treatment. *Journal of Water Process Engineering, 34*, 101158. doi:https://doi.org/10.1016/j.jwpe.2020.101158

Wildayana, E. (2017). Challenging constraints of livelihoods for farmers on the South Sumatra Peatlands, Indonesia. *Bulgarian Journal of Agricultural Science*, *23*(6), 894-905. doi:https://www.agrojournal.org/23/06-02.pdf

Wilson, R., & George, G. (2020). 4 - Pervaporation performance of polymer/clay nanocomposites. In Thomas, S., George, S. C., & Jose, T. (Eds.), *Polymer Nanocomposite Membranes for Pervaporation* (pp. 81-104): Elsevier. doi: https://doi.org/10.1016/B978-0-12-816785-4.00004-5

Wu, Z., Dong, J., Yao, Y., Yang, Y., & Wei, F. (2021). Continuous flowing electrocoagulation reactor for efficient removal of azo dyes: Kinetic and isotherm studies of adsorption. *Environmental Technology & Innovation, 22*, 101448. doi:10.1016/j.eti.2021.101448

Yavuz, Y., & Ögütveren, Ü. B. (2018). Treatment of industrial estate wastewater by the application of electrocoagulation process using iron electrodes. *Journal of Environmental Management, 207*, 151-158. doi:https://doi.org/10.1016/j.jenvman.2017.11.034

Yolmeh, M., & Jafari, S. M. (2017). Applications of response surface methodology in the food industry processes. *Food and Bioprocess Technology, 10*(3), 413-433. doi:10.1007/s11947-016-1855-2

Yu, W., Xu, L., Lei, K., & Gregory, J. (2018). Effect of crystallization of settled aluminium hydroxide precipitate on “dissolved Al”. *Water Research, 143*, 346-354. doi:https://doi.org/10.1016/j.watres.2018.06.063

Zaied, B. K., Rashid, M., Nasrullah, M., Zularisam, A. W., Pant, D., & Singh, L. (2020). A comprehensive review on contaminants removal from pharmaceutical wastewater by electrocoagulation process. *Science of The Total Environment, 726*, 138095. doi:https://doi.org/10.1016/j.scitotenv.2020.138095

Zampeta, C., Mastrantonaki, M., Katsaouni, N., Frontistis, Z., Koutsoukos, P., & Vayenas, D. (2022). Treatment of printing ink wastewater using a continuous flow electrocoagulation reactor. *Journal of Environmental Management, 314*, 115033. doi:10.1016/j.jenvman.2022.115033

Zarei, A., Biglari, H., Mobini, M., Ebrahimzadeh, G., Yari, A. R., Narooie, M. R., & Mazloomi, S. (2018). Enhancing electrocoagulation process efficiency using Astraglus Gossypinus Tragacanth in turbidity removal from brackish water samples. *Polish Journal of Environmental Studies, 27(*4), 1851-1858. doi:10.15244/pjoes/77960

Zhang, X., Lu, M., Idrus, M. A. M., Crombie, C., & Jegatheesan, V. (2019). Performance of precipitation and electrocoagulation as pretreatment of silica removal in brackish water and seawater. *Process Safety and Environmental Protection, 126*, 18-24. doi:https://doi.org/10.1016/j.psep.2019.03.024

Zhang, Q., Ye, X., Li, H., Chen, D., Xiao, W., Zhao, S., & Li, J. (2020). Cumulative effects of pyrolysis temperature and process on properties, chemical speciation, and environmental risks of heavy metals in magnetic biochar derived from coagulation-flocculation sludge of swine wastewater. *Journal of Environmental Chemical Engineering, 8*(6), 104472. doi:https://doi.org/10.1016/j.jece.2020.104472

APPENDICES

APPENDIX A: Publications

Journal Publications (SCOPUS)

1. Rahman, N. A., **Jose Jol, C**., Albania Linus, A., Dampam, F. L., Abdul Jalal, N. S., Baharudin, N., & Wan Borhan, W. W. S. (2022). Desalination of Borneo tropical brackish peat water with adsorption process in continuous electrocoagulation treatment. *Desalination, 527 (April 2022)*, 115574. doi:https://doi.org/10.1016/j.desal.2022.115574

   (Journal Indexed in Q1, SCOPUS, & WOS, Impact Factor: 11.211, Cite Score: 16.3)

2. Rahman, N. A., **Jose Jol, C.**, Albania Linus, A., Dampam, F.L., Abdul Jalal, N.S, Baharudin, N. & Wan Borhan, W.W.S (2022). Continuous electrocoagulation treatment of Borneo tropical brackish peat water from palm oil plantation region for domestic consumption in coastal rural areas. *Chemical Engineering and Processing – Process Intensification, 176* (June 2022), 108967. doi: https://doi.org/10.1016/j.cep.2022.108967

   (Journal Indexed in Q1, SCOPUS, & WOS, Impact Factor: 4.264, Cite Score: 6.9)

3. Rahman, N. A., **Jose Jol, C.**, Linus, A. A., & Ismail, V. (2021). Emerging application of electrocoagulation for tropical peat water treatment: A review. *Chemical Engineering and Processing - Process Intensification*, *165 (August 2021),* 108449. doi: https://doi.org/10.1016/j.cep.2021.108449

   (Journal Indexed in Q1, SCOPUS, & WOS, Impact Factor: 4.264, Cite Score: 6.9)

Conference Proceedings

1. Rahman, N. A., Albania Linus, A., **Jose Jol, C.**, Abdul Jalal, N.S., Baharudin, N., & Wan Borhan, W.W.S. (2022, July 19-20). *Characterization of peat water electrocoagulation flocs from Sarawak southern region* [Paper Presentation]. 7th International Conference on Recent Advances in Materials, Minerals & Environment (RAMM) 2022: Nibong Tebal, Penang, Malaysia.

2. Rahman, N.A., **Jose Jol, C**., Albania Linus, A., Lizza Dampan, F., Abdul Jalan, N.S.A., Baharudin, N., & Wan Borhan, W.W.S. (2022, February 23-24). *Continuous electrocoagulation treatment with aluminium electrodes for desalination of tropical brackish peat water in Sarawak* [Paper Presentation]. The 14th International UNIMAS Engineering Conference 2022: Kota Samarahan, Sarawak, Malaysia.

3. Rahman, N.A., Albania Linus, A., **Jose Jol, C**., Andok, A.I., Lizza Dampan, F., Abdul Jalan, N.S.A., Baharudin, N., & Wan Borhan, W.W.S. (2022, February 23-24). *Continuous electrocoagulation treatment with aluminium electrodes of midstream Batang Kayan and Batang Sadong.* [Paper Presentation]. The 14th International UNIMAS Engineering Conference 2022: Kota Samarahan, Sarawak, Malaysia.

4. Rahman, N.A., **Jose Jol, C**., Albania Linus, A., & Ismail, V. (2021, September 13-15*). Treatment of tropical brackish peat water with continuous electrocoagulation* [Accepted Abstract]. MDPI: The 9th World Sustainability Forum: MDPI: The 9th World Sustainability Forum. Basel: Switzerland

APPENDIX B: Gantt Chart

No.	*Activities*	*Start*	*Finish*	*Duration*	*Milestones*
1	Characterization of Brackish Peat Water	1/10/2020	9/12/2020	10w	*5%*
2	Continuous Electrocoagulation Treatment System	15/10/2020	12/5/2021	30w	*20%*
3	Effects of Seawater Percentage and Electric Current	1/11/2020	13/2/2021	15w	*25%*
4	Effects of Seawater Percentage and Flow Rate	13/1/2021	27/4/2021	15w	*30%*
5	Water Quality Analysis	3/12/2020	26/5/2021	25w	*35%*
6	Energy Operating Cost Analysis	2/4/2021	15/7/2021	15w	*40%*
7	Formulation of Adsorption Isotherm Models	10/5/2021	1/8/2021	12w	*45%*
8	Formulation of Pseudo-First Order Models	6/6/2021	18/9/2021	15w	*50%*
9	Model Validation	2/7/2021	4/11/2021	18w	*60%*
10	Electrocoagulation Flocs Analysis	1/2/2021	1/8/2021	26w	*70%*
11	Design of Experiment	2/8/2021	14/11/2021	15w	*73%*
12	Mathematical Model Fitting	1/9/2021	11/1/2022	19w	*75%*
13	Analysis of Variance	20/9/2021	6/2/2022	20w	*78%*
14	Statistical Model Analysis	8/10/2021	5/5/2022	30w	*80%*
15	Results and Discussion	1/7/2021	24/8/2022	60w	*90%*
16	Journal Publications	1/1/2022	16/12/2022	50w	*100%*

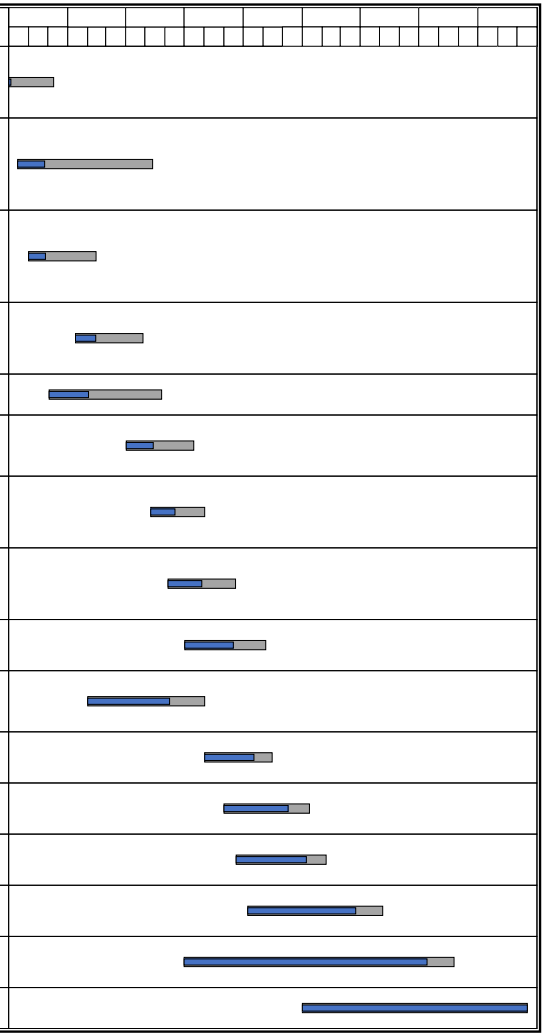

Figure 1: Gantt Chart

APPENDIX C: Supplementary Data

Table 1: Effect of Electric Current on Salinity Level Changes with Varied Seawater Percentage

Seawater Percentage (%)	Electric Current (A)	Changes in Salinity Levels (mg/L)						
		0 min	3 min	5 min	10 min	15 min	20 min	30 min
0	1	316	300	294	287	285	285	285
	2	316	271	256	245	241	241	241
	3	316	242	218	202	197	196	196
	4	316	213	181	160	153	152	152
	5	316	184	143	118	109	108	108
10	1	2,530	2,202	1,976	1,641	1,456	1,390	1,365
	2	2,530	2,009	1,732	1,368	1,200	1,150	1,131
	3	2,530	1,816	1,489	1,094	943	910	898
	4	2,530	1,623	1,245	821	687	670	664
	5	2,530	1,430	1,001	547	430	430	430
30	1	5,010	3,965	3,554	2,910	2,465	2,187	1,765
	2	5,010	3,562	3,052	2,422	2,035	1,805	1,489
	3	5,010	3,160	2,550	1,933	1,605	1,423	1,212
	4	5,010	2,757	2,047	1,445	1,175	1041	936
	5	5,010	2,354	1,545	956	745	659	659
50	1	7,490	6,536	6,024	5,223	4,776	4,567	4,423
	2	7,490	5,840	5,262	4,514	4,091	3,904	3,796
	3	7,490	5,144	4,500	3,805	3,406	3,241	3,169
	4	7,490	4,447	3,738	3,096	2,720	2,578	2,542
	5	7,490	3,751	2,976	2,387	2,035	1,915	1,915
70	1	9,976	8,912	8,293	7,679	7,178	6,780	6,380
	2	9,976	8,270	7,535	6,856	6,372	6,022	5,722
	3	9,976	7,629	6,777	6,033	5,566	5,265	5,065
	4	9,976	6,987	6,018	5,210	4,759	4,507	4,407
	5	9,976	6,345	5,260	4,387	3,953	3,750	3,750
80	1	12,497	12,134	11,921	11,354	10,970	10,770	10,334
	2	12,497	11,648	11,244	10,562	10,091	9,844	9,517
	3	12,497	11,162	10,567	9,769	9,212	8,918	8,700
	4	12,497	10,675	9,889	8,977	8,333	7,991	7,882
	5	12,497	10,189	9,212	8,184	7,454	7,065	7,065
90	1	14,987	14,723	14,524	14,034	13,476	13,132	12,587
	2	14,987	14,262	13,912	13,315	12,729	12,384	11,975
	3	14,987	13,801	13,300	12,597	11,982	11,636	11,364
	4	14,987	13,340	12,688	11,878	11,234	10,888	10,752
	5	14,987	12,878	12,076	11,159	10,487	10,140	10,140

Table 2: Effect of Electric Current on Salinity Reduction Efficiency with Varied Seawater Percentage

Seawater Percentage (%)	Electric Current (A)	Salinity Reduction Efficiency (%)						
		0 min	3 min	5 min	10 min	15 min	20 min	30 min
0	1	0	5.06	6.96	9.18	9.81	9.81	9.81
	2	0	14.22	18.93	22.57	23.71	23.83	23.85
	3	0	23.38	30.89	35.96	37.62	37.86	37.90
	4	0	32.54	42.86	49.35	51.52	51.88	51.94
	5	0	41.69	54.83	62.74	65.43	65.90	65.98
10	1	0	12.96	21.90	35.14	42.45	45.06	46.05
	2	0	20.59	31.53	45.95	52.59	54.55	55.29
	3	0	28.22	41.17	56.76	62.73	64.03	64.53
	4	0	35.85	50.80	67.57	72.87	73.52	73.76
	5	0	43.48	60.43	78.38	83.00	83.00	83.00
30	1	0	20.86	29.06	41.92	50.80	56.35	64.77
	2	0	28.90	39.09	51.67	59.38	63.97	70.29
	3	0	36.94	49.11	61.42	67.96	71.60	75.81
	4	0	44.98	59.14	71.17	76.55	79.22	81.33
	5	0	53.01	69.16	80.92	85.13	86.85	86.85
50	1	0	12.74	19.57	30.27	36.23	39.03	40.95
	2	0	22.03	29.75	39.73	45.38	47.88	49.32
	3	0	31.33	39.92	49.20	54.53	56.73	57.69
	4	0	40.62	50.09	58.66	63.68	65.58	66.06
	5	0	49.92	60.27	68.13	72.83	74.43	74.43
70	1	0	10.67	16.87	23.03	28.05	32.04	36.05
	2	0	17.10	24.47	31.28	36.13	39.63	42.64
	3	0	23.53	32.07	39.52	44.21	47.23	49.23
	4	0	29.96	39.67	47.77	52.29	54.82	55.82
	5	0	36.40	47.27	56.02	60.37	62.41	62.41
80	1	0	2.90	4.61	9.15	12.22	13.82	17.31
	2	0	6.80	10.03	15.49	19.25	21.23	23.85
	3	0	10.69	15.45	21.83	26.29	28.64	30.39
	4	0	14.58	20.87	28.17	33.32	36.05	36.93
	5	0	18.47	26.29	34.51	40.35	43.47	43.47
90	1	0	1.76	3.09	6.36	10.08	12.38	16.01
	2	0	4.84	7.17	11.15	15.07	17.37	20.10
	3	0	7.92	11.26	15.95	20.05	22.36	24.18
	4	0	10.99	15.34	20.75	25.04	27.35	28.26
	5	0	14.07	19.42	25.54	30.03	32.34	32.34

Table 3: Effect of Flow Rate on Salinity Levels Changes with Varied Seawater Percentage

Seawater Percentage (%)	Flow Rate (L/min)	Changes in Salinity Levels (mg/L)						
		0 min	3 min	5 min	10 min	15 min	20 min	30 min
0	0.4	316	234	188	155	145	145	145
	0.8	316	184	143	118	109	108	108
	1.2	316	163	118	97	90	90	90
	1.4	316	206	168	139	129	126	125
	2.0	316	248	217	180	167	161	160
10	0.4	2,530	1,771	1,395	918	742	668	664
	0.8	2,530	1,430	1,001	547	430	430	430
	1.2	2,530	1,221	823	413	303	278	278
	1.4	2,530	1,687	1,243	702	567	532	524
	2.0	2,530	1,854	1,546	1,134	917	804	803
30	0.4	5,010	3,034	2,387	1,686	1,356	1,145	1,023
	0.8	5,010	2,354	1,545	956	745	659	659
	1.2	5,010	1,978	1,232	634	456	412	412
	1.4	5,010	2,765	1,976	1,342	1,038	897	865
	2.0	5,010	3,345	2,776	2,034	1,654	1,445	1,254
50	0.4	7,490	4,644	4,031	3,536	3,233	3,080	3,021
	0.8	7,490	3,751	2,976	2,387	2,035	1,915	1,915
	1.2	7,490	3,445	2,456	1,734	1,367	1,245	1,245
	1.4	7,490	4,057	3,496	3,040	2,703	2,585	2,585
	2.0	7,490	5,231	4,565	4,032	3,763	3,574	3,456
70	0.4	9,976	7,463	6,652	5,889	5,667	5,582	5,582
	0.8	9,976	6,345	5,260	4,387	3,953	3,750	3,750
	1.2	9,976	5,786	4,564	3,586	3,096	2,834	2,834
	1.4	9,976	6,904	5,956	5,088	4,810	4,666	4,666
	2.0	9,976	8,022	7,348	6,640	6,524	6,498	6,498
80	0.4	12,497	11,415	10,928	10,340	9,894	9,643	9,443
	0.8	12,497	10,189	9,212	8,184	7,454	7,065	7,065
	1.2	12,497	95,23	8,387	6,956	6,234	5,876	5,876
	1.4	12,497	10,802	10,070	9,312	8,674	8,354	8,254
	2.0	12,497	12,028	11,786	11,268	10,887	10,732	10,632
90	0.4	14,987	14,203	13,920	13,214	12,813	12,690	12,490
	0.8	14,987	12,878	12,076	11,159	10,487	10,140	10,140
	1.2	14,987	12,216	11,254	10,132	9,324	8,965	8,965
	1.4	14,987	13,541	12,998	12,186	11,650	11,415	11,315
	2.0	14,987	14,806	14,642	14,241	13,976	13,800	13,665

Table 4: Effect of Flow Rate on Salinity Reduction Efficiency with Varied Seawater Percentage

Seawater Percentage (%)	Flow Rate	Salinity Reduction Efficiency (%)						
		0 min	3 min	5 min	10 min	15 min	20 min	30 min
0	0.4	0	25.95	40.51	50.95	54.11	54.11	54.11
	0.8	0	41.69	54.83	62.74	65.43	65.90	65.98
	1.2	0	48.42	62.66	69.30	71.52	71.52	71.52
	1.4	0	34.97	46.99	56.17	59.34	60.28	60.44
	2.0	0	21.52	31.33	43.04	47.15	49.05	49.37
10	0.4	0	30.02	44.88	63.72	70.67	73.60	73.77
	0.8	0	43.48	60.43	78.38	83.00	83.00	83.00
	1.2	0	51.74	67.47	83.68	88.02	89.01	89.01
	1.4	0	33.32	50.87	72.25	77.59	78.97	79.29
	2.0	0	26.72	38.89	55.18	63.75	68.22	68.26
30	0.4	0	39.44	52.36	66.35	72.93	77.15	79.58
	0.8	0	53.01	69.16	80.92	85.13	86.85	86.85
	1.2	0	60.52	75.41	87.35	90.90	91.78	91.78
	1.4	0	44.81	60.56	73.21	79.28	82.10	82.73
	2.0	0	33.23	44.59	59.40	66.99	71.16	74.97
50	0.4	0	38.00	46.19	52.79	56.84	58.89	59.67
	0.8	0	49.92	60.27	68.13	72.83	74.43	74.43
	1.2	0	54.01	67.21	76.85	81.75	83.38	83.38
	1.4	0	45.83	53.32	59.41	63.91	65.49	65.49
	2.0	0	30.16	39.05	46.17	49.76	52.28	53.86
70	0.4	0	25.19	33.32	40.97	43.19	44.05	44.05
	0.8	0	36.40	47.27	56.02	60.37	62.41	62.41
	1.2	0	42.00	54.25	64.05	68.97	71.59	71.59
	1.4	0	30.79	40.30	49.00	51.78	53.23	53.23
	2.0	0	19.59	26.34	33.44	34.60	34.86	34.86
80	0.4	0	8.66	12.56	17.26	20.83	22.84	24.44
	0.8	0	18.47	26.29	34.51	40.35	43.47	43.47
	1.2	0	23.80	32.89	44.34	50.12	52.98	52.98
	1.4	0	13.56	19.42	25.49	30.59	33.15	33.95
	2.0	0	3.75	5.69	9.83	12.88	14.12	14.92
90	0.4	0	5.23	7.12	11.83	14.51	15.33	16.66
	0.8	0	14.07	19.42	25.54	30.03	32.34	32.34
	1.2	0	18.49	24.91	32.39	37.79	40.18	40.18
	1.4	0	9.65	13.27	18.69	22.27	23.83	24.50
	2.0	0	1.21	2.30	4.98	6.75	7.92	8.82

Table 5: Water Quality Standards in terms of Salinity Levels

Seawater Percentage	Salinity Levels (mg/L)		Salinity Reduction Efficiency (%)	National Water Quality Standards Salinity Levels (mg/L)		
	Untreated	Treated		Class I	Class II A/B	Class IV
0	316	90	71.52	500	1,000	2,000
10	2,530	278	89.01			
30	5,010	412	91.78			
50	7,490	1,245	83.38			
70	9,976	2,834	71.59			
80	12,497	5,876	52.98			
90	14,987	8,965	40.18			

Table 6: Effects of Electric Current and Flow Rate on Energy Operating Cost with Electrocoagulation Treatment of Brackish Peat Water with 30% of Seawater Percentage.

Electric Current (A)	Flow Rate (L/min)	Specific Electrical Energy Consumption (kWh/m^3)	Energy Operating Cost (RM/m^3)	Salinity Reduction Efficiency (%)
1	0.4	0.48	0.22	12.34
	0.8	0.24	0.11	16.40
	1.2	0.12	0.06	20.45
	1.4	0.10	0.04	15.00
	2.0	0.07	0.03	9.54
2	0.4	0.95	0.45	29.76
	0.8	0.48	0.22	33.65
	1.2	0.24	0.11	37.54
	1.4	0.19	0.09	30.00
	2.0	0.14	0.07	22.45
3	0.4	1.43	0.67	45.76
	0.8	0.72	0.34	52.20
	1.2	0.36	0.17	58.64
	1.4	0.29	0.13	49.94
	2.0	0.21	0.10	41.23
4	0.4	1.91	0.92	63.24
	0.8	0.95	0.46	69.19
	1.2	0.48	0.23	75.14
	1.4	0.38	0.18	68.24
	2.0	0.29	0.14	61.34
5	0.4	2.38	1.14	79.58
	0.8	1.19	0.57	86.85
	1.2	0.60	0.29	91.78
	1.4	0.48	0.23	82.73
	2.0	0.36	0.17	74.97